THE UNIVERSITY OF MICHIGAN

INDUSTRY PROGRAM OF THE COLLEGE OF ENGINEERING

EFFECTS OF COOLING ON TRANSITION IN THE BOUNDARY LAYER ON A HEMISPHERE IN SIMULATED HYPERSONIC FLOW

Roger Dunlap

A dissertation submitted in partial fulfillment
of the requirements for the degree of
Doctor of Philosophy in the
University of Michigan
1961

February 1961
IP - 499

ergm
UMR0982

Doctoral Committee:

Professor Arnold M. Kuethe, Co-chairman
Associate Professor William W. Willmarth, Co-chairman
Associate Professor Thomas C. Adamson, Jr.
Mr. James L. Amick
Professor Richard B. Morrison
Professor Erich H. Rothe

ACKNOWLEDGMENTS

This investigation was partially supported by the United States Air Force under Contract No.s AF 49(638)-336 and AF 33(616)-6856, monitored by the Aeronautical Research Laboratories, Air Force Research Division, Air Research and Development Command.

The author wishes to thank the doctoral committee for their efforts and especially Professors Arnold M. Kuethe and William W. Willmarth, co-chairman, who provided valuable guidance, advice, and encouragement throughout the course of the investigation. Helpful discussions with Mr. James L. Amick are also deeply appreciated.

Special appreciation is extended to Mr. A. M. Rickel of the Bendix Corporation Research Laboratories who took the photomicrographs and provided valuable information concerning the polishing of the model. The profilometer tracings were made through the courtesy of the Micrometrical Manufacturing Company, Ann Arbor, Michigan.

The assistance of Messrs. G. E. Chmielewski, R. E. Deitrick, A. J. Kuprenas, R. J. Brando, and F. L. Donovan in the construction and execution of the experiments is gratefully acknowledged.

TABLE OF CONTENTS

LIST OF FIGURES

LIST OF FIGURES CONT'D

LIST OF FIGURES CONT'D

NOMENCLATURE

a	speed of sound
a_2, a_4	defined by Equation 11
b	defined by Equation 8
C_f	local skin-friction coefficient, $C_f = \frac{2\tau_w}{\rho_w u_e^2}$
c_m	mean specific heat of model material
C_p	pressure coefficient, $C_p = \frac{2(P - P_\infty)}{\rho_\infty u_\infty^2}$
C	specific heat at constant pressure
D	diameter of body
e'	rms voltage fluctuation
h	altitude in the standard atmosphere
k	roughness height
k	thermal conductivity
M	Mach number
Nu	Nusselt number
P	pressure
Pr	Prandtl number
q	heat transfer rate, $q = -k\frac{\partial T}{\partial y}$
r	radius in spherical coordiantes
$r_{avg.}$	mean radius of a hemispherical shell
Δr	thickness of a hemispherical shell
R	gas constant
R	radius of model
Re	Reynolds number
t	time

T	temperature
u, v	velocities in the η (or x) and r directions
u'	rms velocity fluctuation of u
x	distance along the surface of a body measured from the stagnation point
y	distance normal to a body surface
γ	ratio of specific heats
δ	boundary-layer thickness
δ^*	boundary-layer displacement thickness
η	angle between the free stream direction and the normal to a body surface
θ	boundary-layer momentum thickness
μ	viscosity
ρ	density
ρ_m	density of model material
τ	shear stress, $\tau = \mu \frac{\partial u}{\partial y}$
ψ	stream function defined by Equation 6

Subscripts

0	initial value
e	local value just outside boundary layer
k	value at the top of a roughness element
p	value at point of measurement, pitot probe
s	stagnation value at the nose of a body
w	surface value
aw	adiabatic surface value

I. INTRODUCTION

One of the most difficult problems in the flow of a viscous fluid adjacent to a solid boundary is that of predicting the transition from laminar to turbulent motion in the boundary layer. The transition process is governed by the non-linear terms in the Navier-Stokes equations and, according to experiment, may occur in one of two ways: 1) if the laminar boundary layer is unstable to infinitesimal transient perturbations (termed linear instability), small disturbances, originating at roughness elements or as turbulence in the outside stream, are amplified until the nonlinear terms in the governing equations become large enough to determine the remainder of the flow process culminating in the turbulent layer, 2) if the disturbances in the laminar layer are initially so large that their subsequent behavior cannot be described by the theory for infinitesimal perturbations the non-linear terms in the equations describe the entire process. Therefore, the location of transition on a given body generally depends on the various disturbances present, such as pressure waves, stream turbulence, and surface roughness as well as the flow parameters governing the amplification of these disturbances. It is important for an understanding of the work to be described here to realize that if the disturbances are large enough transition may occur in a linearly stable laminar layer.

The stability of the laminar boundary layer to infinitesimal disturbances and the separate influences of Mach number, pressure gradient, heat transfer, and surface curvature have been evaluated theoretically by Tollmien, Schlichting, Goertler, Lees, Lin and others[1].

These stability theories, in addition to providing some understanding of the mechanisms initiating the transition process for the important case when the disturbances are small, have served as valuable guides in designing, conducting, and interpreting experiments which verify and supplement our basic understanding of the transition phenomenon.

Since the extension of the linear stability theories to compressible boundary layers by Lees and Lin[2,3] in 1946, many experiments have been conducted to verify the theoretical predictions concerning the effects of thermal conditions at the surface on boundary layer stability. According to this theory, there is, in the absence of surface curvature, a stabilizing effect of heat transfer from the boundary layer to the surface (boundary-layer cooling) and therefore a corresponding delay in transition when it is initiated by an instability to small disturbances. The experiments of many investigators[4-10] on flat plates, cones and various bodies of revolution, over a wide range of Mach numbers, have indeed shown that cooling promotes higher transition Reynolds numbers while heating has the opposite effect. Recently, however, wind tunnel experiments by Jack, Diaconis, and Wisniewski[11-13] have shown a so-called "transition reversal", in which, when the degree of cooling exceeds a critical value, influenced by nose bluntness and surface roughness, transition Reynolds numbers were observed to decrease markedly. As the nose bluntness or roughness increased the critical degree of cooling decreased. Also, shock tube experiments by Stetson[14] have yielded low transition Reynolds numbers for the highly cooled boundary layer on a hemisphere-cylinder configuration.

On the basis of observations such as these, some controversy has arisen as to whether cooling may under some circumstances actually cause the boundary layer to become linearly unstable. The phenomenon is complicated by the fact that cooling the boundary layer not only affects the stability to disturbances but, because of the relatively high density near the surface, the disturbance caused by a given roughness element will increase with cooling. This latter effect would, in itself, tend to decrease the transition Reynolds numbers with increasing cooling. Further, if boundary-layer cooling occurs on a convex surface the resulting centrifugal acceleration field tends to destabilize the flow. This tendency does not enter into the above mentioned stability theories. The relative importance of these various effects of cooling will be discussed qualitatively in the following section, and some typical experimental results will be presented. Although the effect of cooling in increasing the magnitude of disturbances from fixed roughness elements represents a most plausible explanation for transition reversal, it has not yet been determined whether this is the proper explanation in all cases and there is a need for further experiments to answer specific questions.

An important situation in which extreme boundary layer cooling occurs is during the re-entry of a blunt body into the atmosphere at hypersonic speed. Under these circumstances unsteady boundary layer cooling exists for a short period of time while the surface is cool and the stagnation temperature high. Since the heat transfer rates associated with a turbulent boundary layer may be an order of magnitude higher than those in the laminar case, a knowledge of the transition point

and its location as affected by the cooling is of major practical significance.

Some attempts have been made to study transition under re-entry conditions by means of flight tests (see, for example, References 15 and 16). Aside from the high cost and extreme instrumentation problems the interpretation of flight test data is hampered by the fact that many of the significant parameters vary simultaneously, so that finding the effect of any one presumes a knowledge of the effects of the others.

The purpose of the work to be reported on here was to investigate in the laboratory the effects of cooling on transition in the boundary layer on the nose of a blunt body under conditions similiar to those encountered during hypersonic re-entry, with the aim of gaining some knowledge of the circumstances under which boundary-layer cooling may promote early transition.

The first problem to be considered was that of producing a hypersonic environment which would facilitate the objectives of these transition studies. Important requirements were considered to be; 1) reasonable testing times and stagnation temperatures so that the details of the transition process may ultimately be studied, and 2) the ability to simulate low free stream turbulence and small surface roughness so that the conditions of small disturbances may be realized.

These requirements can be met by testing scale models in a wind tunnel, in which practical cooling rates can be achieved by cooling the model and/or heating the stream. The maximum stagnation temperatures would perhaps be limited by the available instrumentation.

However, in the usual hypersonic or supersonic wind tunnels, small free stream disturbances and surface roughness become more difficult to simulate. At high speeds, pressure waves arising from the turbulent boundary layers on the tunnel walls are known to give rise to free stream disturbances which may be large enough to have an appreciable effect on transition[17-19]. The difficulties with respect to simulating small roughness stem from the fact that the boundary layers will be relatively thin because of the small scale of most wind tunnel models. These thin boundary layers, typically of the order of a few ten-thousandths of an inch on a one inch diameter spherical nose, impose severe limitations on the maximum roughness if transition due to roughness is to be avoided. The limitation becomes even more severe when one considers the effect of cooling in increasing the effect of roughness. It was found for instance[15,16] that transition Reynolds numbers, based on momentum thickness, on an 8-inch diameter hemisphere could be increased from values between 100 and 400 to between 900 and 1200 by reducing the surface roughness from 25 rms microinches to less than 5 microinches.

In the present investigation the problems of high free stream turbulence and small model size were overcome by simulation techniques. Specifically, the subsonic and low supersonic Mach number, pressure, and velocity distributions which exist over most of the nose region of a blunt body in hypersonic flow (on a sphere moving at $M_\infty = 10$, $M_e = 1$ at $\eta = 44^\circ$ and $M_e = 2$ at $\eta = 70.7^\circ$) can be produced in a wind tunnel with

subsonic flow ahead of the body by a properly contoured shroud in the region of the nose*. In such a "shrouded model" test the turbulence in the subsonic "free-stream" can be kept at a low level, and size limitations on the model are reduced. Accordingly, the shroud technique was herein employed to simulate the subsonic boundary layer on the nose of a 9-inch diameter hemisphere in hypersonic flow.

The following chapters are devoted to a discussion of the hypersonic flow simulation, including a theoretical determination of the shroud contour, and a description of the experimental apparatus and techniques, followed by a presentation and discussion of experimental results. The experiments consisted of: 1) "environmental" tests which include the surface pressure distribution on the sphere resulting from the shroud technique, turbulence levels in the wind tunnel and outside the boundary layer on the model, correlation measurements between velocity fluctuations at the stagnation point, and temperature-time histories of the model surface during tests with cooling; 2) hot-wire measurements of the transition caused by several roughness elements, showing qualitative effects of various combinations of cooling and roughness; and 3) effects of cooling on transition in the subsonic boundary layer when the surface is highly polished, determined by means of a small pitot probe at the surface. There are discussions of the roughness caused by dust in the airstream and by condensation films (H_2O, CO_2, and O_2) at low model temperatures.

---

* The idea of shrouding a model to simulate surface pressure and velocity distributions was first reported by Ferri[20].

II. SOME EFFECTS OF COOLING, CURVATURE, AND ROUGHNESS ON BOUNDARY-LAYER TRANSITION

Experimental observations of the influence on transition of such factors as Mach number, pressure gradient, heat transfer, surface curvature, free-stream turbulence, and surface roughness have been reviewed and discussed in light of applicable stability theories by many authors[21-24]. In this section attention will be devoted to a qualitative discussion of the effects of cooling in conjunction with convex surface curvature and with surface roughness. A few of the experimental results pertaining to these effects will also be given.

The effects of heat transfer on the stability of the laminar boundary layer to Tollmien-Schlichting type disturbances was first evaluated theoretically be Lees and Lin in 1946[2,3]. Their calculations showed that cooling stabilized the boundary layer to disturbances of this type. On concave surfaces, transition may result from an entirely different instability mechanism. This so-called centrifugal instability results from the unstable distribution of the centrifugal acceleration field in the boundary layer on a surface with concave curvature, and was first recognized by Taylor[25] in connection with the flow between concentric rotating cylinders and later analyzed by Goertler[26] for boundary-layer flows. Experimental investigations by Liepmann[27], in subsonic flow, showed that increasing concave curvature does decrease the momentum thickness Reynolds number at transition in accordance with the predictions by Goertler. On the other hand, when the surface curvature was convex, Liepmann found that the Reynolds number of transi-

tion, as well as the characteristics of Tollmien-Schlichting type disturbances, were little influenced by the stabilizing effect of the centrifugal acceleration field.

As pointed out in a rough analysis by Lees[28], the density gradient and the resulting centrifugal acceleration field in a cooled boundary layer on a convex surface tends to decrease the stability of the flow but, even with infinite cooling, the criterion for dynamic stability remains satisfied. Whether the transition point in the compressible boundary layer on a convex surface is appreciably influenced by the decreased stability caused by cooling (in contrast to the results of Liepmann for an incompressible flow without heat transfer) has not been determined.

Turning now to the influence of cooling on the magnitude of disturbances, it will be shown that the transition reversal phenomenon can be caused by the effect of cooling in causing an increase in the magnitude of disturbances from fixed roughness elements. The effects of roughness on transition have been explored by many investigators (a comprehensive discussion of past methods of correlating the data, as well as a successful new method, has recently been given by Potter and Whitfield[29]). Various parameters, such as k/δ^*, $Re_k = \frac{\rho_k u_k k}{\mu_k}$, and $Re_k f(M_k)$ (where k = roughness height, ρ_k, u_k, μ_k and M_k are the density, velocity, viscosity, and Mach number, respectively, at the top of the roughness, and $f(M_k)$ is a monotonic increasing function of M_k) have been found to correlate the data well. For purposes of the qualitative discussion here, the roughness Reynolds number, Re_k, will be used. It has been observed by many investigators that as

Re_k is increased above a certain critical value (magnitude of disturbance from the roughness element exceeds a threshold value) the transition point begins to move upstream until, for large enough values of Re_k, it occurs immediately behind the roughness element. Boundary layer cooling may be identified with an increase in Re_k because of the resulting increase in the density and velocity as well as a decrease in the viscosity at the peak of a given element. Thus early transition or transition reversal may be caused by the cooling*.

An illustration of the effect that cooling may have on Re_k is given in Figure 1 which shows the distribution of Re_y/Re_δ through the boundary layer near the nose of a blunt body**. For small roughness elements (small y/δ) it is seen that Re_k may be increased by an order of magnitude as a result of cooling.

In accordance with the above discussion, three ranges of roughness heights, dependent on the cooling rate, would be expected. This is illustrated qualitatively in Figure 2 which shows the effect of increasing cooling in decreasing the threshold roughness height necessary to cause transition. In general a curve such as that shown would also depend on the type of roughness element and its location on

---

* This deduction assumes that Re_k increases faster than the critical value of Re_k. Although little data is available, the observations of Braslow, Knox, and Horton[30] on cones and flat plates indicate that the critical value of Re_k is essentially independent of heat transfer. They also report transition reversals caused by the effect of cooling in increasing Re_k to supercritical values.

** These distributions were computed from the boundary-layer solutions of Cohen and Reshotko[31] for the case of stagnation point flow on a body of revolution.

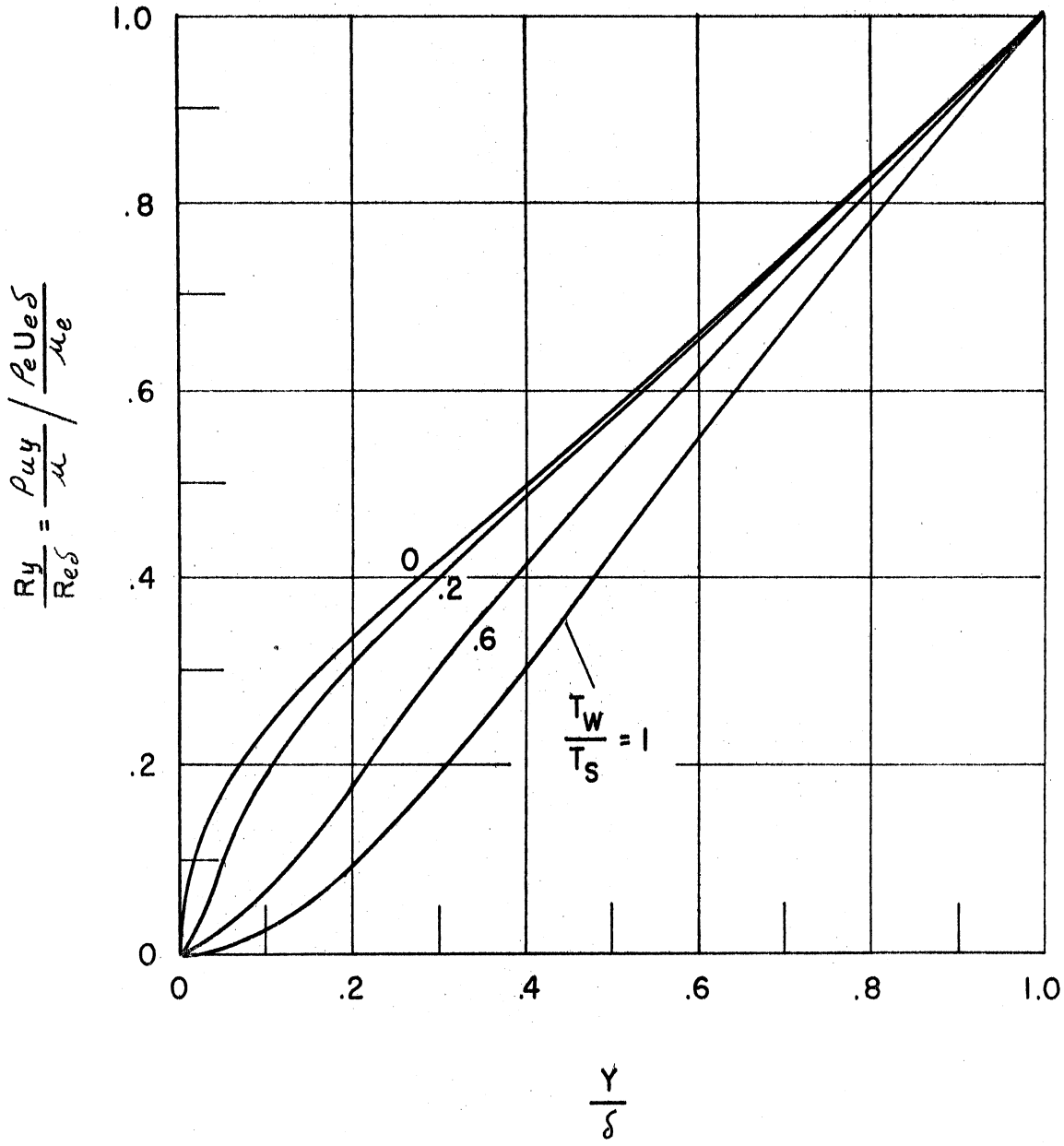

Figure 1. Distribution of Reynolds Number in the Boundary Layer Near the Nose of a Blunt Body.

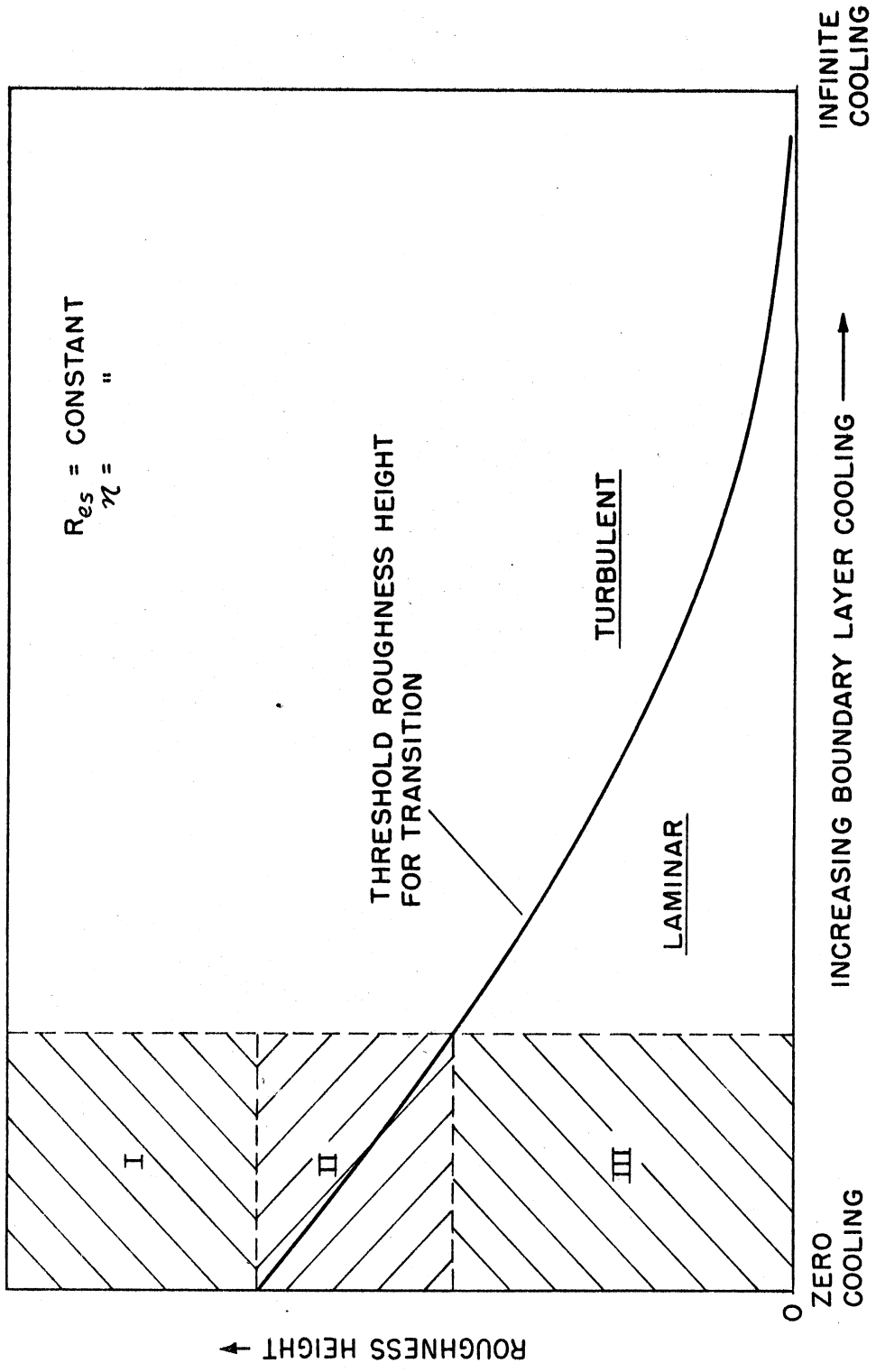

Figure 2. Qualitative Variation of Critical Roughness Height with Boundary-Layer Cooling.

the body as well as Reynolds number. However, for illustrative purposes we may identify the three ranges of roughness height as those corresponding to regions I, II, and III in the figure. For region I the roughness is large enough so that transition always occurs at the roughness independent of the cooling. In region II transition may or may not occur, depending on the cooling rate, while in region III the roughness is small enough so that the value of R_{e_k} remains subcritical up to the maximum cooling rate. One phase of the experimental results to follow will demonstrate these roughness regimes.

Before proceeding to the present work a few of the transition results of other investigators will be given. The purpose here is to illustrate some examples of the opposing trends of the influence of cooling which have been reported. Data of van Driest and Boison[10] on a sharp 10° apex angle cone at $M_e = 2.70$ is shown in Figure 3. In this and the following figures the local Reynolds numbers at transition, based on conditions at the edge of the boundary layer and distance from the stagnation point, is given as a function of the ratio of wall temperature to adiabatic wall temperature. With a smooth surface (rms roughness approximately 10 microinches) and the .0005 inch trip the transition Reynolds number increased with cooling and approached the line indicating complete stability to two-dimensional disturbances. Transition reversal resulting with the .001, .002, and .004 inch trips is also apparent. Observations due to Jack et al[12] on a sharp 9.5° apex angle cone at $M_\infty = 3.12$ is given in Figure 4. They obtain data similiar to that of van Driest, tending asymptotically to complete stabilization at a slightly lower temperature ratio. However they also

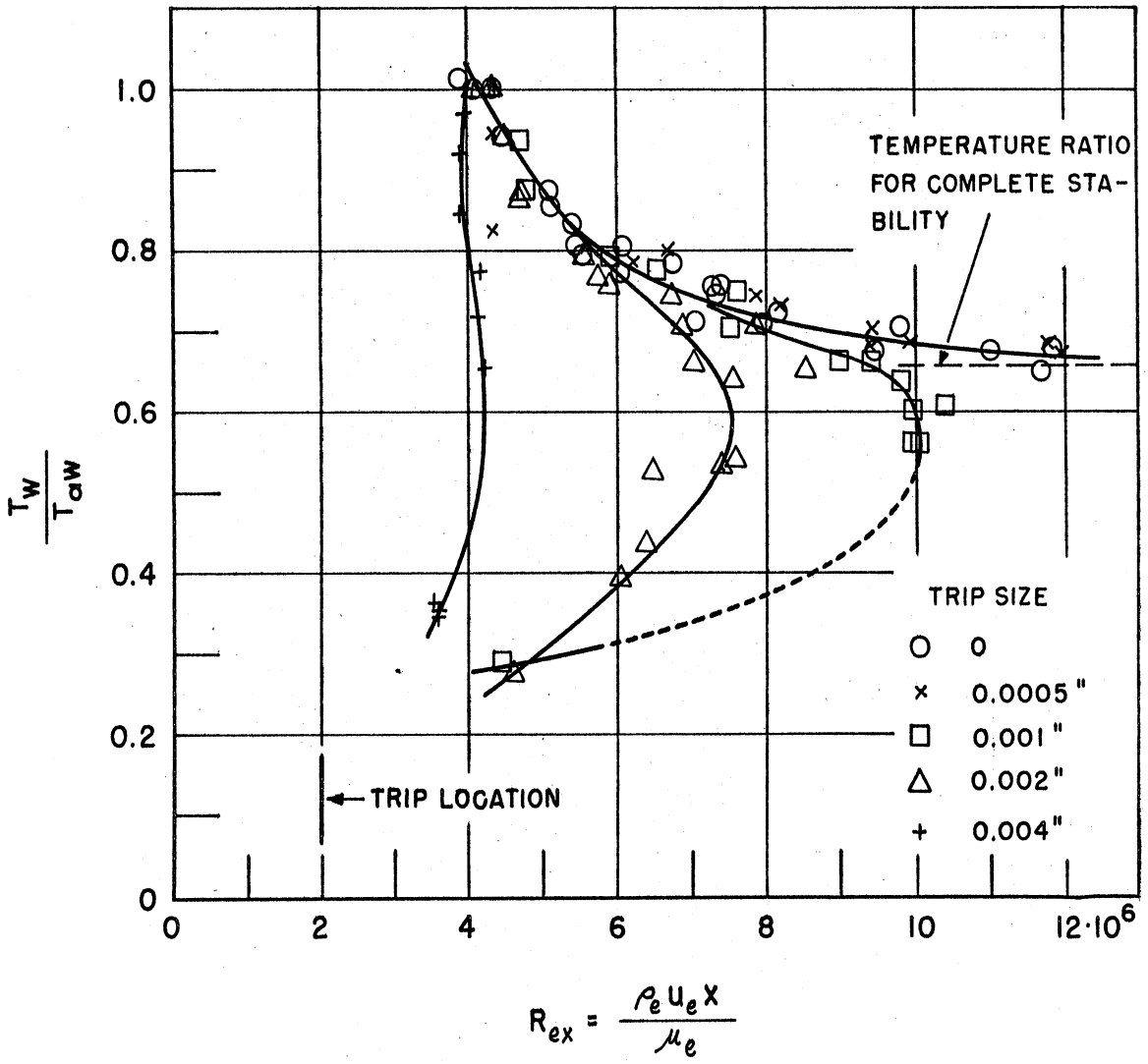

Figure 3. Effect of Cooling and Roughness on Transition on a Sharp 10° Apex Angle cone at M_e = 2.70 (Data of van Driest and Boison[10]).

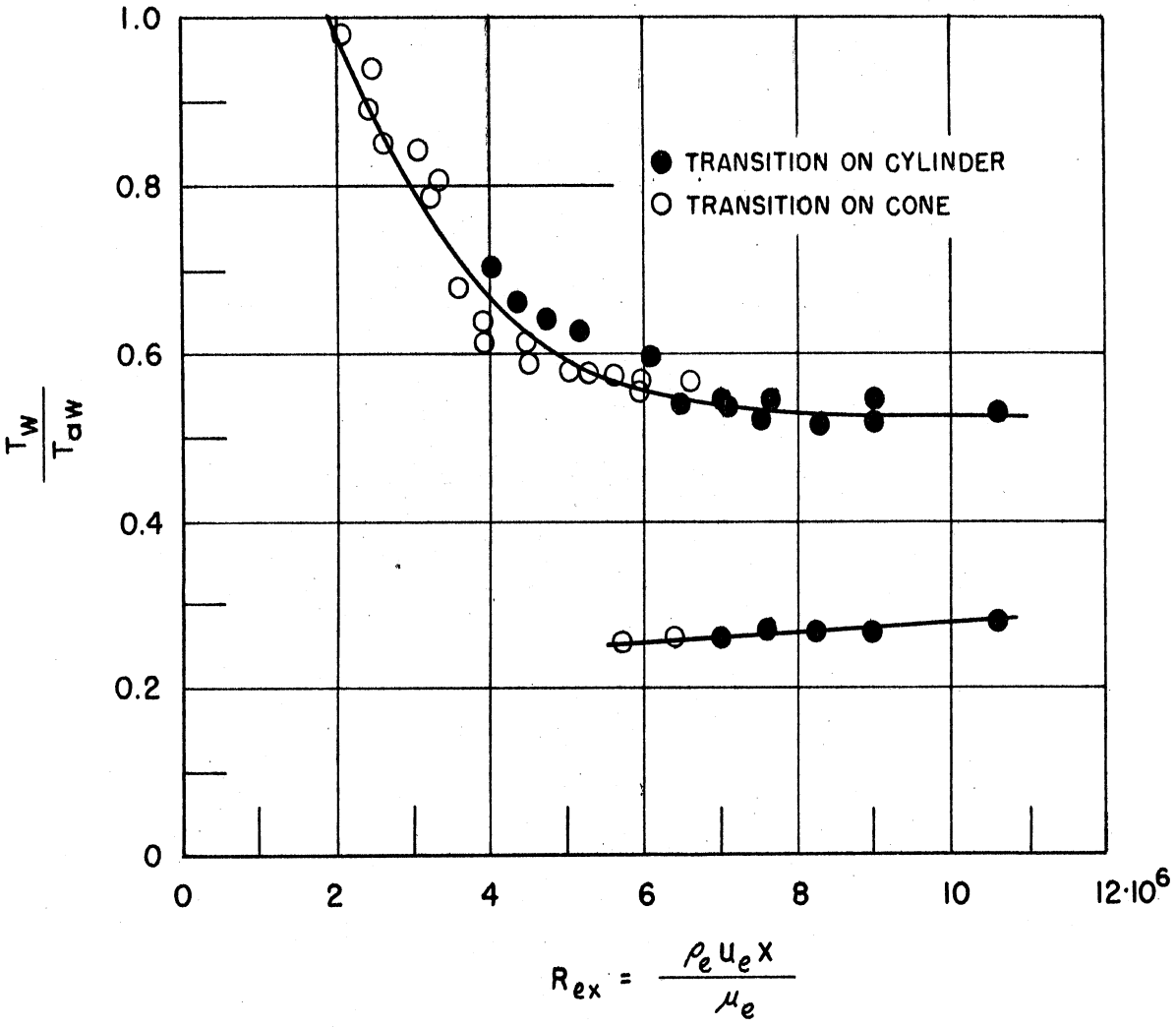

Figure 4. Effect of Cooling on Transition on a Sharp 9.5° Apex Angle Cone at $M_\infty = 3.12$ (Data of Jack et al[12])

find a reversal at lower temperature ratios without placing a trip on the surface (rms surface roughness was 12 microinches). At these temperatures both CO_2 and H_2O films, of undetermined thickness were on the surface. The authors concluded, however, that transition reversal could not be attributed primarily to surface roughness.

An example of the effects of cooling on blunt nosed models (convex surface curvature) is presented in Figure 5. Wind tunnel data of Diaconis et al[13] for a hemisphere-cone-cylinder at $M_\infty = 3.12$ is shown together with the shock tube results of Stetson[14] ($M_\infty = 1.5 - 2.49$) for a hemisphere cylinder. On the blunted cone-cylinder transition reversal occurred at higher temperature ratios than for the sharp cone tests of the same authors (Figure 4). The surface roughness was < 16 microinches. At these temperatures a frost film, of undetermined thickness, was on the surface. The shock tube data of Stetson also show low transition Reynolds numbers at the lower temperature ratios. The rms surface roughness of the 0.25-inch-radius hemisphere-cylinder was less than 1 microinch, but the heat-transfer gages used to detect transition protruded 12 microinches above the surface.

Observations of early transition promoted by boundary layer cooling, such as those presented above, stimulated the investigation to be presented in the following pages.

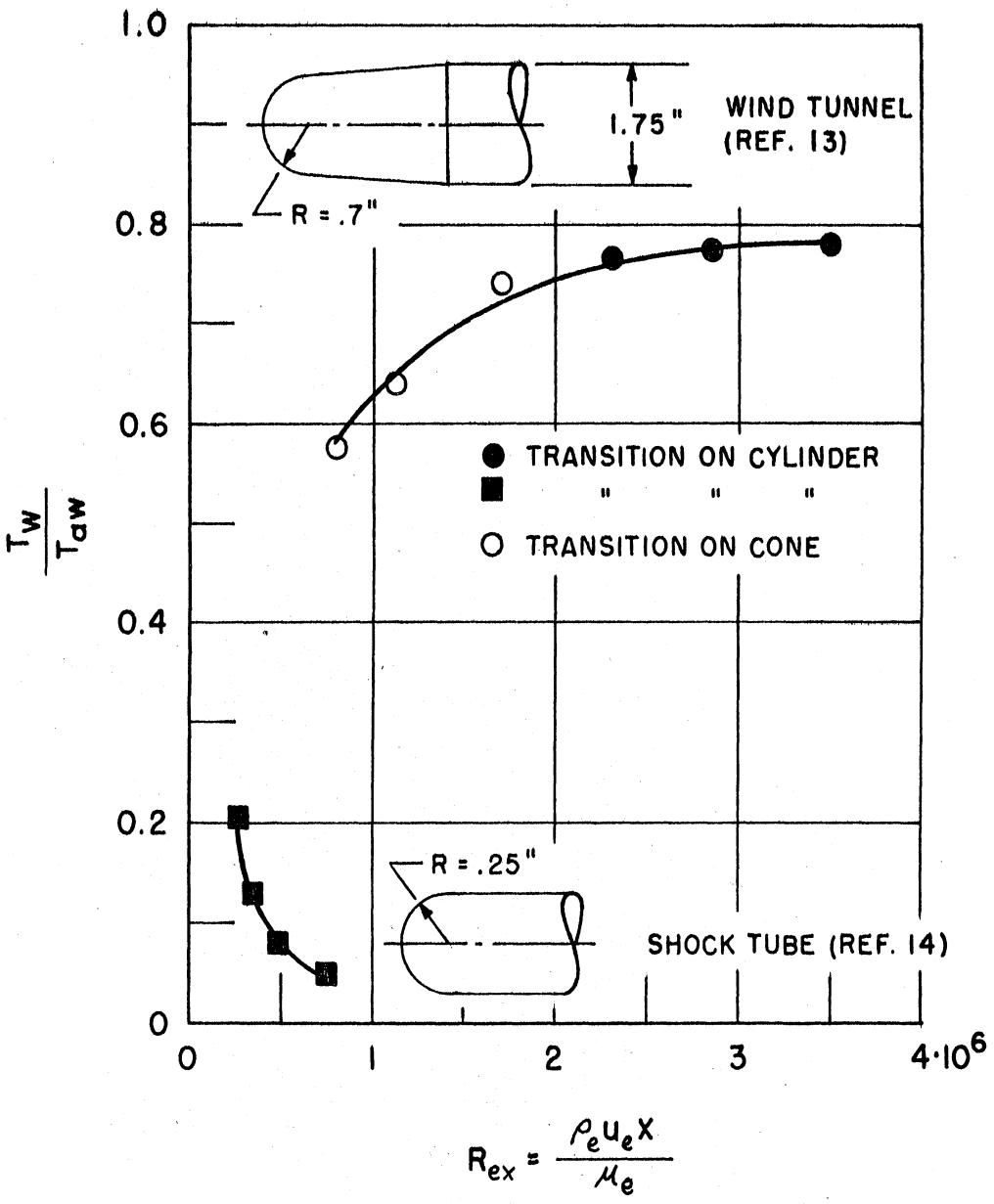

Figure 5. Effects of Cooling on Transition on Blunt Bodies (Data of Diaconis et al[13] and Stetson[14]).

III. FLOW SIMULATION AND SHROUD DESIGN

Similarity Requirements for Boundary Layer Flows - Simplifications for Boundary-Layer Transition Studies on Blunt Bodies in Hypersonic Flow

The fundamental guides for the design of any wind tunnel facility are the non-dimensional similarity parameters, derived from the governing physical equations, which must have the same values for two sets of testing conditions if the detailed flow fields are to be non-dimensionally identical. In the present investigation, it was desired to study the boundary layer flow which occurs over the nose region of blunt bodies at hypersonic speeds. Accordingly, the important similarity parameters for this study are those associated with the boundary-layer equations. It will be shown below that, within certain limitations, when conditions at the stagnation point are used for forming the similarity parameters (as opposed to the usual "free-stream" conditions) the "free-stream" Mach number drops out of the problem. This result is a consequence of the Mach number independence principle[50]. The choice of reference conditions at the stagnation point and the relative unimportance of Mach number as a similarity parameter are consistent with the present shroud technique in which "free-stream" conditions no longer have significance.

A straightforward dimensional analysis of the boundary layer equations, given in Appendix A, shows that when the following conditions are realized in two flow fields:

1. The bodies are geometrically similar.
2. The fluids act as non-reacting gases.
3. Over the range of temperatures encountered, the dependence on temperature of the viscosity, thermal conductivity, and

specific heats can be represented with sufficient accuracy by power laws.

4. The Prandtl number and ratio of specific heats, based on stagnation conditions, are constant.
5. The flow along the edge of the boundary layer can be considered isentropic.

then the important similarity parameters for comparison of the boundary layer flows are

1. The Mach number distribution, $M_e(\frac{x}{D})$, along the edge of the boundary layer;
2. Either the Nusselt number distribution, $Nu_w(\frac{x}{D})$, along the wall or the wall temperature ratio, $\frac{T_w}{T_s}(\frac{x}{D})$;
3. The stagnation Reynolds number, $Re_s = \frac{\rho_s a_s D}{\mu_s}$

where x is measured from the stagnation point along the body in a meridian plane and D is the body diameter. Thus, with the above restrictions, the local boundary layer profiles $\frac{u}{u_e}$, $\frac{T}{T_e}$, and $\frac{\rho}{\rho_e}$ will have the same functional dependence on the non-dimensional co-ordinates in any two flows in which these similarity parameters are the same.

Although, in general, the Mach number distribution along the edge of the boundary layer of a given body implies a unique free-stream Mach number, an exception occurs for the case of blunt bodies in hypersonic flow. In this case, the Mach number and pressure distributions at the edge of the boundary layer are those associated with Newtonian flow and become independent of free stream Mach number over most of the nose region. Actually, the modified Newtonian theory shows that the ratio of surface pressure coefficient to its value at the

stagnation point is independent of free stream Mach number through the relation

$$\frac{C_{pw}}{C_{ps}} \equiv \frac{P_e/P_s - P_\infty/P_s}{1 - P_\infty/P_s} = \cos^2\eta \qquad (1)$$

However, in the hypersonic flow regime P_∞/P_s is negligible compared to unity and can also be neglected compared to P_e/P_s over a considerable portion of the nose region of a blunt body. Thus, the pressure and Mach number distributions are given quite accurately by the equations

$$\frac{P_e}{P_s} = \cos^2\eta \qquad (2)$$

and

$$M_e = \sqrt{\frac{2}{\gamma-1}\left[(\cos\eta)^{\frac{2(1-\gamma)}{\gamma}} - 1\right]}^{1/2} \qquad (3)$$

in the vicinity of the nose of a blunt body in hypersonic flow. Experiments on hemispheres (References 33-38, for example) show that the pressure distribution given by Equation 2 is very accurate over most of the nose region. For example, the data of Reference 34 shows less than 15% deviation from Equation 2 up to $\eta = 45^\circ$ when $M_\infty = 2.0$, and nearly perfect agreement up to $\eta = 65^\circ$ for $M_\infty = 4.15$.

Thus, for the purpose of studying the boundary layer over the nose of a blunt body in hypersonic (and moderate supersonic) flow, when real gas effects and free-stream entropy gradients are of minor importance, the important similarity parameters, based on stagnation

point conditions, are Reynolds number, $\frac{\rho_s a_s D}{\mu_s}$, and either the wall temperature ratio, $\frac{T_w}{T_s}\left(\frac{x}{D}\right)$, or the Nusselt number, $N_{u_w}\left(\frac{x}{D}\right)$. The characteristic velocity in the problem is the speed of sound, and free stream conditions have little significance.

Real gas effects, such as dissociation and ionization and the attendant heat and mass transfers in a multicomponent reacting gas will undoubtedly have some effect on the laminar boundary-layer stability. However, the purpose here was to study the circumstances under which cooling may actually promote a decrease in transition Reynolds number, a phenomenon which has been observed in wind tunnels[11-13] under ambient stagnation conditions, as well as in the shock tube[14] where the temperatures ranged as high as 10,000°R. Therefore, failure to simulate the real gas effects associated with high temperature levels was considered to be of only minor consequence, at least for a first approximation to the effects of cooling and roughness on transition. The effect of not simulating the local "free-stream" vorticity and entropy gradient associated with the bow wave could not be assessed apriori.

On the basis of the arguments presented above, a wind tunnel facility for boundary layer transition studies on a hemisphere in simulated hypersonic flow was designed by shrouding the model so that the Mach number distribution given by Equation 3 could be realized. The analysis used in designing the shroud is presented in the next section.

Since in the use of the tunnel the supply air was unheated, boundary layer cooling was effected by filling the model with various coolants such as liquid nitrogen. In Figure 6 the range of simulation

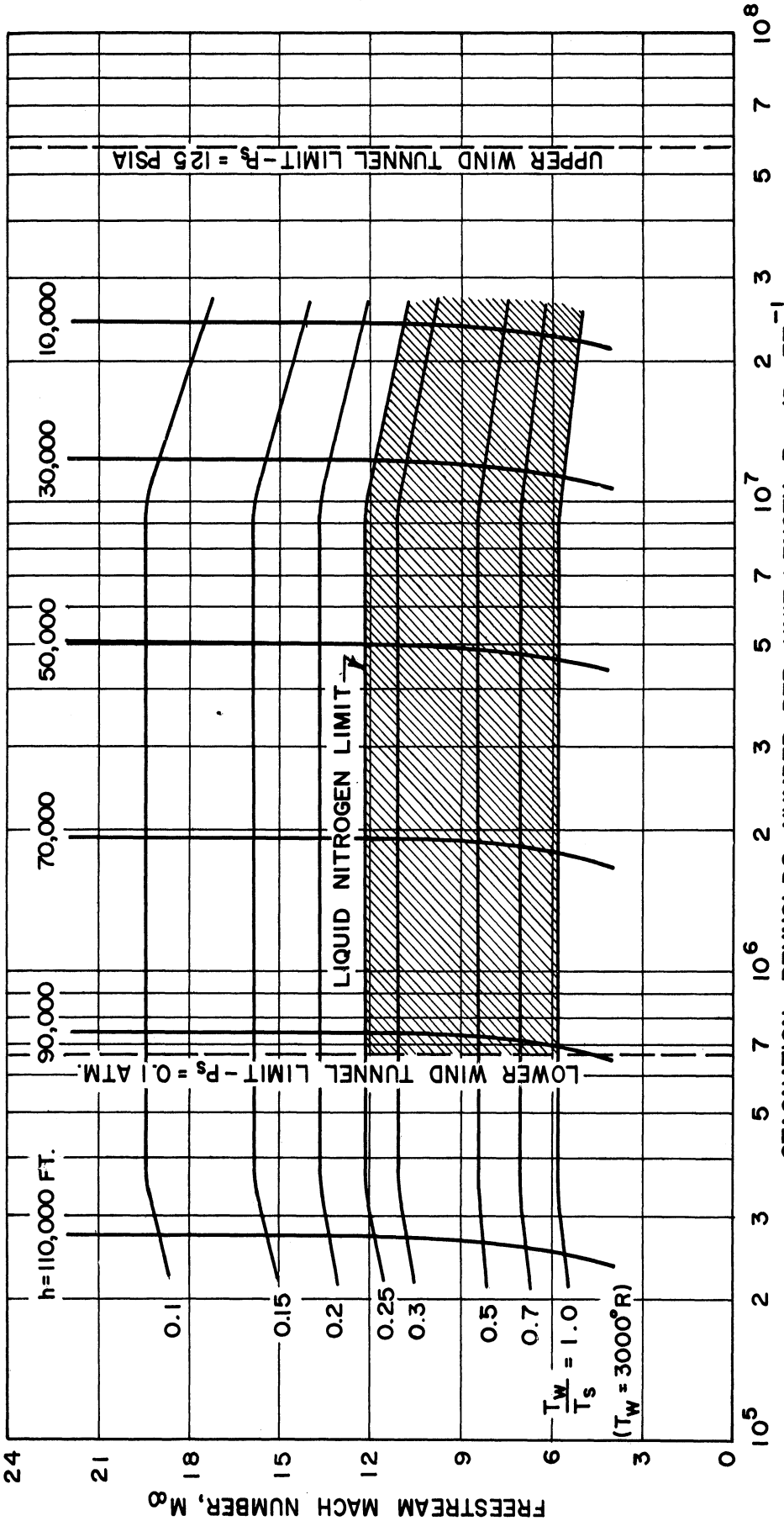

Figure 6. Range of Flow Simulation

provided by the facility is given in terms of the stagnation Reynolds numbers and wall temperature ratios for a re-entry body ($T_w = 3000^\circ R$) at various altitudes and Mach numbers.

Shroud Design

The following analysis predicts the contour of an axi-symmetric shroud enclosing a hemisphere on which, for choking flow, the pressure and Mach number distributions are those for hypersonic flow (Equations 2 and 3). A hemisphere was chosen partially because the spherical coordinate system facilitates the analysis*.

The design of the shroud contour was carried out in two steps. First, an approximate solution for the incompressible, irrotational flow field was found in the region $0^\circ \leq \eta \leq 45^\circ$, and, second, the resulting contour was corrected for compressibility near the sonic region (Me = 1 at $\eta \simeq 44^\circ$) assuming one-dimensional flow**.

---

* Experimentally the spherical surface is convenient because by rotating a sphere a single probe serves for determining a distribution over a meridian plane.

** The contour downstream of the sonic point could also be designed by the method of characteristics. However, this refinement was considered unnecessary because boundary-layer transition was expected to occur in the subsonic region with the testing conditions available. Further, the free stream turbulence generated by the turbulent boundary layer on the shroud would probably seriously affect the transition on the model.

Proceeding to the incompressible problem, the irrotationality condition and conservation of mass, expressed in spherical coordinates, (see Figure 7) are, respectively,

$$\frac{\partial(ur)}{\partial r} - \frac{\partial v}{\partial \eta} = 0 \tag{4}$$

and

$$\frac{\partial}{\partial r}\left(r^2 v \sin\eta\right) + \frac{\partial}{\partial \eta}\left(r u \sin\eta\right) = 0 \tag{5}$$

In view of Equation 5 a stream function, $\psi(r,\eta)$, can be defined by

$$\frac{\partial \psi}{\partial r} = -ru\sin\eta$$

$$\frac{\partial \psi}{\partial \eta} = r^2 v \sin\eta \tag{6}$$

The irrotationality condition, Equation (4), expressed in terms of ψ leads to the following linear equation

$$r^2\frac{\partial^2\psi}{\partial r^2} + \frac{\partial^2\psi}{\partial \eta^2} - \cot\eta\frac{\partial\psi}{\partial\eta} = 0 \tag{7}$$

The boundary conditions to be supplied with Equation 7 are that ψ is zero on the stagnation streamline and the surface of the body, and, in addition, that the velocity distribution derived from Equation 3 exists along the body surface.

Mathematically, the irrotational flow of an incompressible fluid in a "simply connected" region is uniquely determined when either the stream function or the normal component of velocity is known at every point of the boundary[39]. In the present application on the other

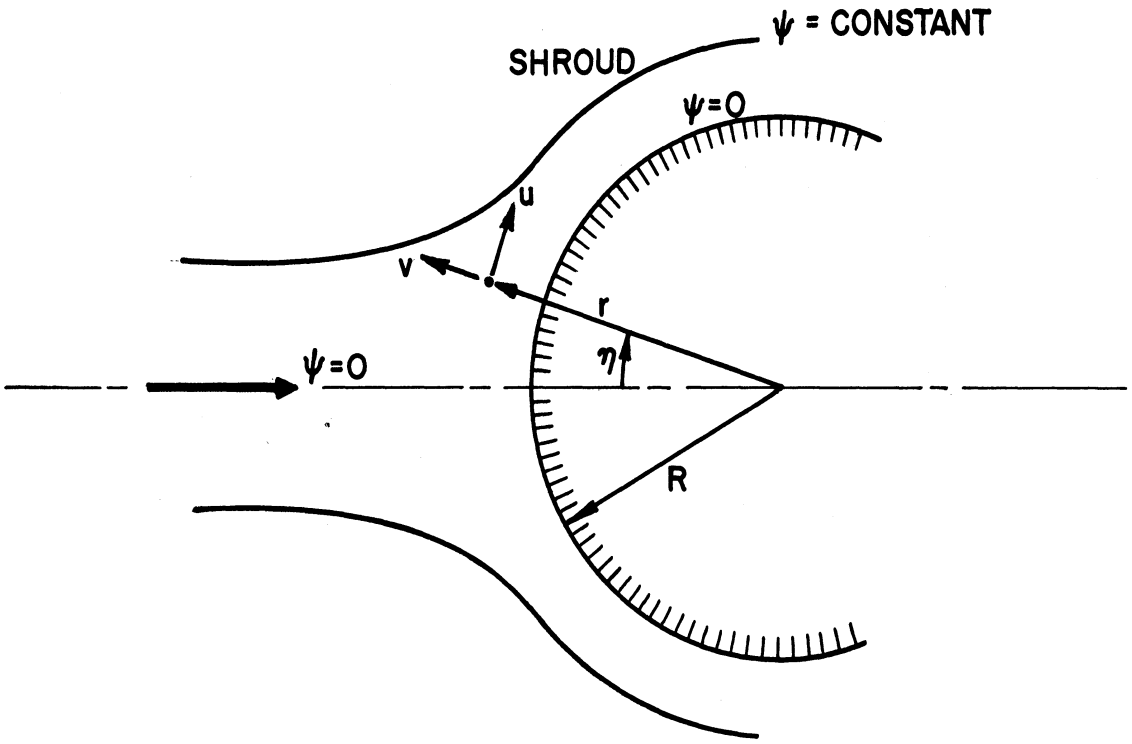

Figure 7. Coordinate System.

hand the problem is to determine the shape of the shroud streamline (Figure 7) such that the hypersonic velocity distribution (Equation 3) will exist over the spherical surface in the range $0 \leq \eta \leq 44^{\circ}$. While we cannot show that the shroud shape so determined represents a unique solution, the agreement with experiment is excellent (see Section V).

The velocity distribution corresponding to Equation 3 is approximated by the first term of its series expansion. Then the boundary conditions on the zero streamline, for $0 \leq \eta \leq \frac{\pi}{4}$ on a sphere of radius R, become

$$\begin{aligned} &\psi(R,\eta) = 0 \\ &\psi(r,0) = 0 \qquad (r \geq R) \\ &\frac{\partial \psi}{\partial r}(R,\eta) = -R\eta \sin\eta\, a_s \sqrt{\frac{2}{\gamma}} = -Rb\eta\sin\eta \end{aligned} \tag{8}$$

Although no straightforward analytical methods appeared to exist for solving Equation 7 with conditions 8, an approximate closed-form solution was obtained by making a few minor simplifications. Since in the range $0 \leq \eta \leq \frac{\pi}{4}$ both $\sin\eta$ and $\cot\eta$ are given to within 1% by the first two terms in their series expansions, Equation 7 becomes, to a high degree of approximation,

$$r^2 \frac{\partial^2 \psi}{\partial r^2} + \frac{\partial^2 \psi}{\partial \eta^2} - \left(\frac{1}{\eta} - \frac{\eta}{3}\right)\frac{\partial \psi}{\partial \eta} = 0 \tag{9}$$

with the boundary conditions

$$\begin{aligned} &\psi(R,\eta) = 0 \qquad (0 \leq \eta \leq \tfrac{\pi}{4}) \\ &\psi(r,0) = 0 \qquad (r \geq R) \\ &\frac{\partial \psi}{\partial r}(R,\eta) = -Rb(\eta^2 - \eta^4/6) \qquad (0 \leq \eta \leq \tfrac{\pi}{4}) \end{aligned} \tag{10}$$

In attempting a power series solution of the form

$$\psi(r,\eta) = \sum_{n=1}^{\infty} a_{2n}(r)\,\eta^{2n} \tag{11}$$

to the above problem, it is found from Equations 10 that the first and third boundary conditions are satisfied if

$$a_{2n}(r) = 0 \qquad (n \geq 3) \tag{12}$$

so that the stream function can be written in the relatively simple form

$$\psi(r,\eta) = a_2(r)\,\eta^2 + a_4(r)\,\eta^4 \tag{13}$$

By substituting Equation 13 into Equation 9 and applying the boundary conditions, Equation 10, the following two simultaneous differential systems result for determining $a_2(r)$ and $a_4(r)$

$$\begin{aligned} r^2 a_2'' + \tfrac{2}{3} a_2 &= -8\, a_4 \\ a_2'(R) &= -Rb \\ a_2(R) &= 0 \end{aligned} \tag{14}$$

and

$$\begin{aligned} r^2 a_4'' + \tfrac{4}{3} a_4 &= 0 \\ a_4'(R) &= \frac{Rb}{6} \\ a_4(R) &= 0 \end{aligned} \tag{15}$$

After solving these equations (Cauchy type) the stream function given by Equation 13 is determined. The final result may be written

$$\psi(r,\eta) = -R^2 b\left(\frac{r}{R}\right)^{1/2}\left\{\left[\sqrt{\frac{108}{5}}\sin\left(\sqrt{\frac{5}{12}}\ln\frac{r}{R}\right) - \sqrt{\frac{48}{13}}\sin\left(\sqrt{\frac{13}{12}}\ln\frac{r}{R}\right)\right]\eta^2 - \left[\frac{1}{\sqrt{39}}\sin\sqrt{\frac{13}{12}}\ln\frac{r}{R}\right]\eta^4\right\} \tag{16}$$

Thus, the (incompressible) shroud contour for any given volume flow is given implicitly by setting ψ = constant in this equation. The shroud contour $\eta = \eta(r)$ is then found by specifying ψ and r and solving the quadratic in η^2 for values of η.

In Figure 8 a scale drawing of the shroud based on the above analysis is shown. Corrections for the effects of compressibility, as mentioned above, have been incorporated. The figure shows that the effect of compressibility is appreciable only in the immediate vicinity and downstream of the sonic point $\eta = 44^\circ$. For $\eta > 45^\circ$, the gap between the shroud and the sphere surface is slightly greater than that specified by theory. This increase in gap was provided so that boundary layer growth would not influence the position of the sonic point.

NOTE:
DOTTED LINE INDICATES SHROUD CONFIGURATION
BASED ON INCOMPRESSIBLE FLOW.

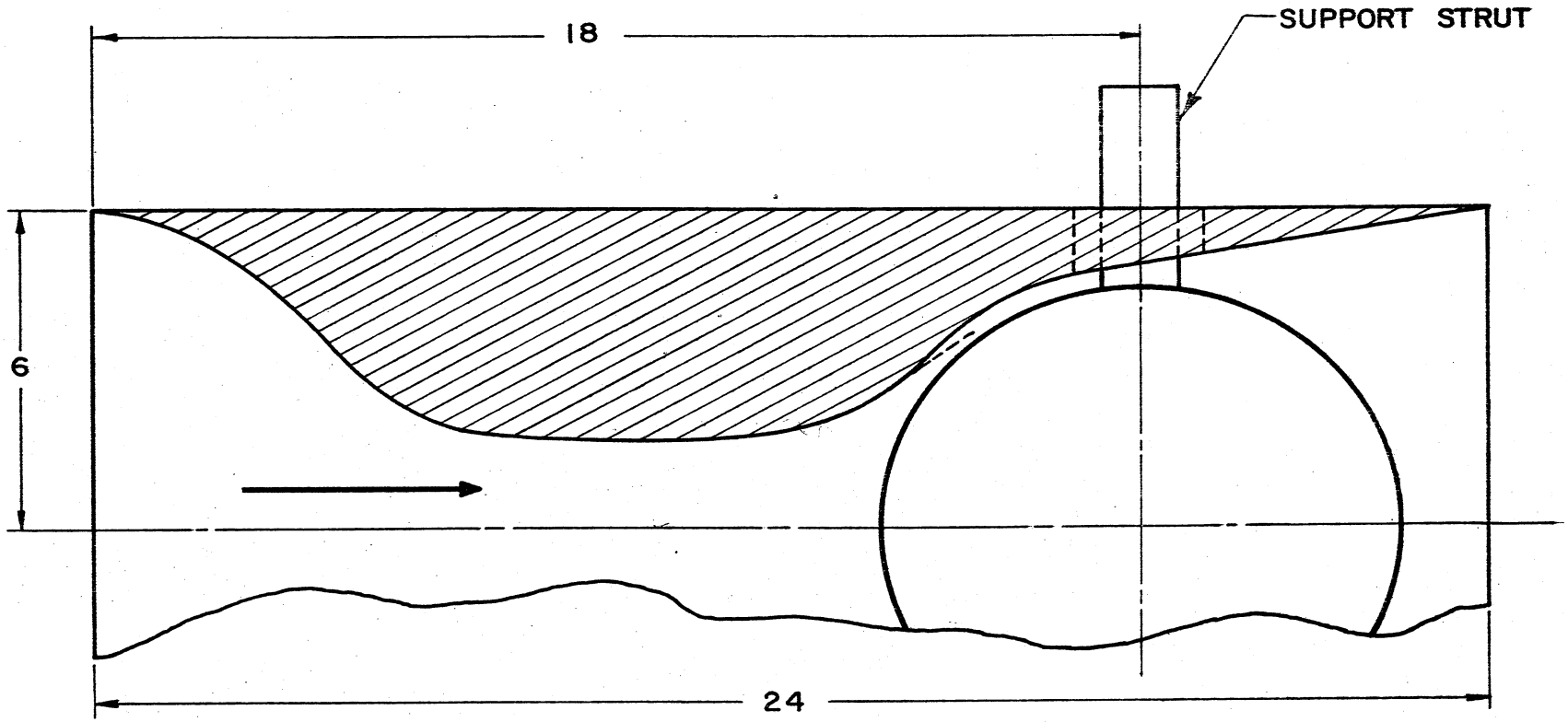

Figure 8. Aluminum Shroud Configuration with Sphere in Place
(Dimensions in Inches)

IV. EXPERIMENTAL APPARATUS AND METHODS

General Wind Tunnel Facility

A schematic diagram showing the general layout and construction of the wind tunnel facility is given in Figure 9. This facility was erected at the Aeronautical Engineering Laboratories of the Department of Aeronautical and Astronautical Engineering, University of Michigan. As indicated in the figure, two air supplies and exhaust systems have been employed. Stagnation pressures of one atmosphere and less can be obtained by using air from a 15,000 cubic foot dry air storage and exhausting into vacuum tanks having a total volume of 13,000 cubic feet. Pressures up to 8.5 atmospheres (structural limit of the tunnel) can be obtained by regulating from a 375 cubic foot 2500 psi. high pressure system and exhausting into either the vacuum tanks or the atmosphere. Both air supplies are unheated.

Air dryers in both systems use activated alumina as the desiccant. The lowest dewpoints obtainable with the atmospheric supply, as well as the length of time they can be maintained, are quite dependent on the atmospheric humidity. Practical dewpoint temperatures range from $-40^{\circ}F$ in the summer to $-60^{\circ}F$ in the winter with this system. In contrast, the high pressure dryer, the installation of which was brought about during the present investigation, is independent of atmospheric conditions and is capable of lower dewpoints. Dewpoints in the range $-70^{\circ}F$ to $-100^{\circ}F$ (measured at one atmosphere pressure), corresponding to specific humidities of 1.8×10^{-5} to 8.9×10^{-7} pounds of water vapor per

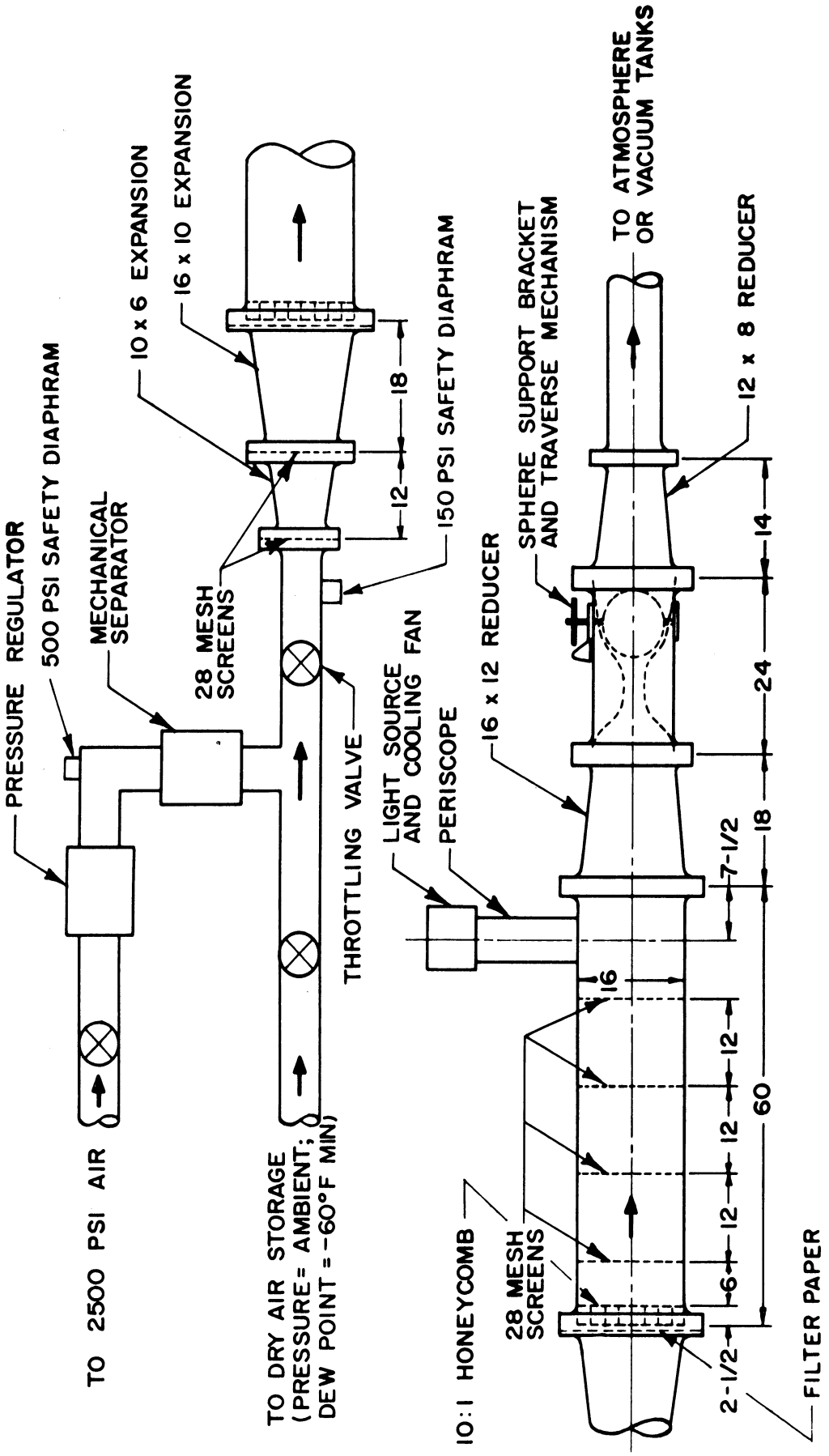

Figure 9. Schematic Diagram of Air Supply System and Wind Tunnel Layout.

pound of air, were usually obtained. No provisions are incorporated for removing carbon dioxide from the air.*

The supply air is throttled, Figure 9, to produce stagnation pressures between 0.1 and 8.5 atmospheres. Steady flow conditions could be established in minimum times of about one second with the atmospheric supply and two to three seconds with the high pressure system. When the high pressure supply is used the air passes through a mechanical separator which traps large scale rust and dirt (95% of all particles larger than 10 microns in size, according to the manufacturer) which may have accumulated in the storage tanks and lines prior to the dryer installation.

After pressure regulation, the air enters a 16-inch diameter 5-foot long settling chamber through the diffusers shown. Screens are provided at the junction of the two diffusers to prevent flow separation. The settling chamber contains a 10:1 (length to width ratio of the cells) honeycomb, $2\frac{1}{2}$ inches thick, four 28-mesh screens of .0065" wire

* Air samples taken from the high pressure supply showed a condensation temperature for dry ice of approximately -230°F which corresponds closely to that predicted on the basis of the carbon dioxide content in the standard atmosphere (.03% by volume). However, several analyses of the compressed air showed that the CO_2 content varied up to as much as 30 times that in the atmosphere. The corresponding "specific humidity" for CO_2 ranged from 4.5×10^{-4} to 1.5×10^{-2} pounds of CO_2 vapor per pound of air, so that for the limiting temperatures in these tests (condensation of liquid oxygen around -300°F, depending on the pressure) the problem of frost build-up on the model surface was of minor importance compared to the condensation of CO_2 in affecting boundary-layer transition. A discussion of the effects of frost and CO_2 on transition is given in the Results and Discussion, Section V.

diameter, and a paper dust-filter* at the entrance. After passing through the 2-foot long test section the air is exhausted to either the atmosphere or vacuum tanks, depending on the pressure level. A scale drawing of the test section interior showing the shroud contour and sphere is given in Figure 8.

Figure 10 is a photograph of the wind tunnel. The reducer downstream of the test section can be unbolted and lifted out of position, as shown, providing access to the model and its instrumentation. The photograph also shows a travelling periscope mounted on the downstream end of the settling chamber. The general construction and operation of this device is sketched in Figure 11. The main purpose of the periscope, whose field of view covers a region up to 20° from the stagnation point, is to provide a means of checking for ice and carbon dioxide formation on the sphere. It is also a convenient device for determining accurately when an instrument on the surface is at the stagnation point. When flow measurements are being made the periscope is retracted so that the bottom is flush with the wall of the settling chamber.

The tunnel weight flow (in pounds per second), based on measured velocities in the settling chamber, is approximately .17 times the stagnation pressure (in pounds per square inch absolute) for the

---

* The purpose of the filter is to remove fine scale rust and dirt not trapped by the mechanical separator. The paper, called 5 ply Airmat, is manufactured by the American Air Filter Co., Louisville 8, Kentucky. The dynamic pressure at the filter was 10,000 to 50,000 times that for which it is normally used so that it had to be backed by screens to provide physical strength. It was found necessary to remove the oil normally in the filter since the particles which did get through would stick to the model quite readily. A surprising amount of rust was stopped by the filter under these circumstances.

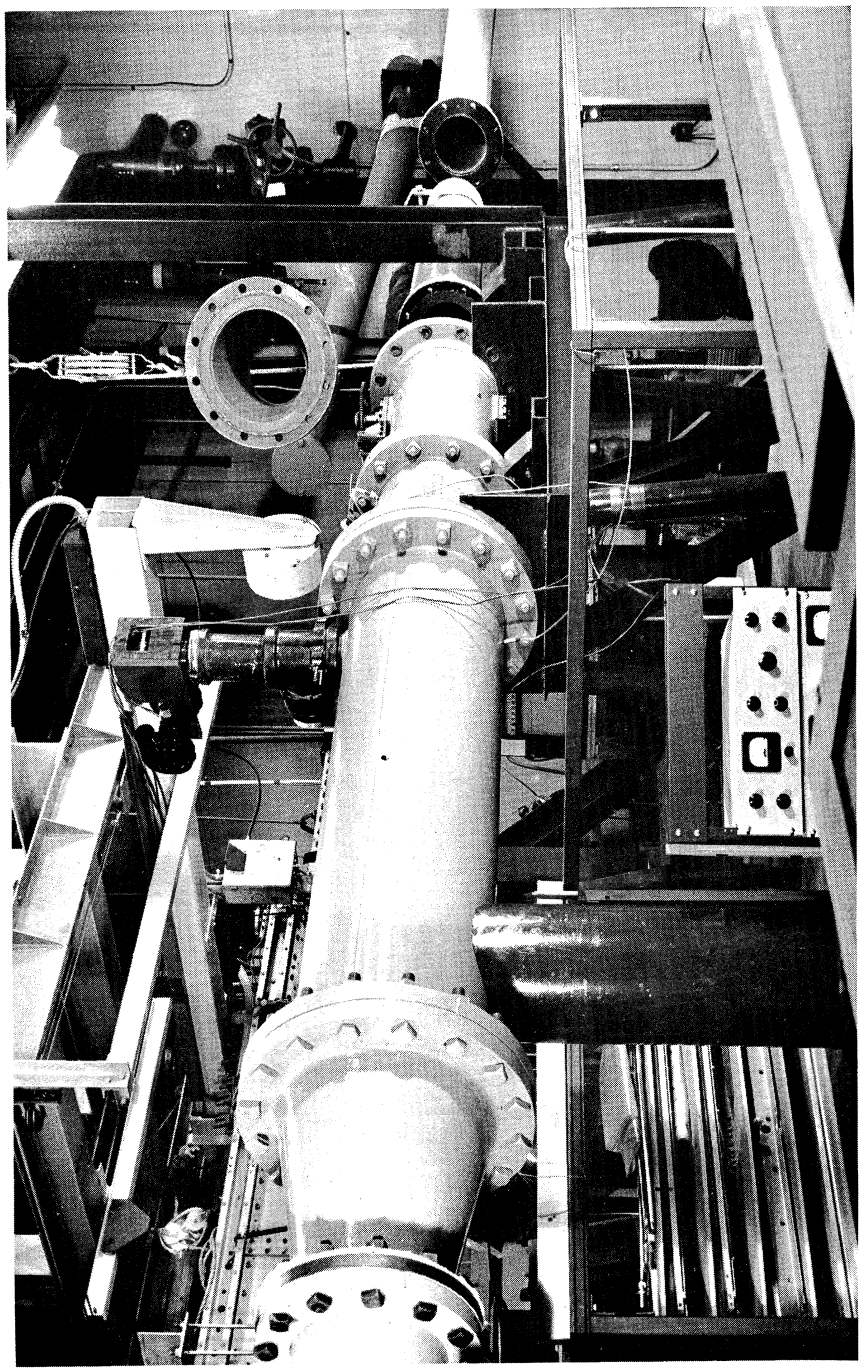

Figure 10. Photograph of Wind Tunnel

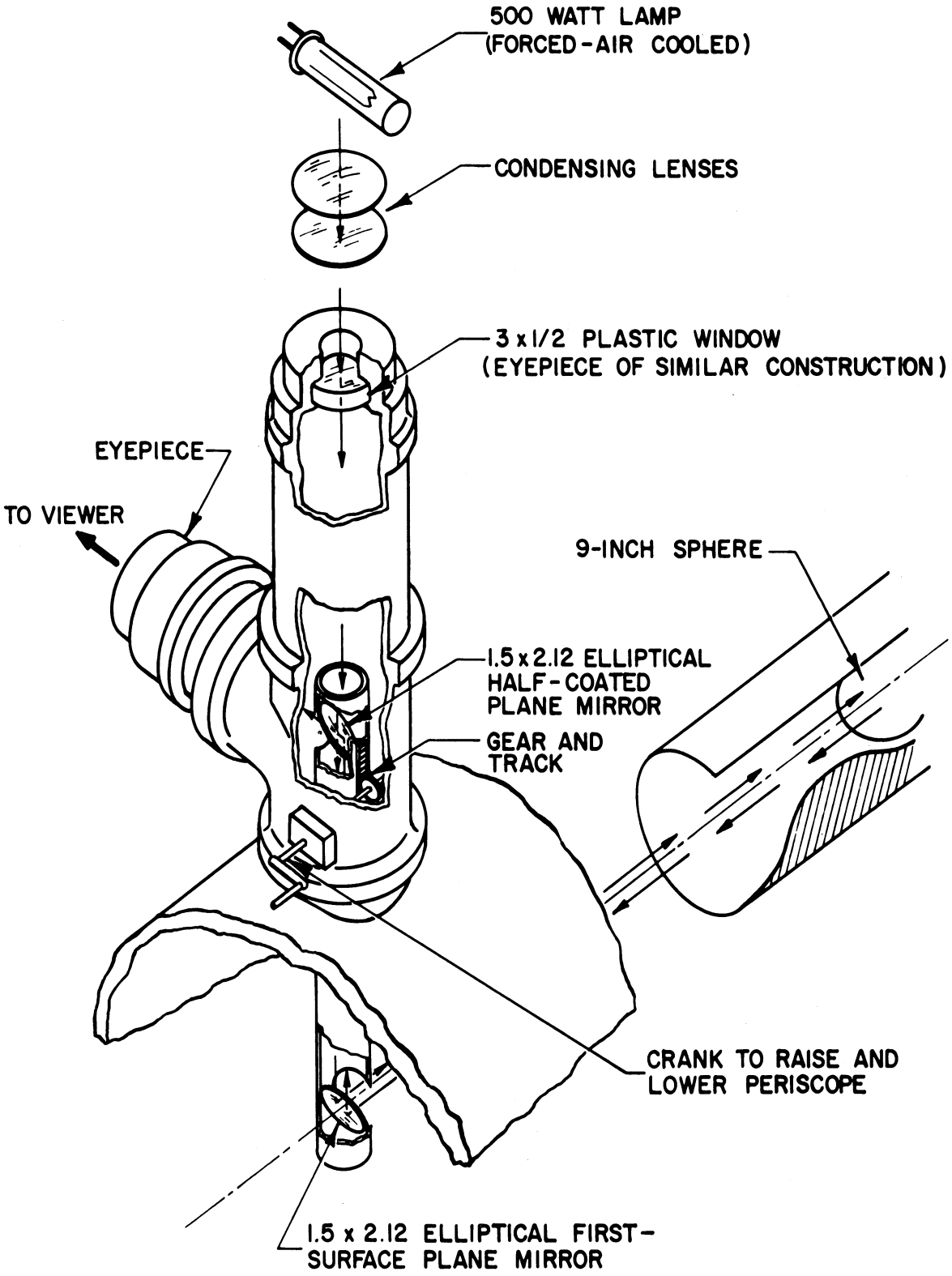

Figure 11. General Construction of Traveling Periscope.

conditions of the experiments. At the maximum allowable tunnel pressure of 125 psi, the high pressure storage system, containing approximately 4700 pounds of air at 2500 psi and 70°F, would be emptied in 3.3 minutes. This represents the minimum length of run for the facility. When running from the atmospheric supply the vacuum tanks limit the length of run with chocked flow to about 9 minutes, nearly independent of stagnation pressure.

A Bourdon-type gage, a 60-inch mercury manometer, and strain-gage-type transducers were used separately and in conjunction, where applicable or necessary, to measure and record tunnel stagnation pressures. A thermocouple upstream of the settling chamber was used to measure stagnation temperatures. The sphere and its associated instrumentation are discussed below.

Sphere and Associated Instrumentation

The 9-inch diameter sphere was machined in two hemispheres from solid 60/40 brass forgings. The purpose of this method, as opposed to casting the hemispheres, was to avoid, as much as possible, gas holes in the final machined surface. The wall thickness is 1/4 inch except in the region of the support struts where it gradually increases to a maximum thickness of 3/4 inch. The installation of the sphere in the shroud permits fore and aft movement of $\pm$1/4 inch. By means of this adjustment the pressure distribution on the hemisphere can be varied somewhat from the Newtonian case. This was not done, however, in the present study.

Six copper-constantan thermocouples are installed within 0.020 inches of the outside surface at 10° intervals, as shown in

Figure 12. Also shown in this figure is the location and construction of two hot-wire probes and a pressure tap. The purpose of using two hot-wires was to measure correlations of the fluctuations at the stagnation point outside the boundary layer. When boundary-layer disturbances were being studied the wire nearest the thermocouples was removed and a plug inserted in its place. The second wire was then turned 180° so that any roughness caused by the plug or thermocouples would be downstream and therefore would not influence the measurements.

Originally it was planned to use both the thermocouples and the hot-wire to detect boundary-layer transition. The thermocouples were installed before the final .010 inch was machined from the surface so that a smooth finish would result after final machining. However, this did not happen. Several gas pockets formed at the constantan connection, appearing as deep pits after machining. Also, the action of the lathe cutting tool was such that a slight depression existed in the softer soldered region. This is illustrated in Figure 13 which shows a profilometer tracing* across one of the thermocouple junctions. Subsequent methods of filling the depressions, such as by soldering or copper plating and then polishing, were not considered satisfactory in view of the importance of roughness in these experiments. Thus, the thermocouples were used mainly as a means for measuring the surface temperature as a function of time during the cooling and heating

---

* All profilometer measurements reported in this paper were made courtesy of the Micrometrical Manufacturing Company, Ann Arbor, Michigan.

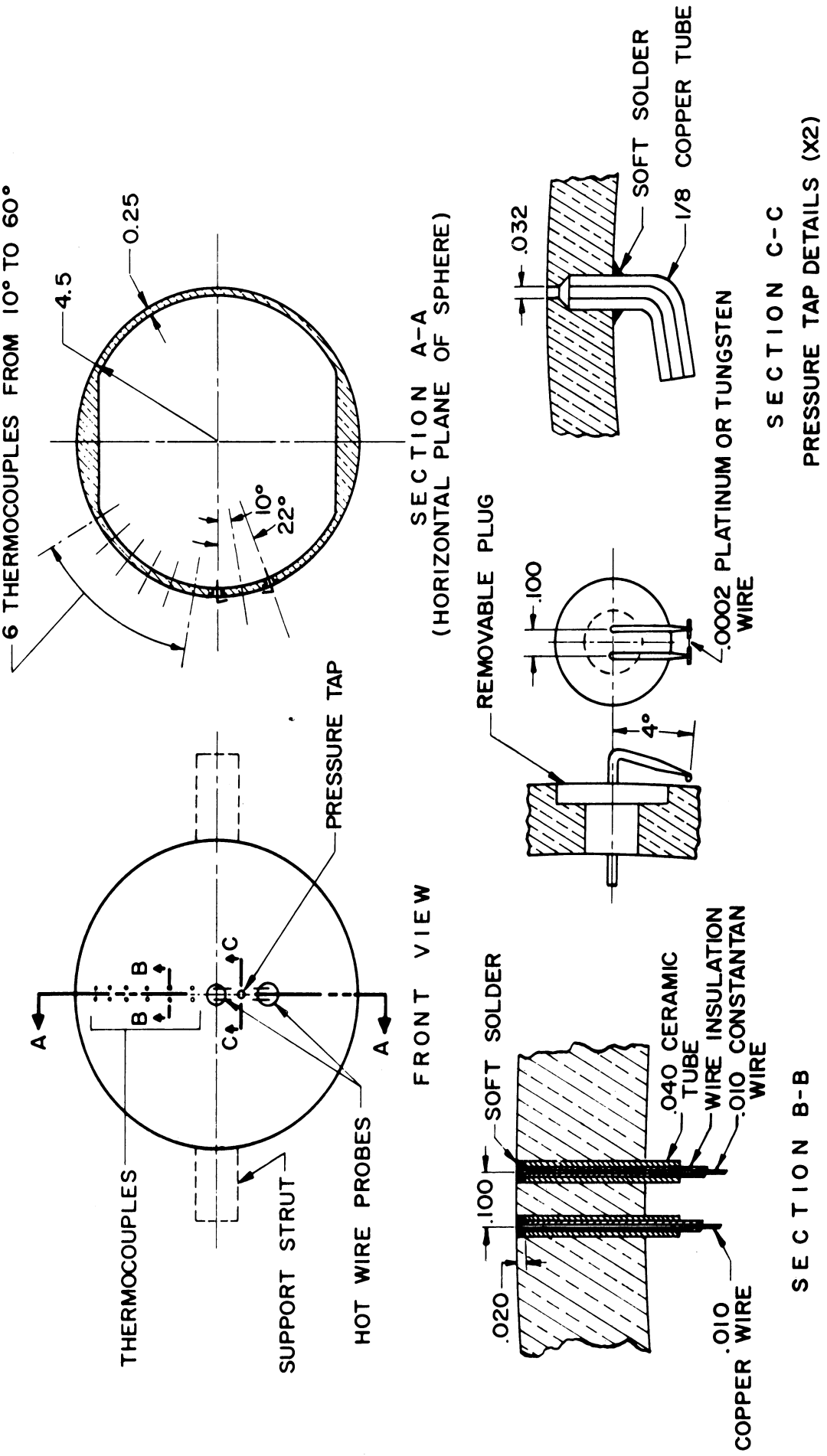

Figure 12. Details of Sphere Instrumentation. All Dimensions in inches.

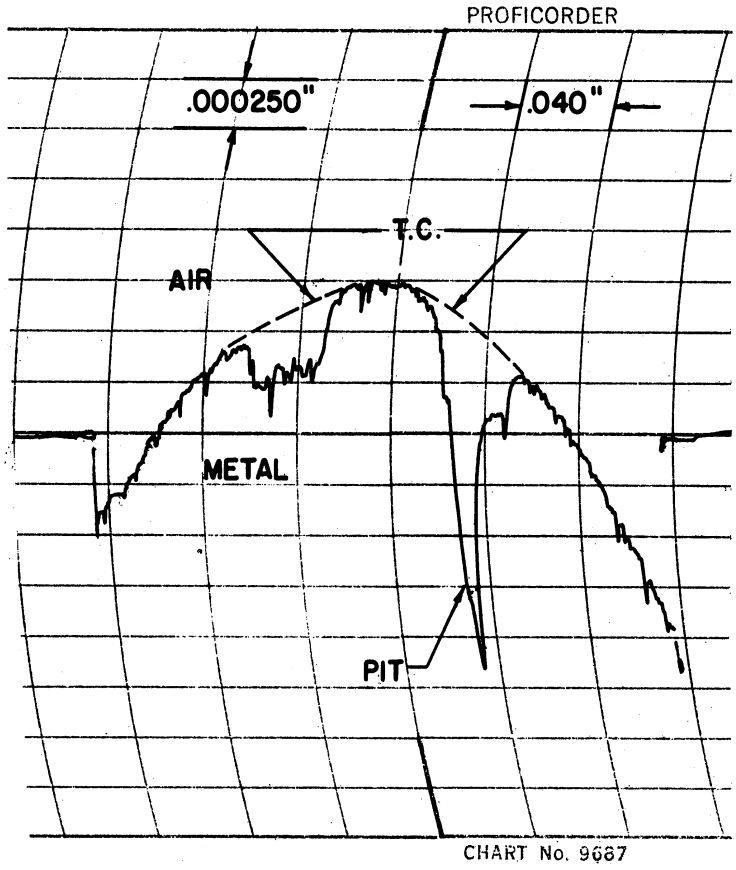

Figure 13. Profilometer Tracing Across Thermocouple.

periods of a test. When transition experiments were conducted, these surface thermocouples were always downstream of the measuring station.

Use of the hot-wire anemometer to obtain quantitative information concerning boundary-layer fluctuations presented an extremely difficult experimental problem in the present case. Immersed in the cooled boundary layer between the stagnation point and the sonic position ($\eta = 44^{\circ}$), the hot-wire can experience a wide range of "local free-stream" conditions upon which its response will depend; viz., Nusselt number, Reynolds number, Mach number, and stagnation temperature. In general, a hot-wire in compressible flow* is sensitive to fluctuations in velocity, temperature, and density, and its mean square output is dependent, in addition, on cross correlations between these variables. When viewed in terms of vorticity, entropy, and sound, the number of unknown quantities making up a single measurement can usually be reduced from six to three or four by neglecting correlations between sound and entropy or vorticity and in the proper circumstances by neglecting sound altogether. To extract a single fluctuation, then, requires at least three or four measurements for which the sensitivities to the various fluctuations are varied between measurements by varying the wire heating. For a given wire, these sensitivities generally depend on the local Nusselt number, Mach number, Reynolds number, recovery factor, (nonlinear) variation of wire resistance with temperature, temperature loading, and various derivatives between these variables. Because the dependence on the above variables can vary

* Reference (40) gives an excellent discussion of the hot-wire in compressible flow.

greatly among individual wires (end loss effect and method of construction) a given wire must first be subjected to a series of calibration tests. Thus, preparing a wire to make measurements and extracting information in a compressible flow is not an easy task - especially in view of the breakage which is often encountered.

In the present application the real difficulty comes in knowing what the conditions are at the wire. Assuming (machine) calculations have been made so that the boundary-layer variables are known as a function of space and time while the model heats up, it is then necessary to know exactly where the wire is in the boundary layer and to be able to place it back in the same position if it should break. The difficulty here is due to the thinness of the boundary layer which varied from about .002 to .008 inches in the range of conditions tested.

In view of the expected difficulties in seeking quantitative information of fluctuations in the boundary layer, the hot wire was used in these initial investigations as a tool for viewing the overall type of fluctuations (regular or random) present and their relative amplitudes at various angular stations and under different conditions of boundary-layer cooling. It also served to measure "free-stream" turbulence distributions and for measurements of the "free-stream" velocity correlations at the stagnation point. A Shapiro-Edwards hot-wire set was used in conjunction with an oscilloscope and tape recorder for viewing and recording the signals.

Even as a qualitative instrument the high mortality of the hot-wires at relatively low dynamic pressures made it desirable

to seek a more rugged instrument. Since the thermocouple method had been abandoned and no windows existed in the tunnel, a surface pitot-tube appeared to be the next possibility as a transition probe. Such an instrument was developed to detect the increase in total pressure near the surface when transition occurred.

This instrument is called a Stanton-tube when the ratio of tube height to boundary-layer thickness is small, and can be used to measure skin friction at the surface.* The small thickness of the boundary layer under consideration made it impractical to satisfy this requirement so that the tube served only as a transition indicator. Even to serve this function it was necessary to make the height of the probe as small as possible, consistent with a reasonable response time, if it was to be fairly sensitive to transition. The lower limit on size was determined mainly by physical limitations in construction.

Figure 14 shows the size and construction of the pitot-tube, a static tube beside it, and the pressure leads. The tube was made by copper plating a horseshoe shape around a static pressure tap, inserting a .001-inch brass shim painted with silver conducting paint, and then plating a thin cover. After removing the spacer the paint was dissolved by sucking a thinner through the opening. The 1/2-inch copper tubing was placed around the 1/8-inch pressure leads to insulate them from the liquid nitrogen which filled the inside of the sphere. Before this was done, liquid oxygen would form inside the pressure leads and cause

* See Reference 41 for example.

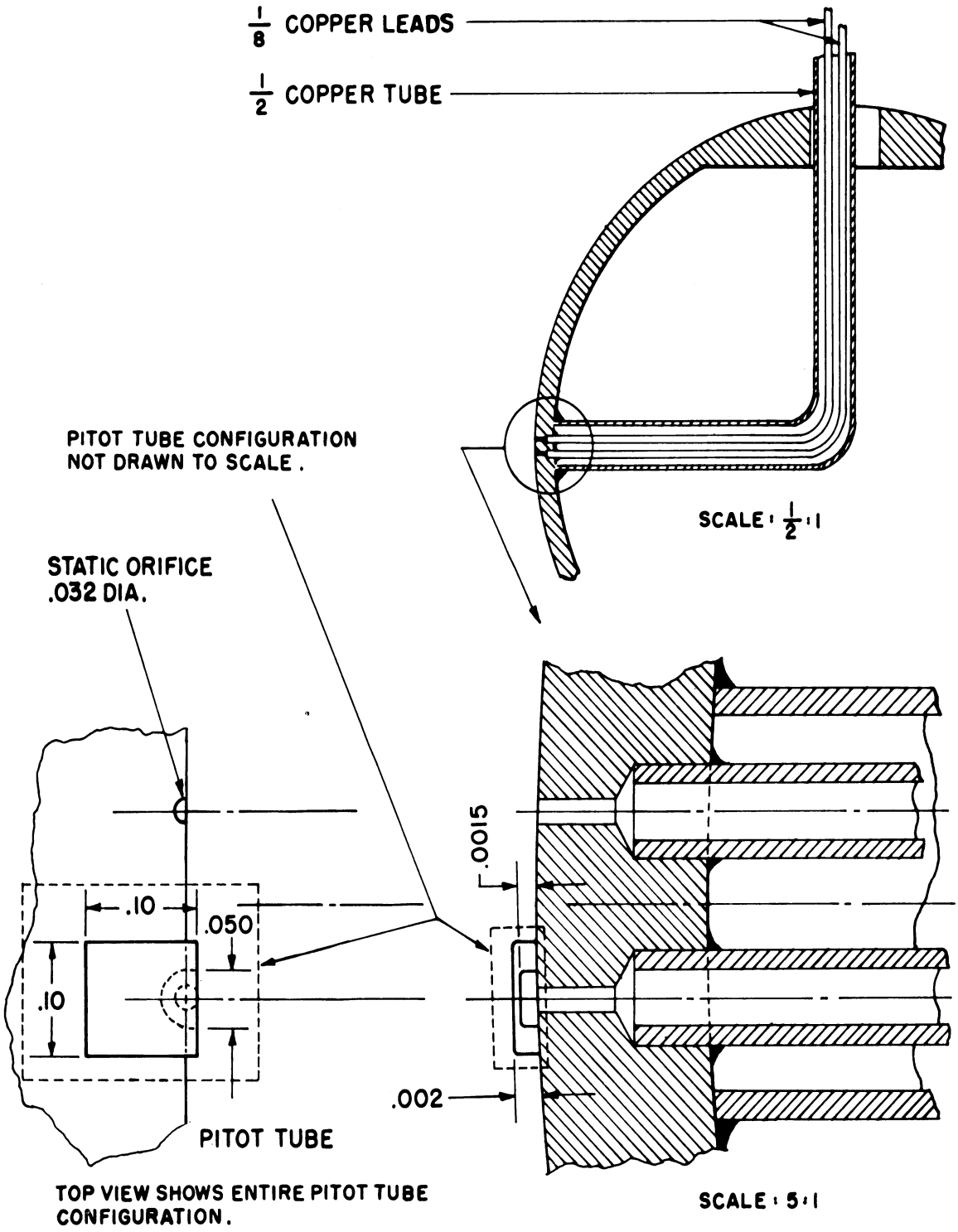

Figure 14. Size and Construction of Pitot and Static Pressure Probes.

erratic readings. The static and pitot pressures were measured differentially by a strain-gage-type pressure transducer whose output was measured continuously on Sanborn pen recorders.

A schematic diagram showing the method used to cool the sphere, together with a typical thermocouple circuit, is given in Figure 15. Two coolants, dry ice mixed with acetone and liquid nitrogen, were used. The corresponding minimum wall temperatures attainable were -110°F with dry ice-acetone and -320°F with liquid nitrogen. The dry ice-acetone mixture was emptied into the sphere by hand and removed with a vacuum pump. Liquid nitrogen was pumped into the model from a self pressurizing (22 psi) 110 liter container and left to evaporate at the end of a run.

The cooling procedure consisted of filling the sphere until the desired initial temperature was reached and then starting the tunnel. While pre-cooling to the lowest temperatures, the model would be exposed to the essentially stagnant dry air in the tunnel for a few minutes during which the surface temperature was below the dewpoint temperature of the air. For a dewpoint of -75°F the total amount of water in the air contained by the tunnel is about 10^{-5} pounds. Even assuming all of this water could deposit on the surface only results in a uniform layer about 10^{-6} inches thick. Therefore, water condensation prior to a run was not considered to be of importance in influencing the data taken*. Examination of the stagnation point

* Of more importance is the condensation of CO_2 that may take place while steady flow conditions are being established during start up. This is discussed in Section V.

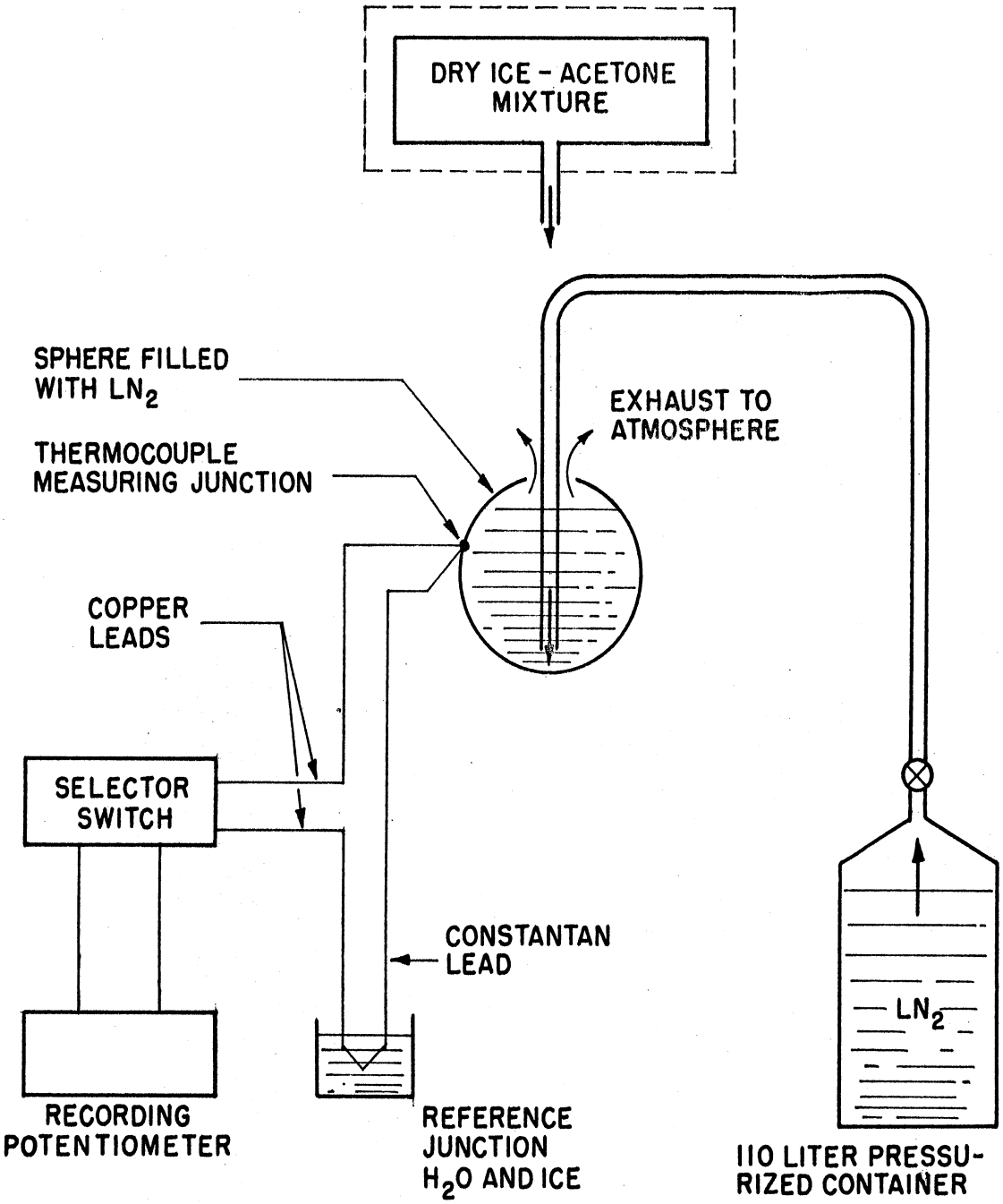

Figure 15. Schematic Diagram of Cooling Procedure and Thermocouple Circuit.

region of the surface through the periscope never showed any visible evidence of frost just prior to starting the tunnel. Actually, when the air dewpoint was about -70°F or less, a minute or so of run time was required before the frost was visible. However, if a relatively short run was made the sphere would be allowed to warm to a temperature above the air dewpoint before making a second run.

The internal cooling of the model was not forced but depended on the natural heat transfer from the coolant reservoir inside. Although this reservoir could be maintained during a run, the heat transfer from the air was usually much greater than that to either the dry ice-acetone or liquid nitrogen so that the surface temperature would increase as the run progressed. For the coldest tests the temperature rise was of the order of 5 to 10°F/sec at the stagnation point for the first 10 to 15 seconds.

Preparation and Inspection of Model Surface

In many experimental boundary-layer studies the combination of Reynolds number, Mach number and body lengths are such that the boundary-layer thickness is large enough so that the avoidance of roughness effects on transition does not require a highly polished surface. High Reynolds numbers per unit length, which tend to reduce this thickness, are usually associated with high Mach numbers, which have the opposite effect. One important exception is the case at hand, that is, boundary layer studies on blunt bodies in hypersonic flow. Here the unit Reynolds numbers are relatively high because of the high "free-stream" Mach number while the Mach numbers at the edge of the boundary layer are low near the nose. Thus, typical boundary layer thicknesses

on the 9-inch hemispherical nose were only a few thousands of an inch. Since the effect of boundary-layer cooling is to cause a given roughness height to be even more effective in promoting transition it becomes a necessity to pay close attention to the surface finish.

Mechanical hand polishing was the method used for preparing the surface after final machining. The entire hemisphere was sanded and rough polished until no deep scratches could be seen. The final polish was concentrated only in a region bisected by the meridian on which the measurements were made. This region was considerably larger than the "transverse contamination zone", in which transition caused by roughness at the edge of the zone would spread to the measurement meridian within the latitude range of the tests. A conservative estimate for this half angle of spread of transition was taken to be 10°.

Chromic oxide and aluminum oxide, having particle sizes ranging from 15 microns initially down to 0.1 microns for the last polish, were used in the final polishing stages. It was found that special care had to be taken in applying the final polish to the brass surface in order to avoid so-called relief polishing, wherein the grain structure of the hard and soft phases polish at different rates and give an etching effect, which can result in significant surface roughness. The relief polishing was kept at a minimum by using a cloth without nap, such as silk, for most of the polishing operations, and polishing only a short time with the softest cloths to take out scratches made with the silk. There is, then, a limit other than time to which an alloy such as brass can be polished. If one continues to polish

with the finest powders and softest cloths available, relief polishing will begin to appear before "all" scratches from the harder cloths containing no nap have been obliterated.

Figures 16 and 17 show photomicrographs* and profilometer tracings, respectively, which illustrate the type of surface obtained where relief polishing resulted compared to that finally obtained using the polishing procedure outlined above. Both surfaces had been polished to the point where no scratches were visible to the naked eye. Figure 16a was made with the microscope and lighting directed normal to the surface, while the lighting in Figure 16b was directed at a slight angle to the surface normal so as to accentuate the ruggedness of the relief polish. The grain structure is still visible in Figure 16a but shows up mainly due to the differential staining of the phases rather than differential height and shape. The black spots are apparently blow holes in the surface. These photographs and profile tracings show a considerable difference in surface roughness between the two polishing techniques.

Both microscopic examinations and profilometer tracings were used to inspect the surface finish. The stylus used with the profilometer was .0007 inches in diameter and had 1 gram of applied pressure. The traces were, of course, carried out in a region where the groves due to the stylus could not influence transition at the position of measure-

---

* All photomicrographs were made through the courtesy of Mr. A. M. Rickel of the Bendix Corporation Research Laboratories, Detroit, Michigan.

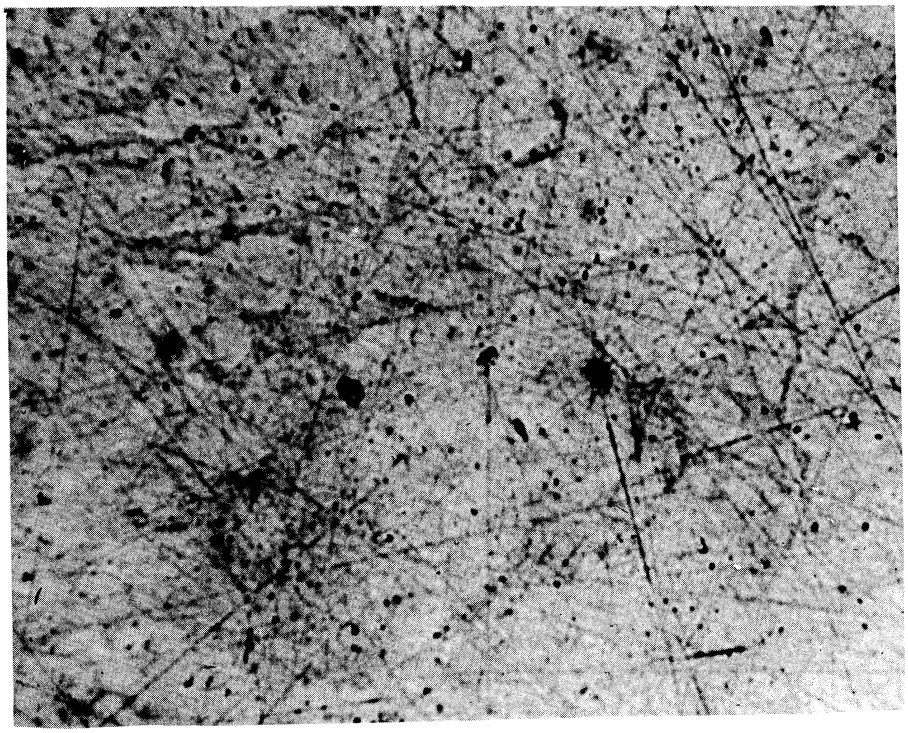

a. no relief

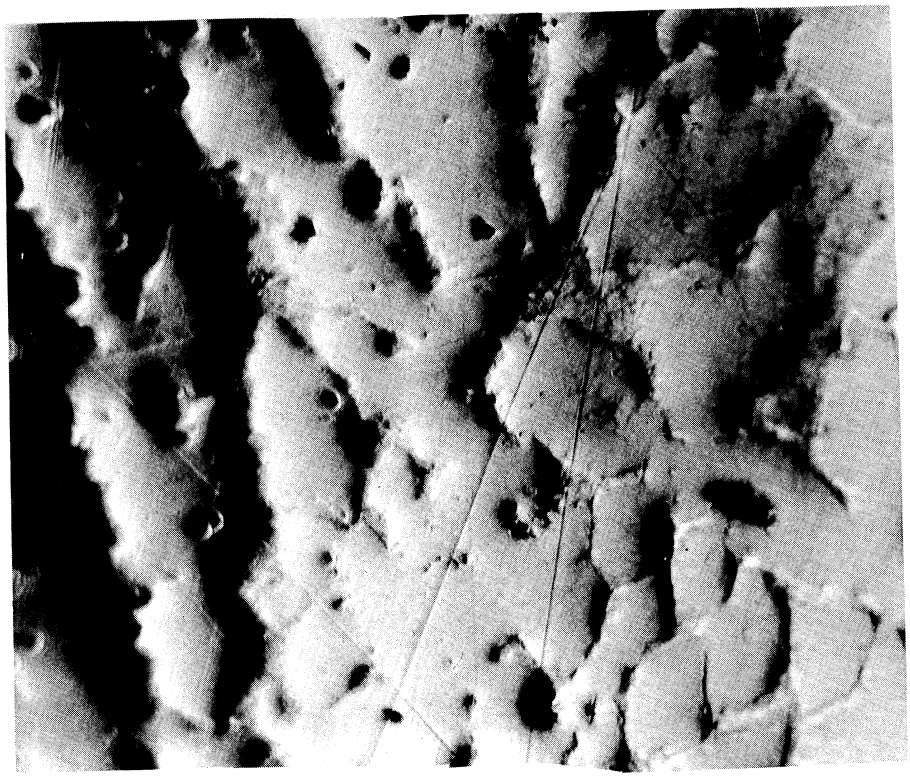

b. relief

Figure 16. Photomicrographs of Surface at a Magnification of 350

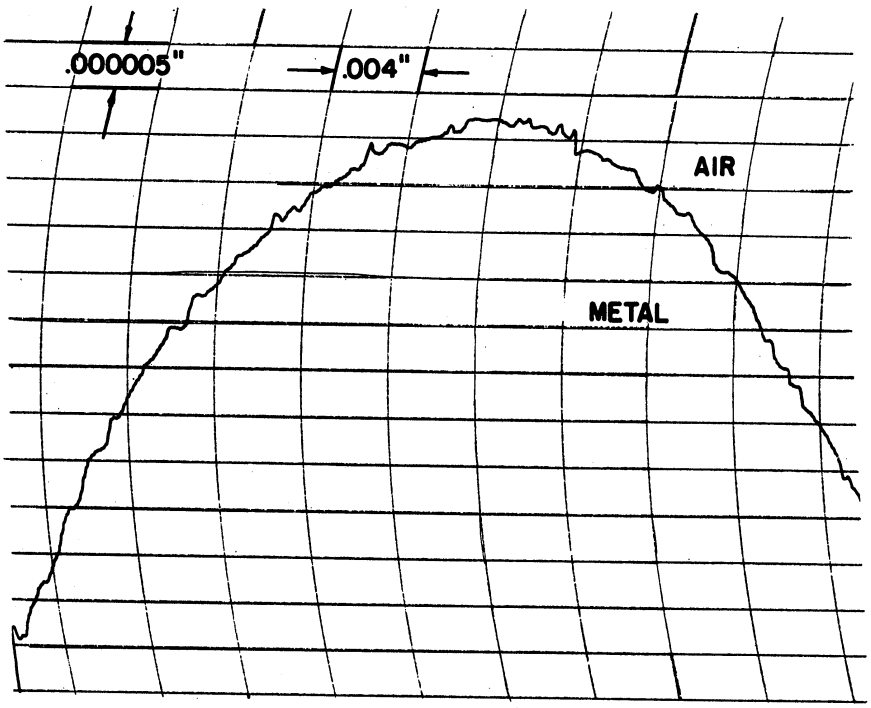

a) NO RELIEF

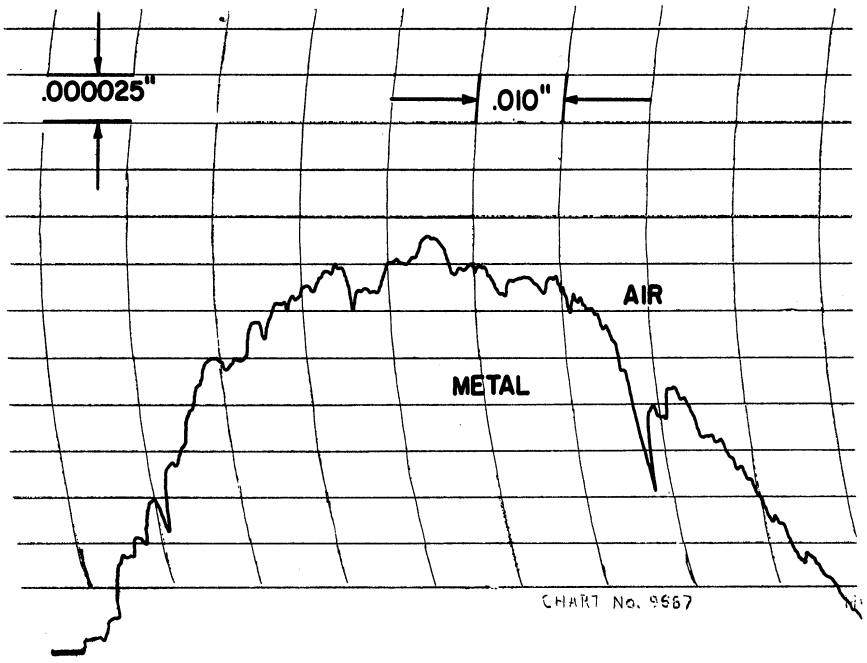

b) RELIEF

Figure 17. Profilometer Tracings of Surface.

ment. One or two traces were assumed to be typical of the entire polished surface prior to placing the model in the wind tunnel.

The best surface obtained had an rms roughness less than one microinch according to profilometer measurements, Figure 17a. Although this is undoubtedly on the low side due to deficiencies of this type of instrument on very smooth surfaces[42], it is indicative of a high quality finish. In this report, rms roughness reported in connection with the present study were those obtained with a profilometer. It should be pointed out that an rms roughness measurement on a "smooth" surface, regardless of how accurate the method used in obtaining it, is very often only indicitive of the care used in polishing rather than an important aerodynamic parameter characterizing the roughness. That is, the relatively few scratches, pits, and protrusions often present during and after, if not before, a wind tunnel test may be of much more significance in effecting boundary-layer transition than the many smaller irregularities which usually make up the sample rms measurement.

During tests with the smoothest surface some microscopic inspections were made of small dust particles deposited near the stagnation point. These are discussed with the experimental results which follow.

V. RESULTS AND DISCUSSION

The experimental results to be described below are presented in three parts. First are the tests which check and describe the "environmental" conditions under which the boundary-layer transition studies were conducted. They include the surface pressure distribution on the sphere resulting from the shroud technique, turbulence levels in the wind tunnel and outside the boundary layer on the model, correlation measurements between velocity fluctuations at the stagnation point, and temperature-time histories of the model surface during tests with boundary-layer cooling.

The second and third parts are concerned with the investigations of transition in moderately cooled boundary layers. When these studies were first begun the pressure range was limited to a maximum of one atmosphere while the high pressure driers and dirt separators were being installed. Accordingly, a series of preliminary experiments were run at a constant stagnation Reynolds number, $R_{e_s} = \frac{\rho_s a_s D}{\mu_s}$, of approximately 4.3×10^6. Dry ice and acetone was used as the coolant so that the minimum ratio of wall temperature to stagnation temperature was about 0.72. The hot-wire anemometer served to determine the character of fluctuations in the boundary layer. Although "natural" transition was not observed in the subsonic boundary layer under these conditions, some experiments were made to ascertain the effects of boundary-layer cooling on the disturbances caused by various two-and three-dimensional single roughness elements glued to the surface.

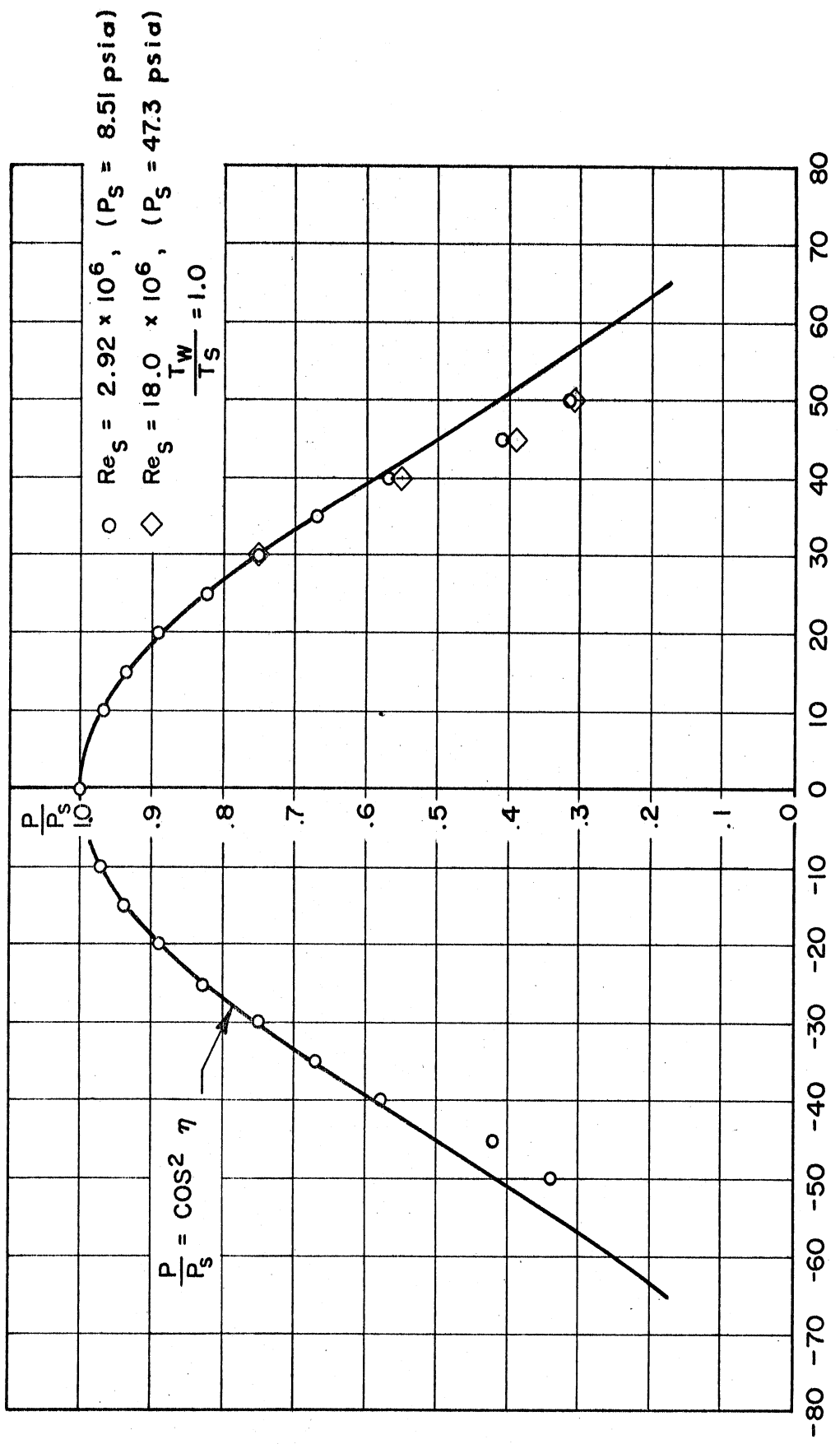

Figure 18. Measured Pressure Distribution on 9-inch Diameter Sphere.

occur a few degrees ahead of the theoretical position ($\eta = 43.8^{\circ}$). This error is probably a result of the simple one-dimensional correction used in the neighborhood of the sonic point. That is, the deviation from one-dimensional flow, due to the curving boundaries of the shroud and sphere, causes the sonic line near the sphere to move upstream of the minimum area.

While pressure distribution measurements were being made, a one percent low frequency oscillation in stagnation chamber pressure was observed. This was traced to intermittent separation in a curved inlet pipe which in turn was coupled with an unsteadiness in an upstream valve. After eliminating this fluctuation the turbulence level distribution at the shroud inlet was that shown in Figure 19. Measurements of the velocity profile are also shown. The rms mainstream velocity fluctuations in the axial direction are about 0.3% of the centerline velocity. A turbulent boundary layer extending about 2 1/2 inches from the wall is also apparent.

The turbulence level is reduced considerably as the flow passes over the nose of the sphere. Measurement in the "free-stream" outside the boundary layer, at a height of .071 inches from the surface, showed the rms streamwise velocity fluctuations to be less than 0.1% of the local velocity in the range $7^{\circ} \leq \eta \leq 46^{\circ}$. Although the gap between the shroud and sphere reaches a minimum of 3/8 of an inch in the sonic region, the shroud boundary layer, 2 1/2 inch thick in the settling chamber, does not appear to introduce unreasonable values of "free-stream" turbulence in the range of the investigation. The relatively low "free-stream" turbulence level is important particularly

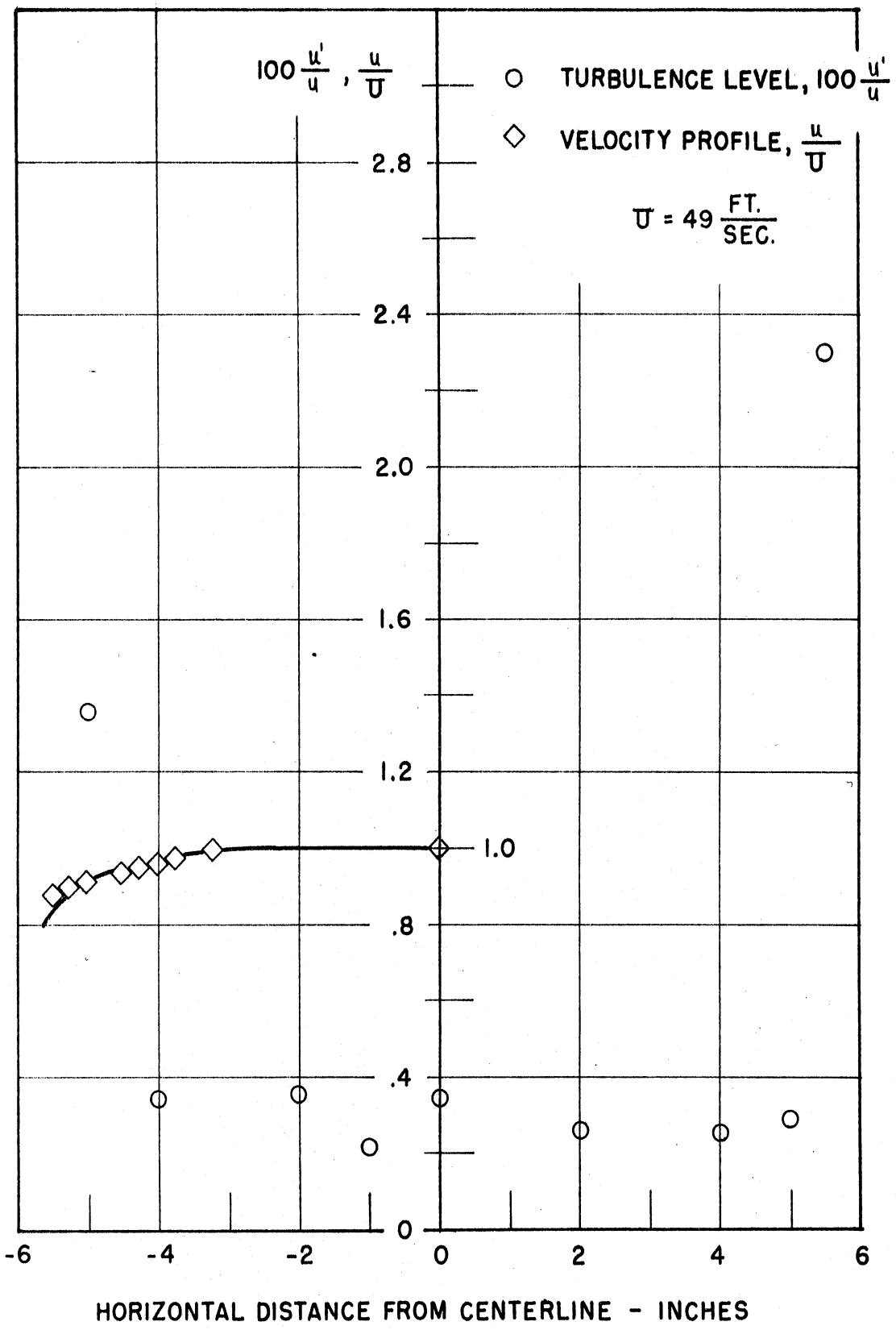

Figure 19. Turbulence Level and Velocity Distribution in the Settling Chamber.

because no quantitative information of the effect of "free-stream" turbulence on transition, pertaining to the present study, is available at present.

Recent measurements by Kuethe, Willmarth, and Crocker[43,44] of the correlation between velocity fluctuations on opposite sides of the nose of hemispheres have shown the occurence of a random, low frequency, stagnation point motion. In subsonic flow, they found high negative correlations to exist at $\pm 7^{o}$ from the stagnation point when the hot-wire frequency band was 0.1 to 20,000 cps. At $M_{\infty} = 2.44$ nearly zero correlation was reported for the frequency range 10 to 20,000 cps, although significant negative correlation did exist when the frequency band was restricted to the range 0.1 to 50 cps.

Of basic interest in itself, the stagnation point motion is also significant since it represents a source of disturbance to the boundary layer flow which could be of importance in the transition process. In the present shrouded sphere tests the correlation was measured at the same angular position, $\pm 7^{o}$, with the hot wires .05 inches from the surface. Measurements were made with the wire compensated to respond in the frequency range 0.1 to 20,000 cps and without compensation which limited the high frequency response to about 300 cps. In these frequency bands, no appreciable motion of the stagnation point was found. Further measurements still need to be made to determine whether a motion, whose amplitude is small compared to the overall rms fluctuation level, exists at low frequencies, as in the supersonic case above, or whether the stagnation

point remains fixed due, perhaps, to the "confining" effects of the shroud on the main stream flow.

Finally, the model wall temperature-time histories will be considered. Results for typical testing conditions are presented in Figure 20 which shows the time variation of the difference between instantaneous and initial wall temperature at the stagnation point, divided by the difference between the air stagnation temperature and initial wall temperature. Data are shown for both liquid nitrogen and dry ice-acetone coolants. The effectiveness of the coolants is shown by comparison with the corresponding theoretical* time variation of the temperature ratio neglecting the heat transferred by lateral conduction, and assuming that the inside wall is insulated. The opposite extreme of infinite cooling is, of course, represented by the abcissa, $T_{w_s} = T_{w_o}$. The results show that the heat transferred to the coolant from the model was generally small in comparison with that transferred to the model from the air. Nearly equilibrium conditions were established only at the lower heating rates with the dry ice-acetone coolant.

It is seen that the experimental points for the liquid nitrogen data have a nearly exponential variation with time. If the net heat transferred to the wall per second is modified to be a constant fraction of that transferred from the air, i.e., q_{w_s} is replaced by αq_{w_s} where α is less than one, then the modified theoretical curve

---

* The exponential solution is based on a constant mean specific heat for the metal and results from the fact that $q_{w_s}/T_s - T_w$ is very nearly independent of T_w. The theoretical heat transfer at the stagnation point, q_{w_s} was computed from the solution of References 31 and 32.

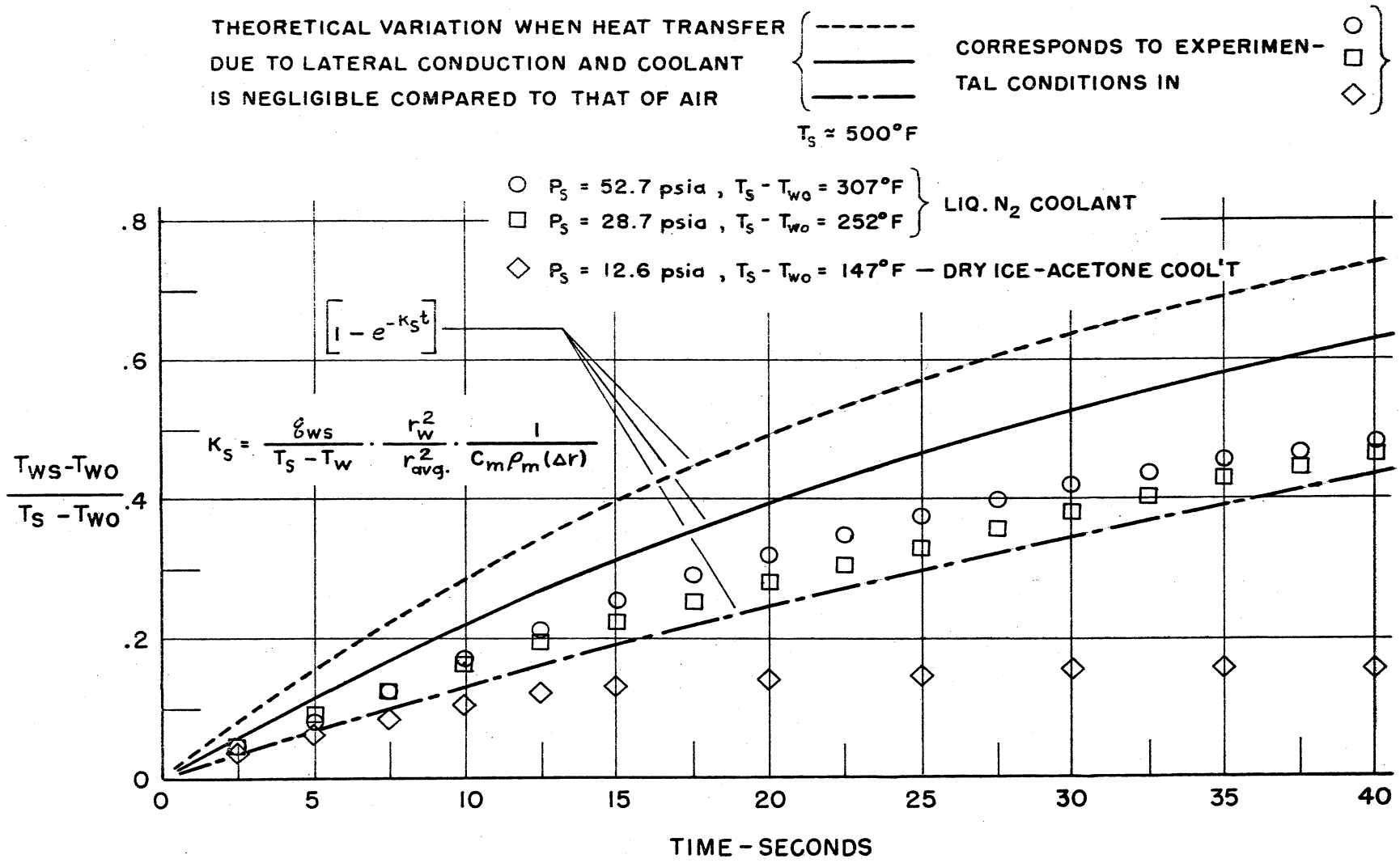

Figure 20. Typical Surface Temperature-Time Histories for Tests with Cooling.

can be made to fall on the data. This results in a "figure of merit" for the cooling effectiveness. For example, the solid curve will fall on the corresponding data if q_{w_s} is replaced by 0.65 q_{w_s}, that is, about 35% of the heat transferred from the air was absorbed by the coolant.

With the experimental techniques used for cooling and for detecting transition (Section IV), the minimum wall temperatures for which transition data could be obtained were limited by the temperature rise during the establishment of steady flow conditions and the instrument response. The time required for the pitot tube to reach equilibrium was about 3 seconds. If the model was cooled to liquid nitrogen temperature (140°R) initially the stagnation point temperature would rise to about 155°R in three seconds. For an air stagnation temperature of 500°R, the corresponding minimum value of T_w/T_s was 0.31.

Actually, the minimum wall temperatures for which reliable data could be obtained will be seen to be nearer 250°R because of the condensation of carbon dioxide on the model surface at lower temperatures.

Effects of Boundary-Layer Cooling on Transition Caused by Roughness

A series of transition experiments, carried out at a constant stagnation Reynolds number of approximately 4.3×10^6, were made to verify the qualitative effects of cooling on boundary-layer transition caused by various roughness elements. As pointed out in Section II, three ranges of roughness height, dependent on the stagnation Reynolds number, angular position from the stagnation point, and amount of boundary layer cooling, are expected. The three ranges are, (see Figure 2)

1) the roughness may be small enough so that transition does not occur either with or without a given amount of cooling, or 2) the roughness may be of such a height that transition occurs only when the boundary layer is cooled, or 3) the roughness is large enough so that transition always occurs, independent of the amount of cooling.

The data to be presented, illustrating the above ranges of roughness, were obtained with the same hot wire heated to nearly the same temperature. Since the angular position of the wire from the stagnation point was varied by rotating the sphere, the wire height from the surface was exactly the same in all of the tests*. This distance was between .002 and .003 inches. The boundary layer thickness** varied from .0057 inches at $\eta = 0^{\circ}$ to .0078 inches at $\eta = 45^{\circ}$, nearly independent of the small amount of cooling. The wall temperature was nominally 0.8 of the stagnation temperature for the tests with cooling. The hot wire data is given in terms of the rms wire voltage fluctuations as a function of wire position from the stagnation point. Although no attempt was made to calibrate the hot wire and decompose the voltage signal into the various flow fluctuations (Section IV), it should be

* Other data with different hot-wires showed the same general effects of cooling. However, the fluctuation levels were not sufficiently repeatable due to the difficulties experienced in locating the wire at the same height in the relatively thin boundary layer.

** The boundary layer thickness, displacement thickness, momentum thickness, heat transfer, and skin friction for the laminar boundary layer were computed using the techniques and solutions of References 31 and 32. Their variation with η and T_w/T_s is shown in Appendix B.

pointed out that, with the conditions outlined above, the wire sensitivities had nearly the same variation with position from the stagnation point in all of the tests. The voltage fluctuations are therefore comparable.

Measurements were made with two types of disturbances glued to the surface. They were, 1) a .004" x .025" dia. disk placed 15° ahead of the wire, and 2) three ribbons, .004", .006", and .010" high, .030" wide, and approximately 1 1/2" long, placed 10° ahead of the wire. In addition, data was taken with no disturbance added to the surface. In this case the rms surface roughness was 10 to 15 microinches, with pits ranging up to 100 microinches in depth.

Typical fluctuation levels at transition are shown in Figure 21. The difference between total and static pressure in the boundary layer is also given*. Distributions are shown for the case of no disturbance placed on the surface, and for the case when the .004 inch disk was placed 15° ahead of the sensing probes. It should be emphasized that in this figure and the ones to follow the angular position of the probe was varied by rotating the sphere. Consequently the roughness elements rotate at the same time. It can be seen that with the disk forward of 15 to 20° (probe angle 30 to 35 degrees) the disturbances caused by the disk are damped before they reach the hot wire. In this region, the rapid rise in fluctuations is interpreted as indicating the occurence of transition. This interpretation is

---

* The total head tube opening spanned the boundary layer between .0015 and .0045 inches from the surface. This tube was not mentioned in the description of the experimental apparatus (Section IV) since it was only used for a few measurements.

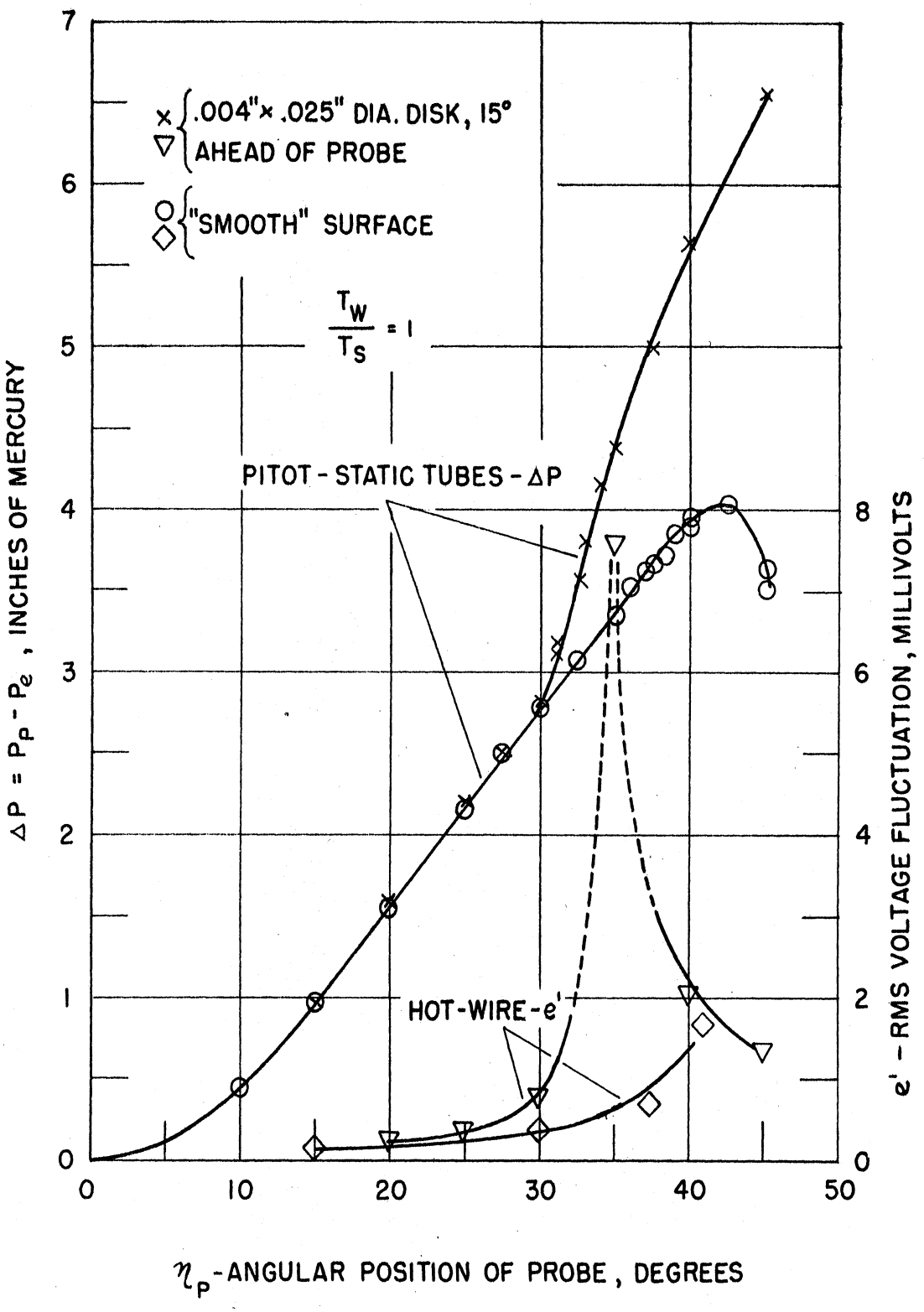

Figure 21. Hot-wire and Pitot Tube Measurements of Transition Caused by a .004" x .025" Diameter Disk.

verified by the pitot pressure measurements which indicate much higher velocities (skin friction) in the lower portions of the boundary layer. Subsequent increases in the angle show a decreasing fluctuation level at the wire and an increasing deviation from the laminar pitot pressure distribution. For these angles the pitot pressure results are consistent with the development of a fully turbulent boundary layer at the probes as the transition point moves closer to the disturbance.

The fluctuation distributions in the transitional and turbulent regions depend, among other things, on the Mach number[29,45], pressure gradient[43], and, as will be seen, the type of trip. Of course, they also depend on the relative position of measurement which, in this instance, changes considerably in the thicker transitional and turbulent boundary layer. However, the rather large decrease in indicated fluctuations is probably caused by the fact that the high frequency response of the hot-wire amplifier was cut off at 10,000 cps to keep the noise low. An estimate of the turbulent frequencies to be expected in this case shows, however, that much of the energy is contained above the frequency range used. For example, on the basis of measured energy spectrums[46] in the turbulent boundary layer at low speed on a flat plate, it is estimated that for the measurements shown, near 90% of the turbulent energy is contained in fluctuations above 10,000 cps.

The rising voltage fluctuations at the largest angles for the smooth surface is caused in part by the increasing wire sensitivity to percentage velocity fluctuations at the higher speeds. Also, the sound level may be increasing near the sonic region. The

pitot pressure distribution indicates, however, that transition does not occur up to $\eta = 45^{\circ}$ for the smooth surface condition.

Cooling of the boundary layer causes the position of transition due to the disturbance in Figure 21 to move forward, as illustrated in Figure 22. Hot wire fluctuation levels are given for $T_w/T_s = 1.0$ and 0.8. Transition with boundary layer cooling occurs about 5° ahead of the position without cooling, in accordance with the roughness regime II of Figure 2, Section II.

Oscillograms of the fluctuations are also shown in Figure 22. In the transition region, frequencies ranging up to about 2500 cps can be seen. These frequencies are considerably lower than those corresponding to disturbances of the order of the boundary layer or disk size, being transmitted at the free stream speed ($\frac{u_e}{\delta} \sim 10^6$ sec.$^{-1}$, $\frac{u_e}{D_{DISK}} \sim 5 \times 10^5$ sec.$^{-1}$). Presumably, they are associated with turbulent bursts in the initial stages of transition.

The effect of small boundary layer cooling rates on transition caused by the three two-dimensional ribbons is given in Figures 23a-23c. Figure 23a also shows results for the smooth surface. These results illustrate the three ranges of roughness discussed previously in Figure 2. Thus, transition did not occur on the smooth surface, with or without cooling. The roughness of the smooth surface therefore falls in regime III. When the .004 and .006 inch disturbances were introduced transition occurred and the effect of cooling was to move it further forward, Figures 23a and 23b. These roughness elements therefore fall in regime II. For example, with the .004 inch ribbon transition did not occur at $\eta = 35^{\circ}$ until the boundary layer was cooled.

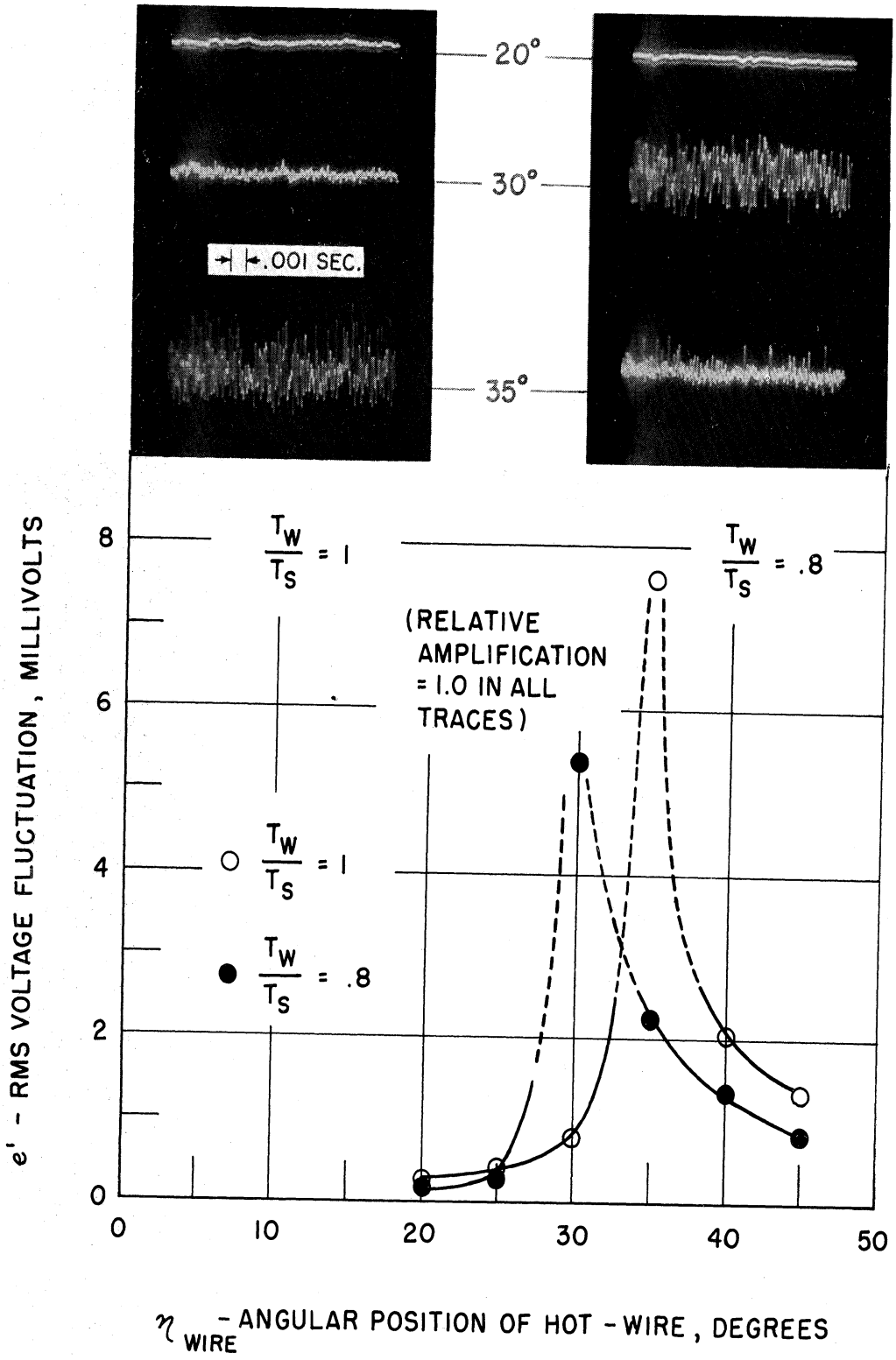

Figure 22. Hot Wire Fluctuation Distributions for T_w/T_s= 1.0 and 0.8, (.004" x .025" Diameter Disk, 15° Ahead of Wire)

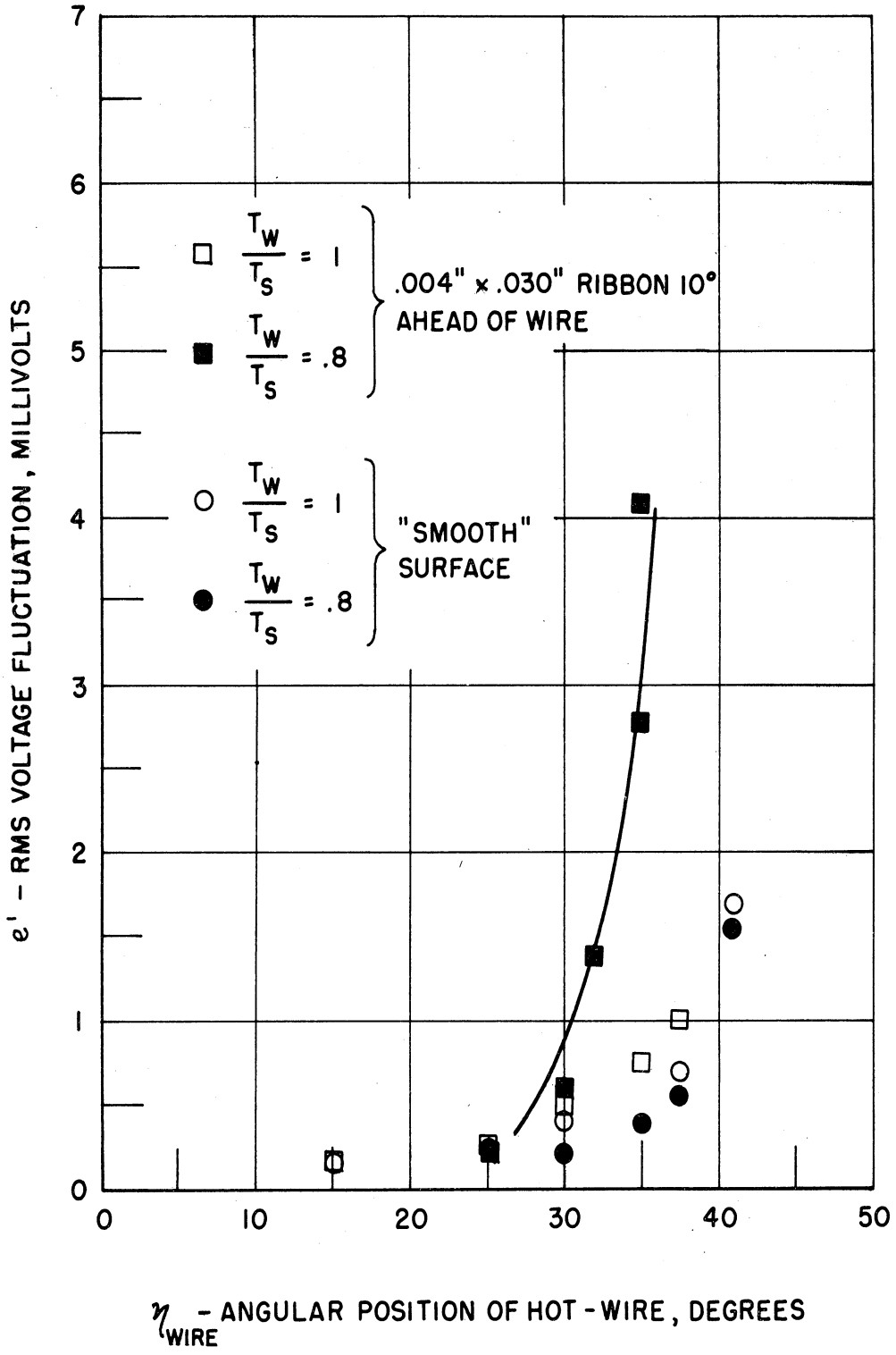

Figure 23. Hot Wire Fluctuation Distributions for T_w/T_s = 1.0 and 0.8, (two-dimensional ribbons 10° ahead of wire)
(a) .004" x .030" ribbon, and "smooth" surface.

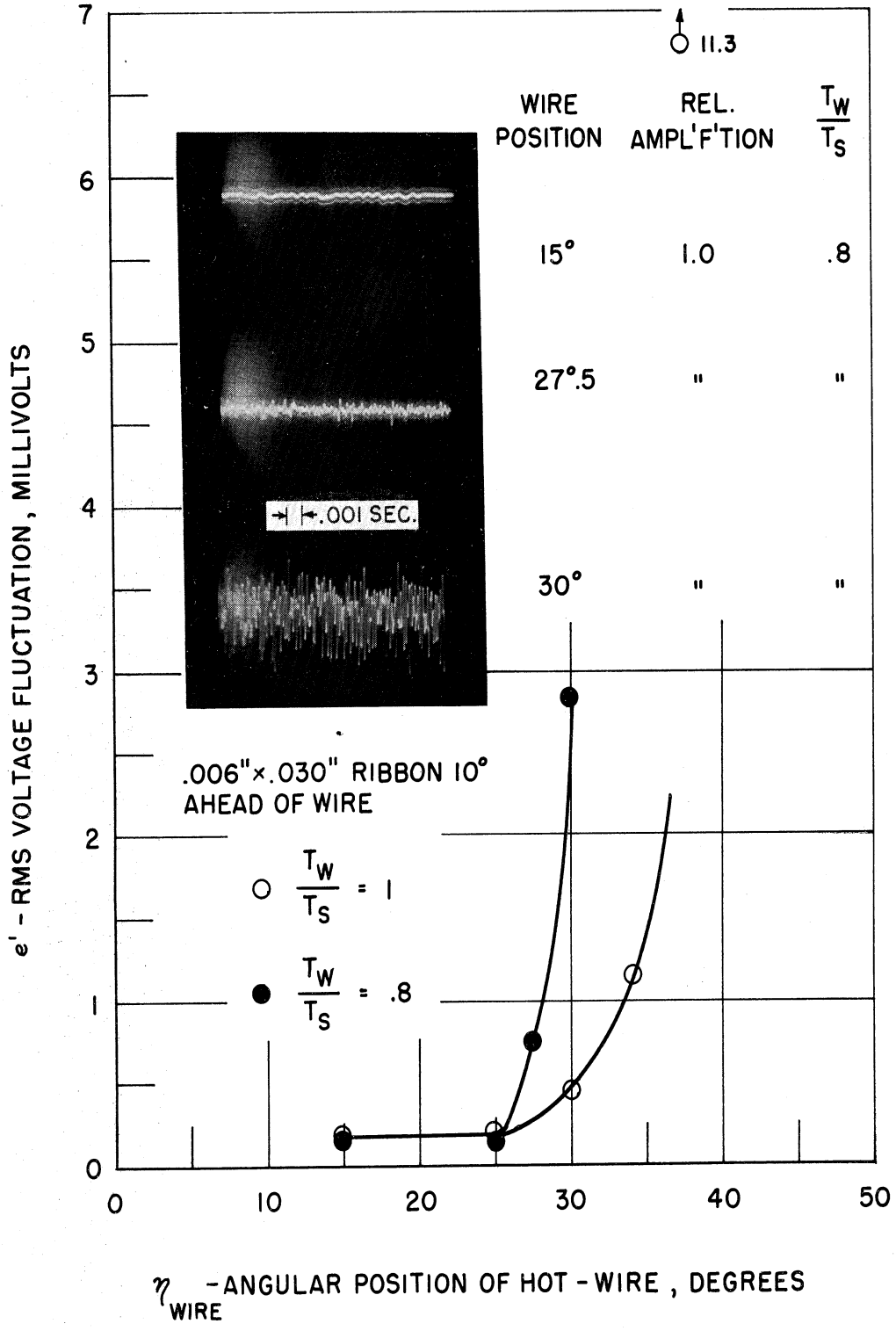

Figure 23. (continued)

(b) .006" x .030" ribbon

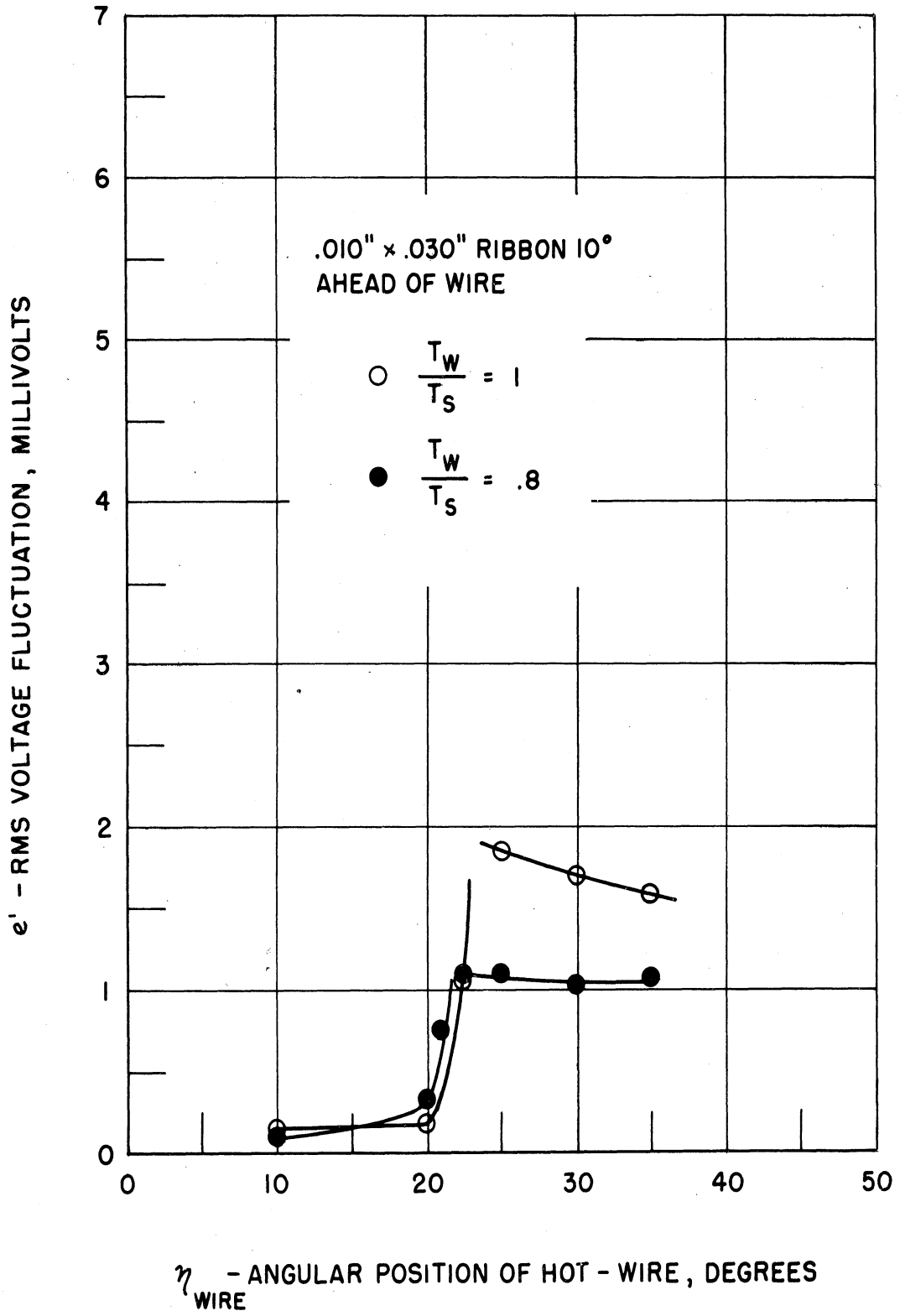

Figure 23. (continued)

(c) .010" x .030" ribbon

Finally, in Figure 23c the transition point moved furthest forward with the .010 inch disturbance and there was no appreciable effect of cooling. This roughness element therefore falls in regime I.

In addition to the effects of cooling it may be noted that the initial stages of transition are quite similar for both the two- and three-dimensional disturbances as evidenced by the oscillograms in Figures 22 and 23b. Also, with the relatively large .010 inch ribbon ($\frac{\text{disturbance height}}{\text{boundary layer thickness}} = 1.7$), the fluctuation amplitudes at transition (below 10,000 cps) were considerably less when compared to those resulting with the smaller disturbance.

In all of the measurements with applied roughness the exact position of transition was found to vary somewhat between experiments where the only change was to replace the disturbance with a (supposedly) identical one. This indicates that the manner in which the elements were glued to the surface was highly critical. Also the increased surface pitting with time may have introduced some scatter into the experiments. However, in the data given in Figures 21-23 the disturbance element was not changed between the tests with and without cooling.

Two extraneous effects were encountered in the earlier tests. During these tests regular voltage fluctuations appeared which were traceable to vibration of the hot wire supports. Since the fluctuation thus generated was considerable compared to the overall signal, it was necessary to support the hot-wire terminals near the tips to eliminate this spurious signal. Also, when the air dewpoint was unusually high, boundary-layer transition would occur due to the roughness caused by frost forming on the surface. The hot wire records were quite striking in this instance. At the beginning of the tests,

the boundary layer was turbulent as far forward as 12.5° from the stagnation point. Then as the surface temperature slowly rose the boundary layer passed rather suddenly through the transitional to the laminar state. At the end of the test the flow was laminar at least to the largest angles investigated ($\eta = 45^{\circ}$). This type of result could not be reproduced when the air dewpoint was close to or below the initial wall temperature ($\sim -60^{\circ}$F).

In conclusion, the data presented has qualitatively demonstrated the combined effects of cooling and roughness on boundary layer transition. The stagnation Reynolds number was held constant and one (relatively small) boundary layer cooling rate was used. The results indicate that a given amount of surface cooling does not affect transition if the roughness is small, or large, but that there is an intermediate range of roughness for which cooling hastens transition. The width of this range and its position in the roughness scale is probably a function of Reynolds number and distance from the stagnation point.

In the following section, experiments are described in which the Reynolds number and surface cooling were varied and the surface roughness was kept as small as possible.

Transition Experiments on a Highly Polished Model with Variable Boundary-Layer Cooling

The purpose of the experiments to be discussed here was to gain further knowledge of the circumstances under which cooling of the boundary layer may promote early transition on a blunt body. One effect of cooling is to increase the Reynolds number at the peak of a

given roughness element. Therefore, a decrease in transition Reynolds number will occur with boundary-layer cooling if, as a consequence of the cooling, a particular roughness Reynolds number exceeds a critical value.

On the other hand, according to our present notions, there appears to be no reason to expect a large reduction in transition Reynolds number due to the effects of cooling on boundary-layer stability. As pointed out in Section II, existing small disturbance theory predicts increasing stability to Tollmien-Schlichting disturbances with increasing cooling, for surfaces without curvature. There is a destabilizing effect of the density gradient in the cooled boundary layer on a convex surface, but rough analysis indicates that the flow in the centrifugal acceleration field remains dynamically stable even if the surface temperature is decreased to $0^{o}R$.

In an effort to determine the effects of cooling on boundary layer stability, experiments were conducted in which the roughness of the model surface was made as small as possible. The results show that, for small roughness, there is little change in transition Reynolds number with cooling for the range of parameters investigated.

The surface roughness was minimized by giving the model an extremely smooth polish (approaching 1-microinch rms, Section III) and placing paper dust filters in the airstream. In addition, the model was continually monitored throughout the test program so that the effects of any change in surface roughness, caused by pitting, deposition of small dust particles, and formation of frost or carbon dioxide

could be detected. Estimates* of the order of magnitude of frost film thickness to be expected when the surface was cooled below the air dewpoint ($\sim -75^{\circ}F$) gave a uniform layer thickness of about 1 microinch per second of run time at the highest mass flow rates. The roughness caused by the frost would, of course, depend on the crystalline pattern and the way in which it was distributed over the surface. However, the rough estimates indicated that for a short run the build up would be of the order of the surface roughness itself, and the frost was expected to have negligible influence. Observations of the surface by means of the periscope showed no visible signs of the frost during a short run. As far as the transition observations were concerned, no noticeable change in the trend of the data was found when the surface was cooled below the dewpoint as long as the low dewpoint was maintained.

An analysis of several air samples showed the percentage of carbon dioxide to vary up to as much as 30 times that for the standard atmosphere. These unusually high amounts of CO_2 were probably caused by contaminated intake air at the compressors and/or partial oxidation of the oil during compression. At the tunnel pressures, and these percentages of CO_2, dry ice would condense on the model surface for temperatures in the range $230^{\circ}R$ to $250^{\circ}R$.

---

* The estimates assumed that all of the water vapor in the velocity boundary layer up to a given angle from the stagnation point deposited uniformily over the included surface area. The results were found to be nearly independent of the angular location chosen. These estimates are conservative as to the total amount of water that could reach the surface when the Lewis number and Prandtl number are equal to one, i.e., when the diffusion boundary-layer thickness is equal to the velocity boundary-layer thickness.

Estimates similar to those for frost, gave uniform layer thickness of from 25 to 1000 microinches per second of run time. For the lowest model temperatures, in contrast to the case with the frost layer, the CO_2 became clearly visible as the tunnel established steady conditions. As will be pointed out, the records of transition from turbulent to laminar flow were often visually correlated with the disappearance of the condensation film as the model warmed. The maximum cooling range for which reliable data was obtained was thus limited to the range in which CO_2 was observed to condense.

Low transition Reynolds numbers (as much as 50% below the highest values observed) were also found to occur as a result of the roughness caused by minute dust particles sticking to the model within about 10° of the stagnation point. Microscopic examinations of six of the larger particles showed their heights to vary from .00075 inches to .0020 inches. The non-repeatibility of the data when the particles were removed suggested that the low transition Reynolds numbers were caused by these roughness elements. This conjecture was also supported by a calculation of the critical roughness height for a particle at 10°. For example, using a critical roughness Reynolds number of 700* and a tunnel pressure of 40 psia, the critical roughness height for a particle at 10° is .0023 inches when $T_w/T_s = 1.0$ and .0013 inches when $T_w/T_s = 0.5$.

---

* In the present investigation, supercritical roughness Reynolds numbers of 640 and 1015 were measured for two-dimensional ribbons at 10° and 12°, and a value of 465 was found for a three-dimensional disk at 12°. Reference 47 gives values between 625 and 770 for spherical roughness elements at 10° on a 10 foot diameter hemisphere in subsonic flow.

The influence of dust particles on the transition data was reduced by removing the oil from the paper filter so that the particles had little tendency to stick to the model. In addition, the surface was cleaned when any specks of dust could be seen.

When real gas effects are of only minor importance, the laminar boundary layer on geometrically similar blunt bodies in hypersonic flow is characterized by a Reynolds number behind the bow shock wave and the ratio of wall to stagnation temperatures. Therefore, if the roughness (and all other disturbances) are also scaled, we would expect, in general, the non-dimensional location of transition to be a function of Reynolds number and temperature ratio. Stated in another way, the local transition Reynolds number should generally depend on the non-dimensional location of transition as well as on the temperature ratio. In the experiments reported here the observations were made at a fixed angular position, and the transition Reynolds number determined as a function of temperature ratio.

Transition was detected with the pitot pressure probe described in Section III. Typical calibration data showing the difference in pitot minus static pressures between the laminar and turbulent boundary layer is shown in Figure 24. The turbulent boundary layers were obtained by using a .0025 inch ribbon trip placed 5^{o}, 15^{o}, and 25^{o} ahead of the probe. It can be seen that the turbulent pitot pressure was fairly insensitive to the trip location, which reflects the slow rate of growth of the turbulent boundary layer in the subsonic region. When the measured pressure difference is divided by the stagnation pressure, the resultant dimensionless parameter has little dependence on

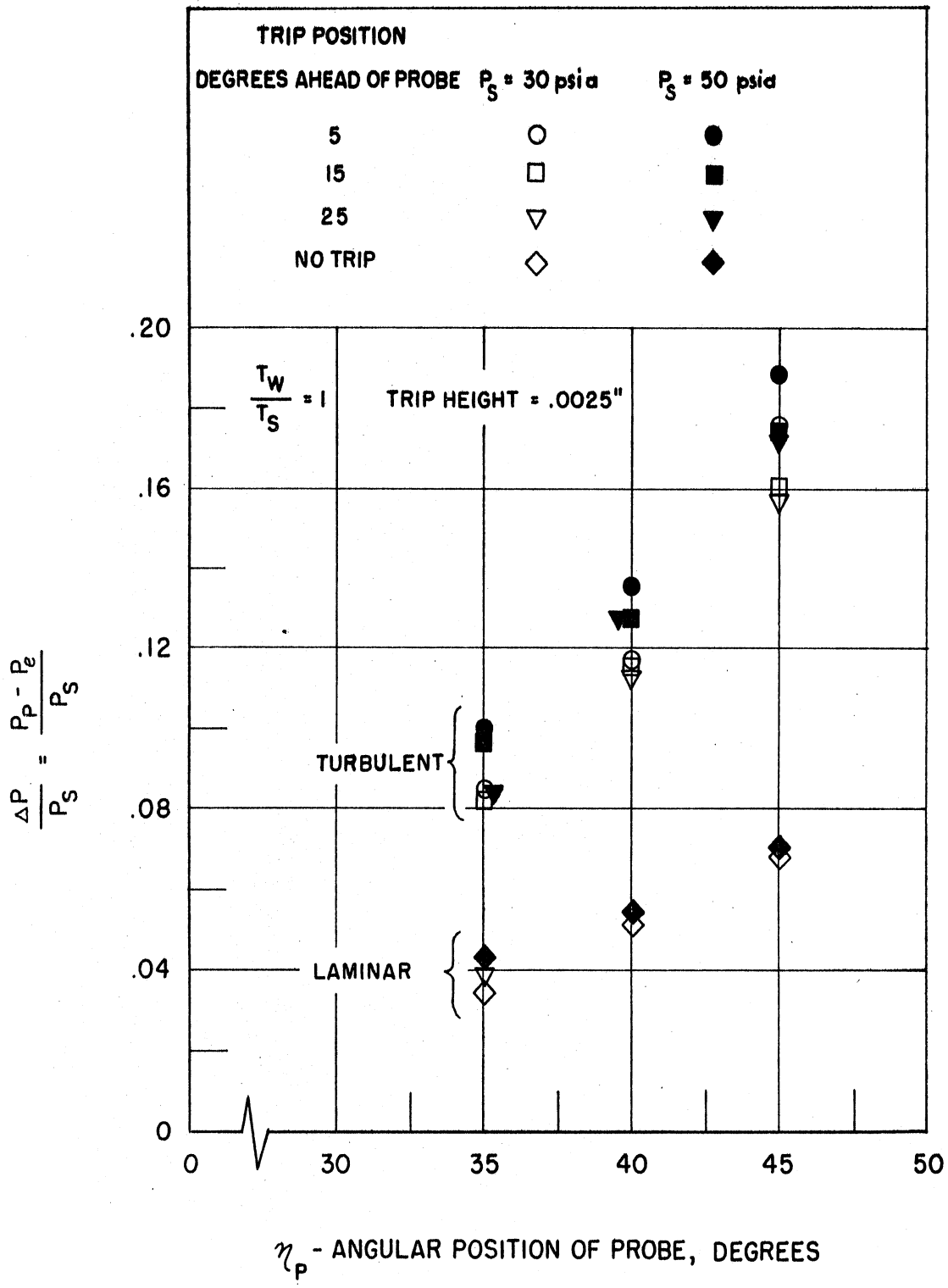

Figure 24. Calibration of Pitot Probe.

the stagnation pressure level. The increase in measured pitot pressure when the boundary layer changes from laminar to turbulent is seen to be more than 100% for the 35, 40, and 45 degree angular locations.

Typical data obtained during a given run are reproduced in Figure 25. In this run the flow began laminar at the lowest temperatures*, changed to turbulent when the stagnation pressure was increased, and then, at constant stagnation pressure, returned to the laminar state as the surface temperature increased. The values of $\Delta p/p_s$ for both laminar and turbulent flows correspond closely to the values found when the probe was calibrated at $T_w/T_s = 1$. The record does in fact indicate that the change in boundary layer temperature close to the surface has negligible effect on the average pitot pressure over the subtended portion of the layer.

In contrast to the data of Figure 25, when the initial wall temperature was decreased slightly to the range in which CO_2 condensed on the model surface, the flow started out turbulent even with a 25% reduction in stagnation pressure (Reynolds number), as is shown in Figure 26. In this run the model was observed through the periscope and the time at which the CO_2 did not extend beyond $\eta = 20^o$ (limit of field of view) was noted. This observation correlates with the change

---

* The first peak in the pressure difference, P_p-P_e, is caused by the slower response time of the pitot probe compared with that of the static tube, during start-up. Thus, for the first few seconds the pitot probe remains at nearly atmospheric pressure while the static tube follows the rapid negative to positive variation of static gage pressure.

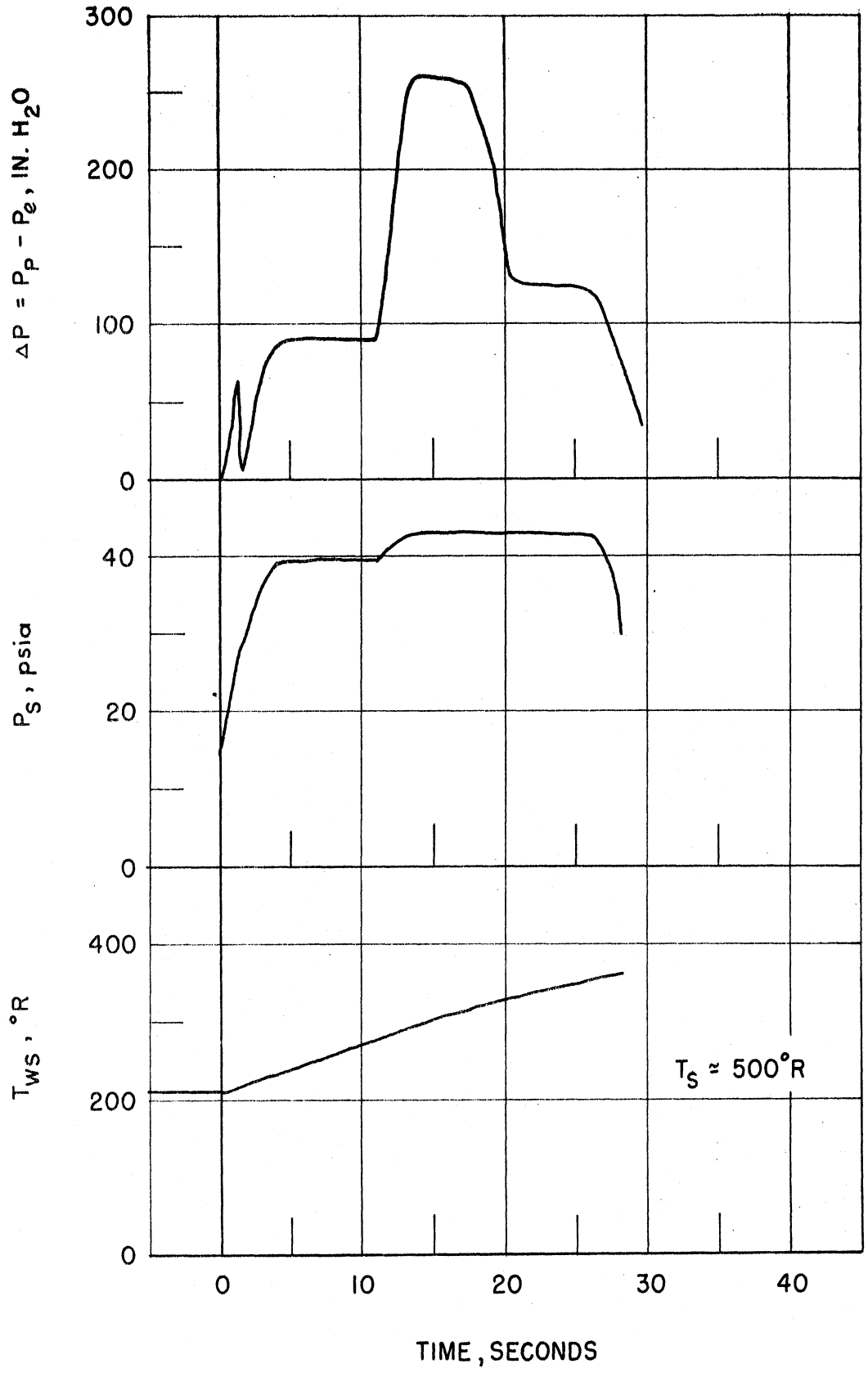

Figure 25. Records of P_p-P_e, P_s, and T_{w_s} During a Typical Transition Experiment.

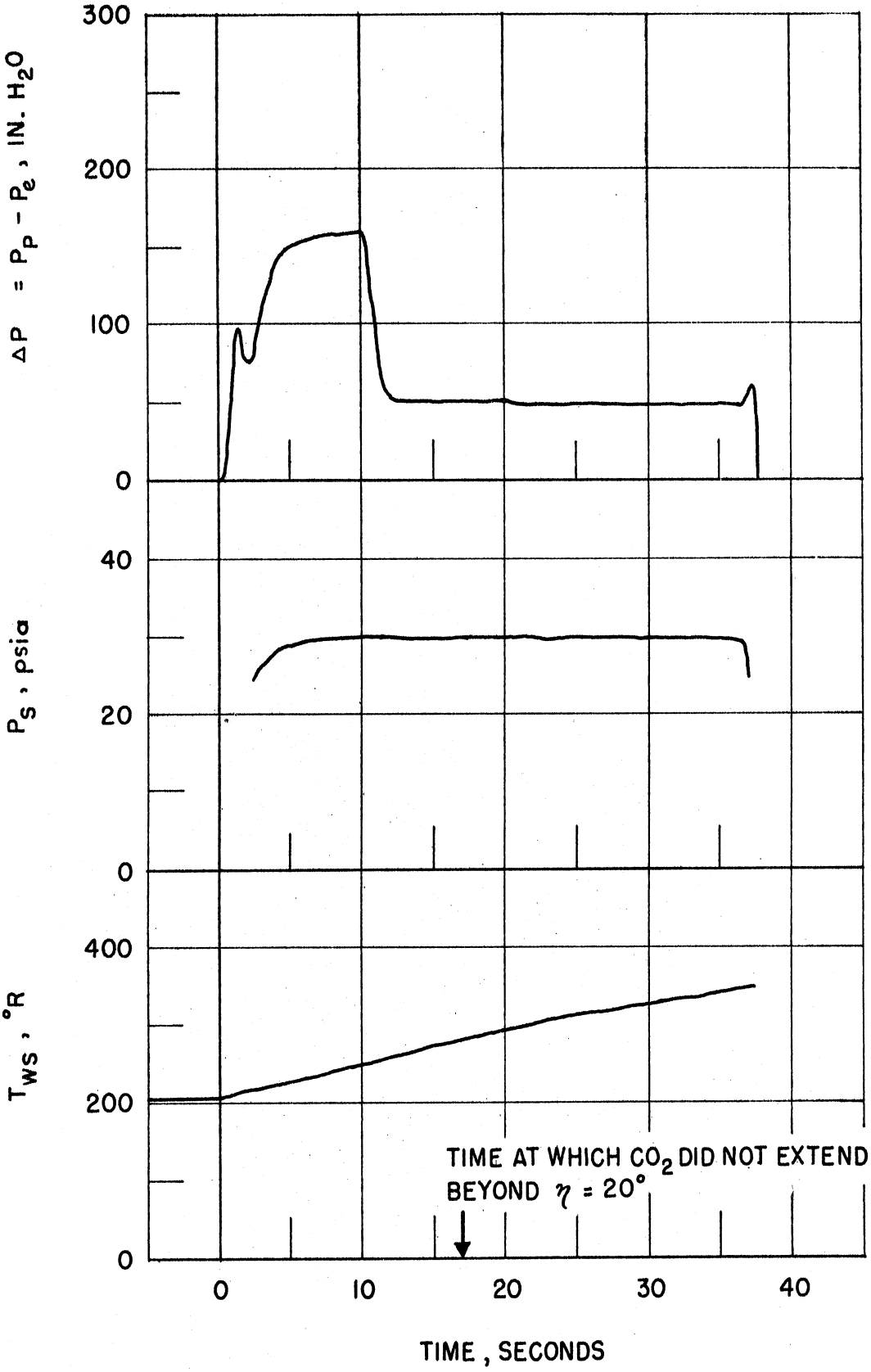

Figure 26. Correlation of Transition with CO_2 Film.

from turbulent to laminar flow indicated by the pressure records. That is, the roughness caused by the CO_2 film promoted turbulent flow at a lower Reynolds number until the film did not extend beyond some angle between 20^o and 45^o. The fact that the CO_2 film disappeared last at the stagnation point as the body warmed is of course caused by the higher heat transfer rates (greater evaporation rates) in the turbulent boundary layer.

Most of the transition data was taken at the 45^o angular position, with a few measurements at 40^o and a single measurement at 30^o. The data is presented in Figure 27 in terms of the local transition Reynolds number based on distance from the stagnation point, Re_x, as a function of T_w/T_s. Results are also given of some other investigations with hemispheres in supersonic flow for which transition was observed ahead of the 90^o point. In the range $1 \geq T_w/T_s \geq 0.5$ the present data show little effect of cooling on the local transition Reynolds number at 40^o and 45^o. For $T_w/T_s < .5$ the scatter, as well as a reduction in Re_x, is caused largely by the presence of varying amounts of CO_2 on the surface. Although data in which dust particles were definitely known to be influencing transition are not shown, there is still some scatter in the present data outside the range in which CO_2 condenses on the surface. These lower values of Re_x did not correlate with the increasing surface abrasion at the stagnation point, i.e., with increasing testing time with the same surface. The scatter may therefore reflect the influence of minute dust particles. In fact, it is possible that the small

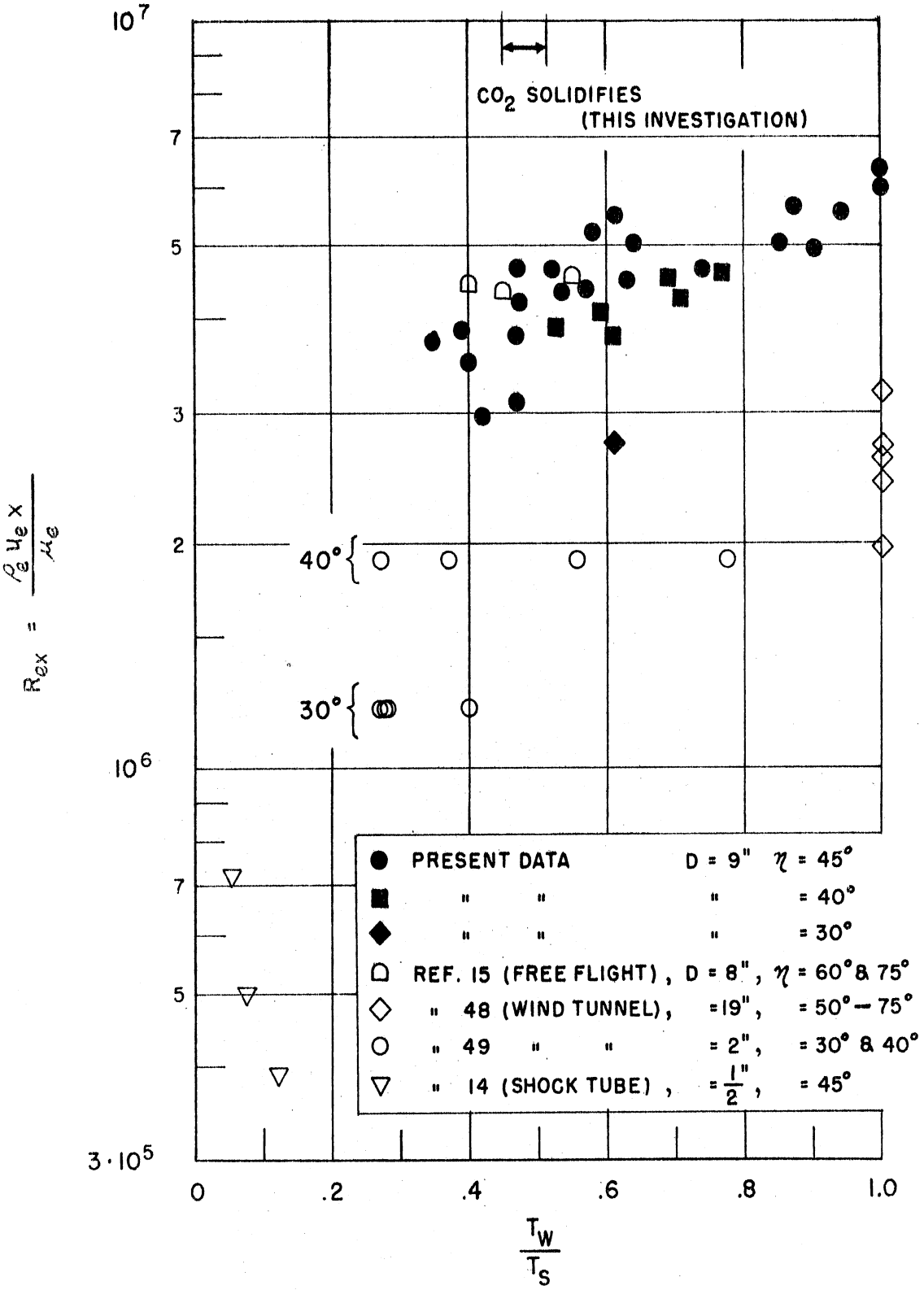

Figure 27. Local Transition Reynolds Numbers Based on Distance From the Stagnation Point, Re_x, vs. T_w/T_s.

decrease in Re_x with cooling may be caused by the increasing importance of any dust particles present as the surface is cooled.

All the data from other sources shown in Figure 27 are for rms surface roughness reported to be less than 5 microinches, except that of Reference 48 which reported a value of 10-15 microinches. The level of Re_x at $T_w/T_s = 1$ for the present investigation is seen to be somewhat higher than that of Reference 48. This result may accordingly be attributed to the differences in surface roughness. Agreement between the present data and the flight test results of Reference 15, for which transition occurred at the 60 and 75 degree location, is also apparent for T_w/T_s near 0.5. The recent wind tunnel data of Reference 49 which extends to a lower temperature ratio than that reached here also indicate an independence of Re_x with cooling. There is, however, a factor of about 2 1/2 in the levels of Re_x between their data and the present data. This disagreement may be due to differences in absolute surface roughness and/or free stream turbulence levels.

With an unheated airstream it was not possible to check the range of temperature ratios corresponding to the shock tube data of Stetson(14). These data show considerably lower values of Re_x at the low temperature ratios. Although the rms surface roughness was less than 1 microinch, the heat transfer gages used to detect transition were approximately 12 microinches in height. A typical value of Re_k at the top of the gage located at 30° was estimated to be about 130*. While

---

* The stagnation point boundary-layer distributions, Figure 1, were used in this calculation.

no information is available on the critical value of Re_k under these circumstances, this value does lie in the range of critical values found in the experiments of Reference 48 on a 19-inch diameter hemisphere without cooling*.

As was pointed out previously, any local transition Reynolds number, such as Re_x, Re_θ, Re_{δ^*}, or Re_δ, would be expected to depend on the angular location and temperature ratio. This dependence was given in terms of Re_x in Figure 27, where the disagreement between data taken under dynamically similar conditions (present data and that of Reference 49) must reflect a difference in the simulation of boundary layer disturbances, viz. free stream turbulence and sound, and surface roughness. It is of interest to view the transition data in terms of Re_θ and Re_{δ^*} which are based on characteristic lengths which depend on the cooling and are generally more characteristic of a boundary layer than is the distance x. The variation with T_w/T_s of Re_θ at transition is given in Figure 28. All the data of Figure 27 is shown except for the present investigation for which only the highest values are given. A small increase in Re_θ with cooling is indicated by the present data for transition at 45° in the range $.5 \leq T_w/T_s \leq 1$. Comparison with Figure 27 shows that Re_θ is less dependent than Re_x on angular position at the lower angles but more dependent at the higher angles, corresponding to the manner in which θ varies with η as opposed to the linear variation of x (see Appendix B).

---

* As pointed out in Section II, Reference 30 found little effect of cooling on the critical value of Re_k for transition on cones and flat plates in supersonic flow.

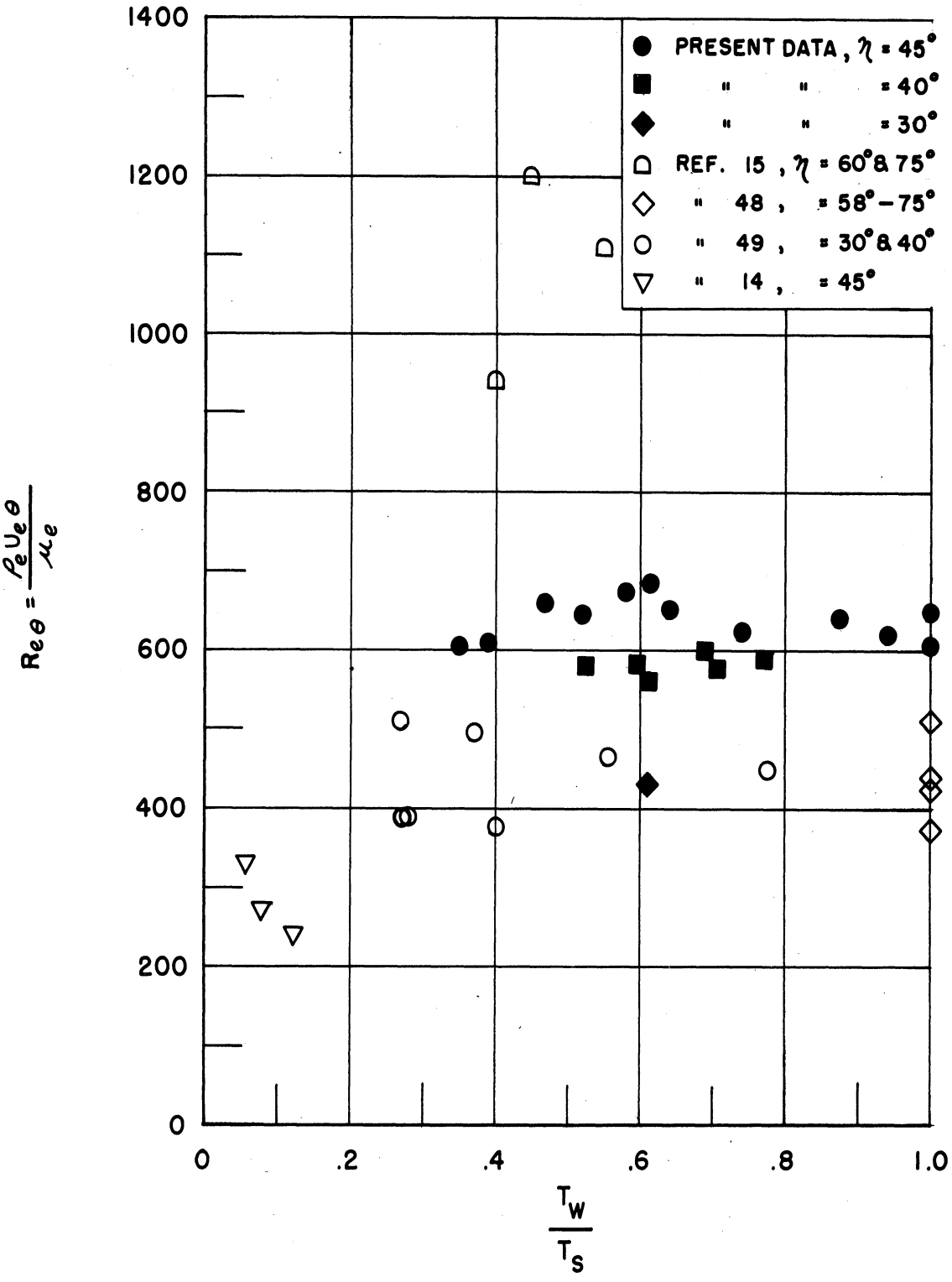

Figure 28. Local Transition Reynolds numbers Based on Boundary-Layer Momentum Thickness, Re_θ, vs. T_W/T_S.

The data of Figure 28 is given in Figure 29 in terms of the variation of Re_{δ^*} at transition. All of the data indicates a rapid decrease in Re_{δ^*} with decreasing T_w/T_s. This behavior reflects the rapid decrease in δ^* with cooling, the effect of which also tends to center the data about a nearly straight line decrease in Re_{δ^*}. The flight data (Reference 15), for which transition occurred at 60 and 75 degrees on an 8-inch diameter hemisphere with rms surface roughness between 0 and 5 microinches, shows considerably higher values of Re_{δ^*} as well as Re_θ. This result may reflect either a smaller absolute roughness and free stream turbulence compared with the roughness and stream turbulence in the wind tunnel tests, or a difference in the stability characteristics and transition process at the higher angles.

It is not possible, on the basis of the few unclassified results shown, to determine whether a particular Reynolds number is most significant for describing transition on "smooth" hemispherical bodies in hypersonic flow. However, concerning the correlation in terms of Re_{δ^*}, one notes that δ^* is practically constant on a hemisphere when T_w/T_s is very small (see Appendix B). In view of this and the fact that $\frac{\rho_e u_e}{\mu_e}$ changes little after the first 20 to 30 degrees, a correlation in terms of Re_{δ^*} becomes of little use as far as predicting the location of transition is concerned. A knowledge of the location of transition, especially when T_w/T_s is small (high heat transfer), is important from the standpoint of those aspects of a design dictated by the heat transfer rates.

The results of the present experiments are summarized as follows:

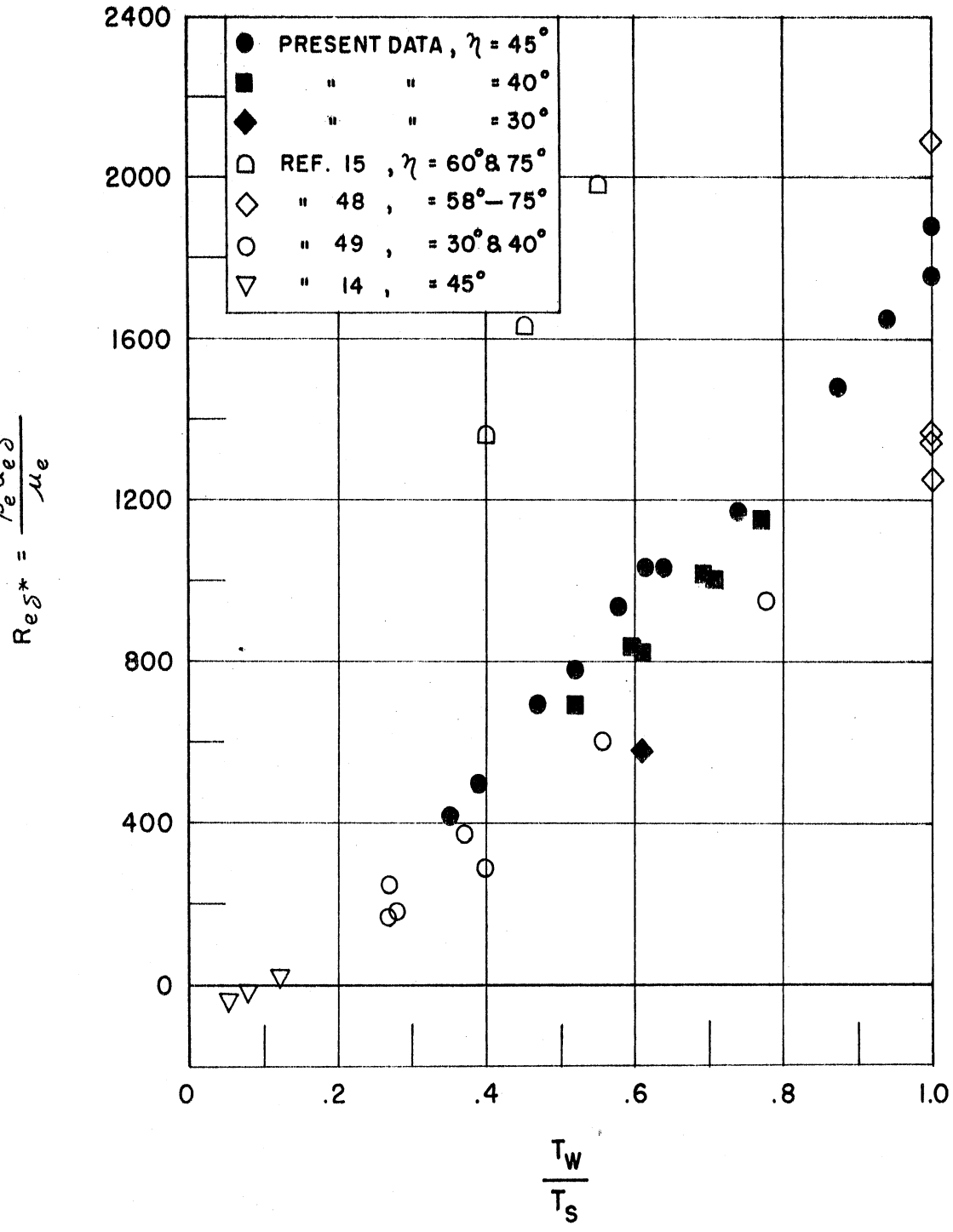

Figure 39. Local Transition Reynolds Number Based on Boundary-Layer Displacement Thickness, Re_{δ^*}, vs. T_w/T_s.

1. In the cooling range investigated, when the roughness was small, little effect of cooling was found on transition when it occurred at 40 and 45 degrees from the stagnation point. Thus, the stability of the subsonic boundary layer is not appreciably decreased by the cooling.

2. The values of Re_x and Re_θ were 5×10^6 to 6.3×10^6 and 600 to 700, respectively, for transition at 45° in the range $0.5 \leq T_w/T_s \leq 1.0$.

While there was no "transition reversal" in the subsonic boundary layer, neither was there a significant increase in Re_x or Re_θ which would have been predicted on the basis of the stabilizing effect of cooling on Tollmien-Schlichting type disturbances on a flat plate. The failure to find an increase in Re_x or Re_θ with cooling could have possibly been caused by the increased magnitude of the disturbances from roughness elements still present, which then cause transition in the cooler more stable boundary layer as soon as smaller disturbances from the same roughness elements in the warmer less stable layer. The effect of cooling in destabilizing the flow in the centrifugal acceleration field may also have been of importance under these circumstances (Section II). There is clearly a need for more experimentation to investigate these effects in detail.

Since the hypersonic pressure distribution was not simulated for angles greater than 45°*, no data was taken at the higher angles. To

---

* Actually, the pressure gradient begins to deviate from that for hypersonic flow around 40° (Figure 18). That this did not have any appreciable effect on the transition Reynolds numbers is indicated by comparison with the data at 40°. Therefore, we conclude that the results at 45° are applicable to a hemisphere in hypersonic flow.

determine whether the turbulent observations at 45^{o} may have resulted from a rapid shift of transition to a position near the nose, the pitot probe was placed at 30^{o} and the tunnel pressure increased until transition occurred. To obtain transition at the 30^{o} position it was necessary to increase the pressure 10 to 15 percent above the values necessary to obtain transition at 40 and 45 degrees. Therefore, when the boundary layer first became turbulent at 45^{o}, it was indeed laminar over most of the upstream portions of the hemisphere. That is, transition did not suddenly move close to the nose as might happen if, say, a centrifugal instability were to develop at the nose where the density gradients are large, or if a roughness element near the nose became supercritical.

VI. CONCLUDING REMARKS

The main results of this investigation are summarized as follows:

1. Simulation of the subsonic boundary layer on a hemisphere in hypersonic flow for the purpose of studying boundary layer transition has been accomplished using the shroud technique. A mathematical analysis was developed for predicting the shroud contour which would cause the hypersonic pressure distribution to prevail up to the sonic point ($\eta = 44^{\circ}$). The measured pressure distribution on the shrouded hemisphere was in excellent agreement with the Newtonian distribution specified in the analysis.

2. Experiments with small cooling rates, in which roughness elements were placed on the model, have qualitatively demonstrated the combined effects of cooling and roughness on boundary layer transition. The results indicate that a given amount of cooling does not affect transition if the roughness is small, or large, but that there is an intermediate range of roughness where cooling hastens transition.

3. An essential feature of transition studies with boundary layer cooling is the close control of surface roughness. In the present experiments this involved, in addition to having a highly polished surface, the necessity for low water vapor dewpoint, the avoidance of carbon dioxide condensation films, and special filtering of the airstream to remove most of the dust particles.

4. When the roughness was small, little effect of cooling was found on transition occurring 40 and 45 degrees from the stagnation

point. The values of Re_x and Re_θ were 5×10^6 to 6.3×10^6 and 600 to 700, respectively, for transition at 45^o in the range $0.5 \leq T_w/T_s \leq 1.0$. It is concluded that the stability of the subsonic boundary layer is not appreciably decreased in this cooling range.

APPENDICES

APPENDIX A

SIMILARITY PARAMETERS FOR BOUNDARY-LAYER FLOWS

Consider the steady boundary-layer flow of a non-reacting perfect gas about a body of revolution. The boundary-layer equations* which govern the motion can be written for the coordinate system shown as:

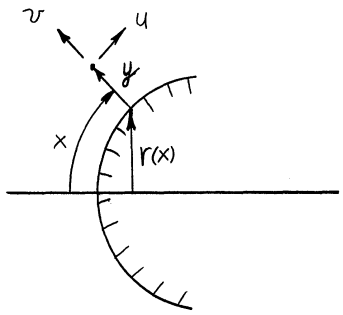

$$\frac{\partial}{\partial x}(\rho u r) + \frac{\partial}{\partial y}(\rho v r) = 0 \tag{A-1}$$

$$\rho u \frac{\partial u}{\partial x} + \rho v \frac{\partial u}{\partial y} = -\frac{\partial P_e}{\partial x} + \frac{\partial}{\partial y}\left(\mu \frac{\partial u}{\partial y}\right) \tag{A-2}$$

$$c_p\left\{\rho u \frac{\partial T}{\partial x} + \rho v \frac{\partial T}{\partial y}\right\} = \frac{\partial}{\partial y}\left(k \frac{\partial T}{\partial y}\right) + u \frac{\partial P_e}{\partial x} + \mu\left(\frac{\partial u}{\partial y}\right)^2 \tag{A-3}$$

$$P = \rho R T \tag{A-4}$$

---

* Assume the surface nearly isothermal so that $\frac{\partial}{\partial x}\left(k \frac{\partial T}{\partial x}\right) << \frac{\partial}{\partial y}\left(k \frac{\partial T}{\partial y}\right)$

These equations are non-dimensionalized in terms of the boundary-layer profiles as follows:

Define the non-dimensional quantities, shown by superscript *, to be

$$x^* = \frac{x}{D}\,, \quad y^* = \frac{y}{D}\,, \quad r^* = \frac{r}{D}$$
$$\mu^* = \frac{\mu}{\mu_e}\,, \quad k^* = \frac{k}{k_e}\,, \quad C_p^* = \frac{C_p}{C_{p_e}} \qquad \text{(A-5)}$$
$$P_e^* = \frac{P_e}{\rho_e u_e^2}\,, \quad T^* = \frac{T}{T_e}\,, \quad \rho^* = \frac{\rho}{\rho_e}\,, \quad u^* = \frac{u}{u_e}\,, \quad v^* = \frac{v}{u_e}$$

Then the governing equations can be written

$$\frac{\partial}{\partial x^*}\left(\rho^* u^* r^*\right) + \frac{\partial}{\partial y^*}\left(\rho^* v^* r^*\right) + \rho^* u^* r^* \frac{\partial}{\partial x^*}\left[\ln \frac{\rho_e}{\rho_s}\frac{a_e}{a_s} M_e\right] = 0 \qquad \text{(A-6)}$$

$$\rho^* u^* \frac{\partial u^*}{\partial x^*} + \rho^* v^* \frac{\partial u^*}{\partial y^*} + \rho^* u^{*2} \frac{\partial}{\partial x^*}\left[\ln \frac{a_e}{a_s} M_e\right] + \left[\frac{1}{\gamma_e M_e}\frac{\partial}{\partial x^*}\left(\ln \frac{\rho_e}{\rho_s}\frac{a_e^2}{a_s^2} M_e^2\right)\right]$$

$$= -\frac{\partial}{\partial x^*}\left[\frac{1}{\gamma_e M_e^2}\right] + \frac{1}{Re_s}\left[\frac{\mu_e/\mu_s}{\rho_e/\rho_s \; u_e/a_s}\right]\frac{\partial}{\partial y^*}\left(\mu^* \frac{\partial u^*}{\partial y^*}\right) \qquad \text{(A-7)}$$

$$c_p^* \rho^* \left\{ u^* \frac{\partial T^*}{\partial x^*} + v^* \frac{\partial T^*}{\partial y^*} + u^* T^* \frac{\partial}{\partial x^*} \left[\ln \frac{T_e}{T_s} \right] \right\}$$

$$= \frac{1}{Pr_s \, Re_s} \left[\frac{k_e/k_s}{\rho_e/\rho_s \;\; u_e/a_s \;\; c_{p_e}/c_{p_s}} \right] \frac{\partial}{\partial y^*} \left(k^* \frac{\partial T^*}{\partial y^*} \right) + \frac{\gamma_e - 1}{Re_s} \left[\frac{M_e^2 \, \mu_e/\mu_s}{\rho_e/\rho_s \;\; u_e/a_s} \right] \mu^* \left(\frac{\partial u^*}{\partial y^*} \right)^2$$

$$+ (\gamma_e - 1) M_e^2 \left\{ u^* \frac{\partial}{\partial x^*} \left[\frac{1}{\gamma_e M_e^2} \right] + \frac{u^*}{\gamma_e M_e^2} \frac{\partial}{\partial x^*} \left[\ln \frac{\gamma_e}{\gamma_s} \frac{\rho_e}{\rho_s} M_e^2 \right] \right\} \qquad \text{(A-8)}$$

and

$$\rho^* T^* = 1 \qquad \text{(A-9)}$$

where $Re_s = \dfrac{\rho_s a_s D}{\mu_s}$

Equations (A-6) to (A-9) are four simultaneous equations for determining the four unknowns u*, v*, T*, ρ*. All other parameters appearing are either given constants or known functions.

Applicable boundary conditions supplied with these equations are

$$u^*(x^*, 0) = v^*(x^*, 0) = 0$$

$$\lim_{y^* \to \infty} u^*(x^*, y^*) = 1 \;, \quad \lim_{y^* \to \infty} T^*(x^*, y^*) = 1 \qquad \text{(A-10)}$$

$$T^*(x^*, 0) = T_w^*(x^*) = \frac{T_w}{T_s}(x^*) \left[1 + \frac{\gamma - 1}{2} M_e^2(x^*) \right] \quad \text{or} \quad Nu(x^*, 0) = Nu_w(x^*)$$

Assuming that k, μ , and C_p vary as powers of the temperature over the range of temperatures for two flow fields, k*, μ*, and C_p* are unique functions of T*. Further, if any gradients in entropy along the edge of the boundary layer are neglected then all the terms in square brackets become functions of $M_e(x^*)$ only. Thus, for two flows in which P_{r_s} and γ_s are the same, the non-dimensional velocity, temperature, and density distributions in the boundary layer on geometrically similar bodies will be identical functions of the non-dimensional coordinates provided the similarity parameters $M_e(x^*)$, T_w/T_s (x^*) or $N_{u_w}(x^*)$, and Re_s are the same.

APPENDIX B

CALCULATED PROPERTIES OF THE LAMINAR BOUNDARY LAYER ON A HEMISPHERE IN HYPERSONIC FLOW

The following figures show the variation of δ , δ^*, θ, C_f and q_w with η and T_w/T_s for a hemisphere in hypersonic flow. The parameters were computed using the methods and solutions due to Cohen and Reshotko[31,32]. λ_w is a constant of proportionality between viscosity and temperature given by the relation $\lambda_w = \frac{\mu_w}{\mu_s}\frac{T_s}{T_w}$.

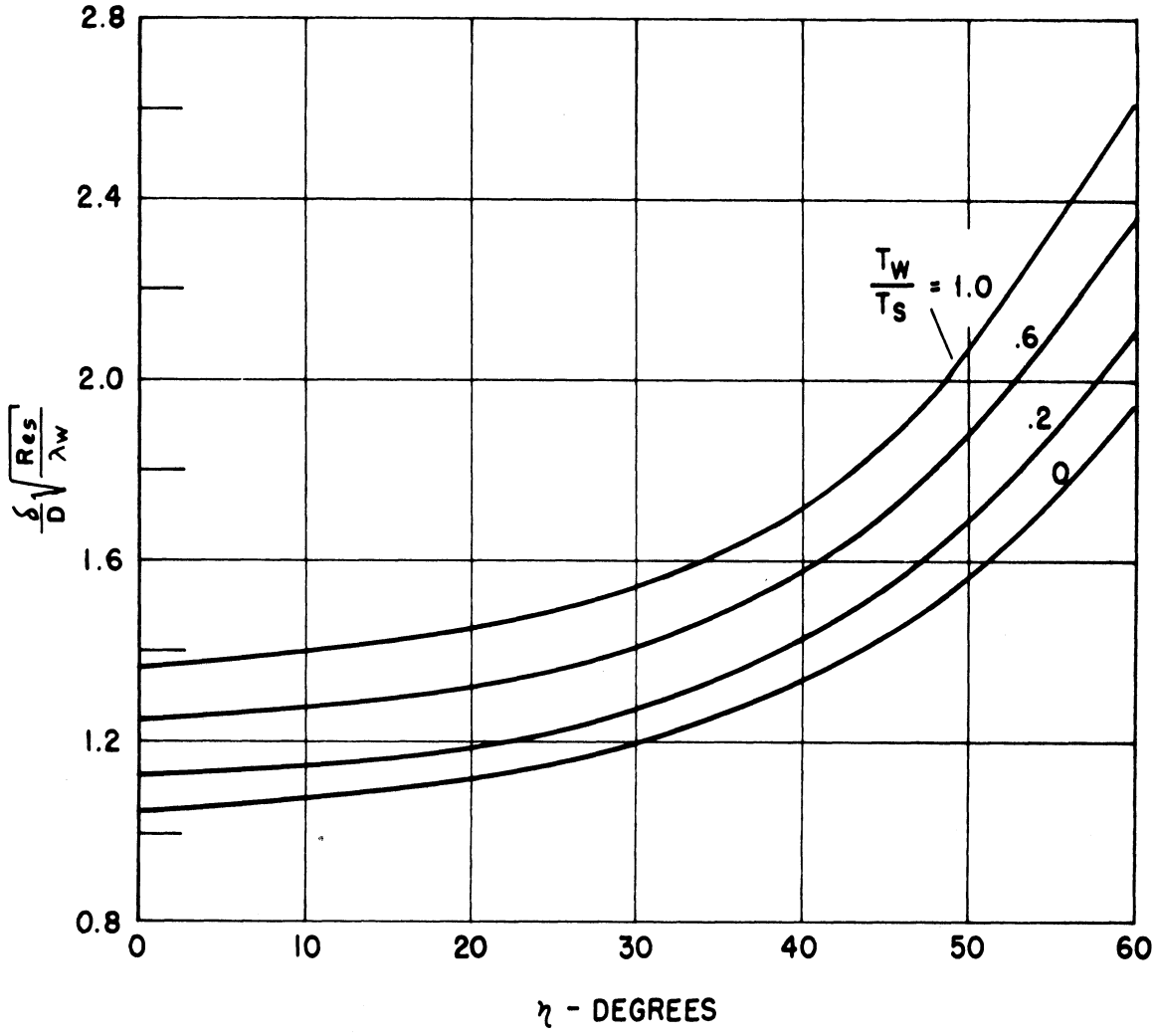

Figure 30. Variation of δ with η and T_w/T_s on a Hemisphere in Hypersonic Flow.

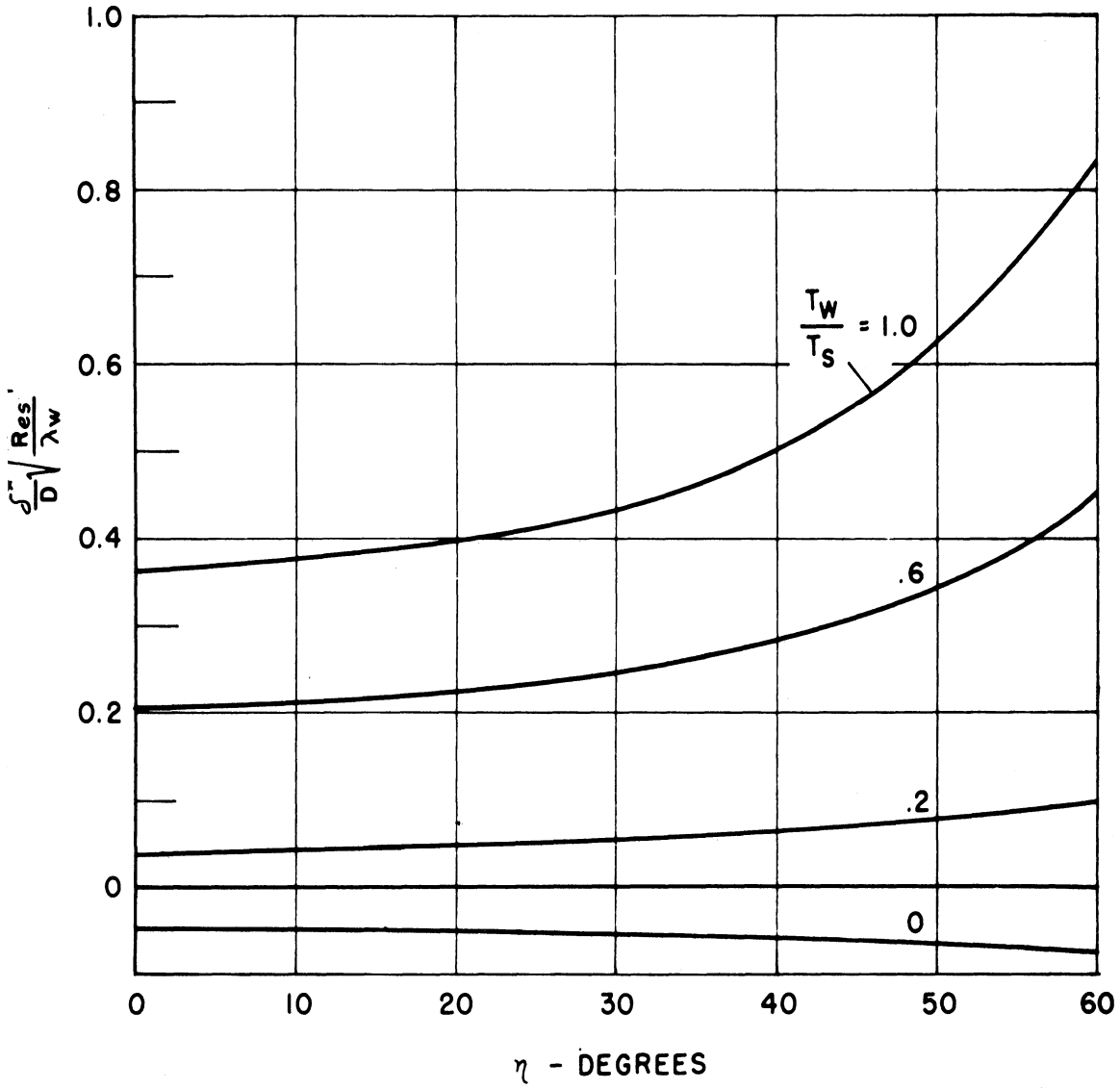

Figure 31. Variation of δ^* with η and T_w/T_s on a Hemisphere in Hypersonic Flow.

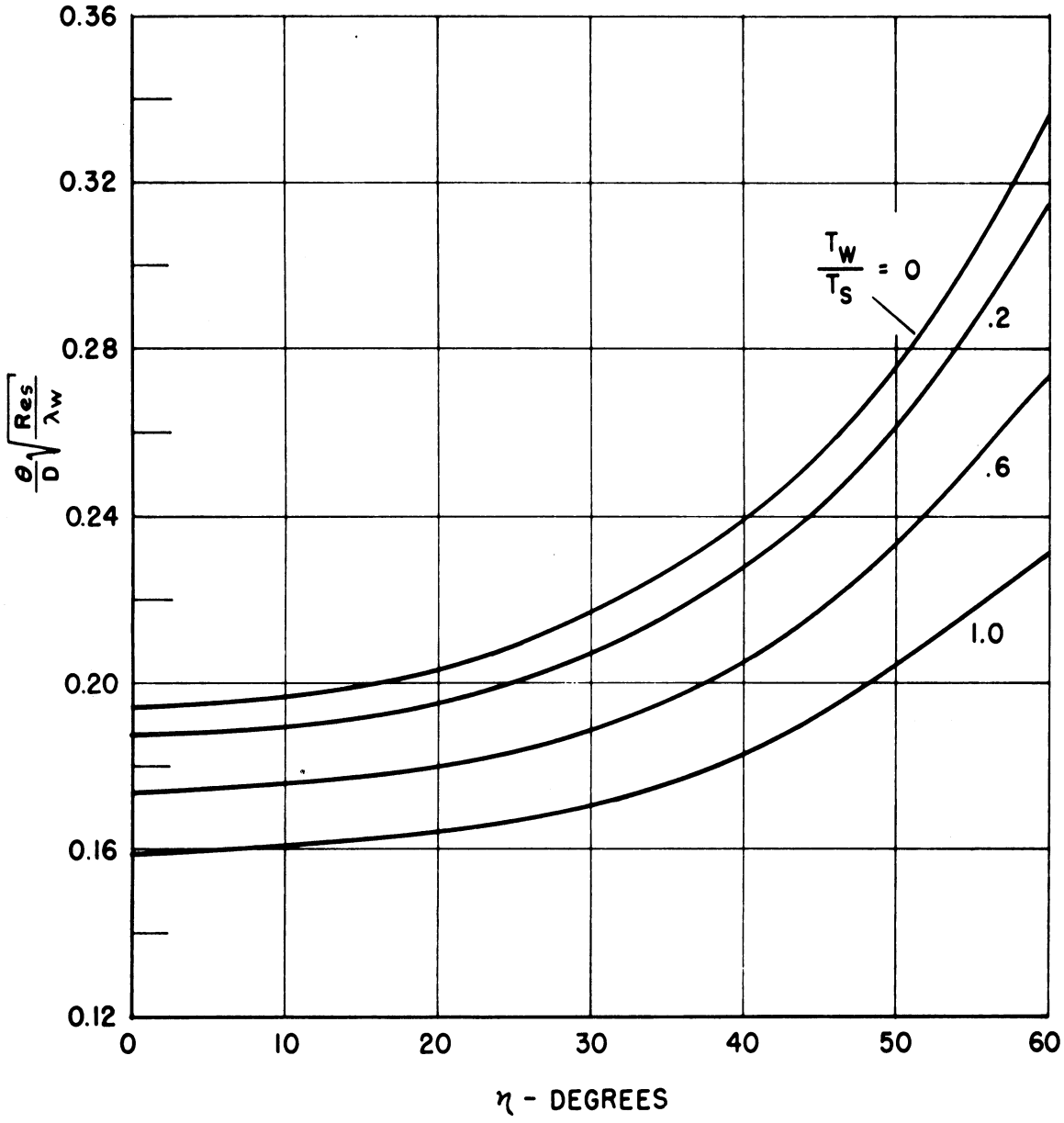

Figure 32. Variation of θ with η and T_w/T_s on a Hemisphere in Hypersonic Flow.

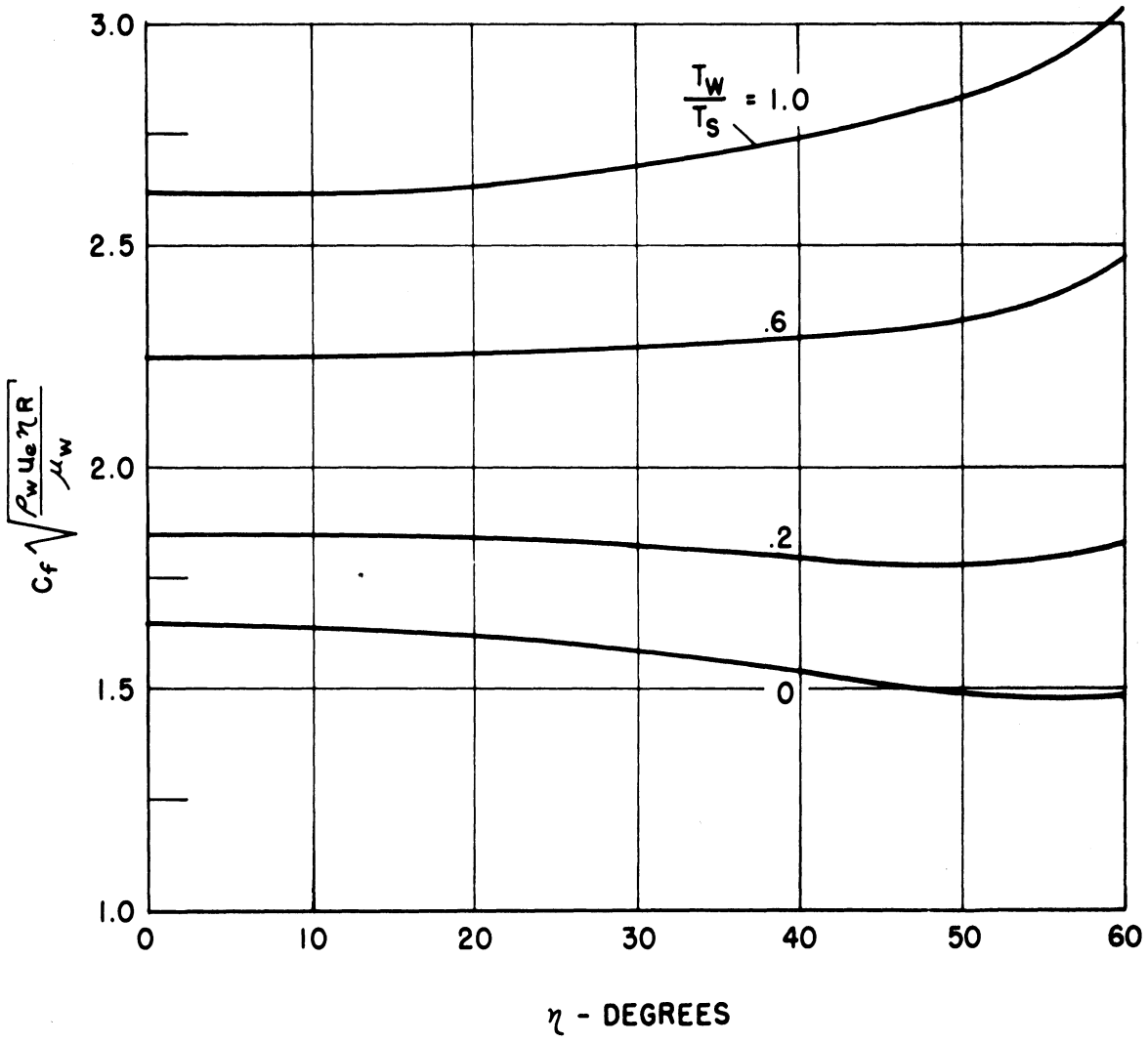

Figure 33. Variation of $C_f\sqrt{\frac{\rho_w u_e \eta R}{\mu_w}}$ with η and T_w/T_s on a Hemisphere in Hypersonic Flow.

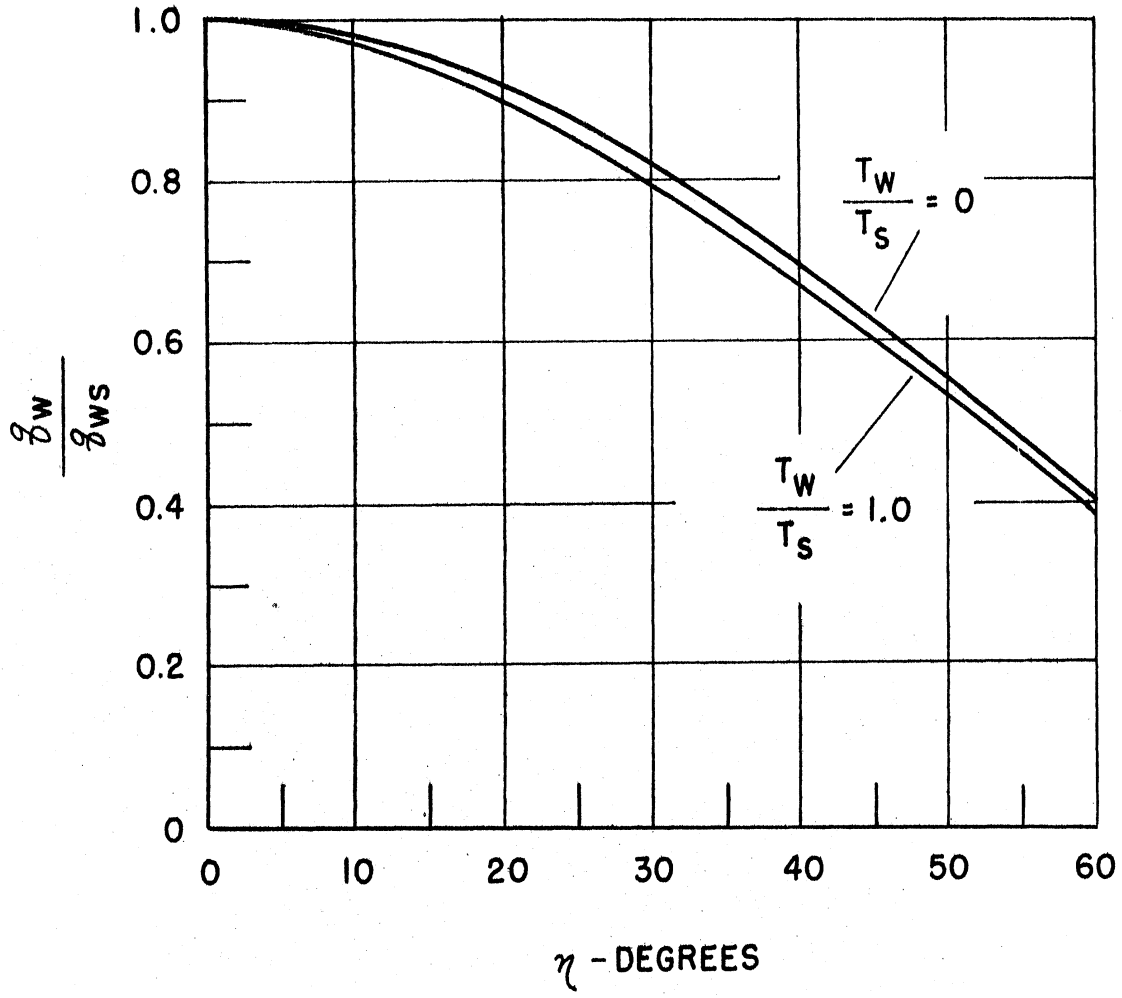

Figure 34. Variation of q_w with η and T_w/T_s on a Hemisphere in Hypersonic Flow.

REFERENCES

1. See for instance: Lin, C. C. The Theory of Hydrodynamic Stability. Cambridge University Press, (1955).

2. Lees, L., and Lin, C. C. "Investigation of the Stability of the Laminar Boundary Layer in a Compressible Fluid." NACA TN 1115, 1946.

3. Lees, L. "The Stability of the Laminar Boundary Layer in a Compressible Fluid." NACA Report No. 876, 1947.

4. Eber, G. R. "Recent Investigations of Temperature Recovery and Heat Transmission on Cones and Cylinders in Axial Flow in the N. O. L. Aeroballistics Wind Tunnel." J. Aero. Sci., 19, (1952), 1-6.

5. Higgins, W., and Pappas, C. C. "An Experimental Investigation of the Effect of Surface Heating on Boundary-Layer Transition on a Flat Plate in Supersonic Flow." NACA TN 2351, 1951.

6. Liepmann, H. W., and Fila, G. H. "Investigations of Effects of Surface Temperature and Single Roughness Elements on Boundary Layer Transition." NACA TN 1196, 1947.

7. Scherrer, R. "Boundary Layer Transition on a Cooled 20° Cone at Mach Numbers of 1.5 and 2.0." NACA TN 2131, 1950.

8. Czarnecki, K. R., and Sinclair, A. R. "Preliminary Investigation of the Effects of Heat Transfer on Boundary Layer Transition on a Parabolic Body of Revolution (NACA RM-10) at a Mach Number of 1.61." NACA TN 3165, 1954. See also NACA TN 3166 by same authors.

9. Jack, J. R. and Diaconis, N. S. "Variation of Boundary Layer Transition on Two Bodies of Revolution at a Mach Number of 3.12." NACA TN 3562.

10. van Driest, E. R., and Boison, J. C. "Experiments on Boundary Layer Transition at Supersonic Speeds." J. Aero. Sci., 24, (1957), 885-889.

11. Diaconis, N. S., Jack, J. R., and Wisniewski, R. J. "Boundary-Layer Transition at Mach 3.12 as Affected by Cooling and Nose Blunting." NACA TN 3928, 1957.

12. Jack, J. R., Wisniewski, R. J., and Diaconis, N. S. "Effects of Extreme Surface Cooling on Boundary Layer Transition." NACA TN 4094, October, 1957.

13. Diaconis, N. S., Wisniewski, R. J., and Jack. J. R. "Heat Transfer and Boundary Layer Transition on Two Blunt Bodies at Mach Number 3.12." NACA TN 4099, October, 1957.

14. Stetson, K. F. "Boundary-Layer Transition on Blunt Bodies with Highly Cooled Boundary Layers." J. Aero. Sci., 27, (1960), 81-90.

15. Hall, J. R., Speegle, K. C., and Piland, R. O. "Preliminary Results from a Free-Flight Investigation of Boundary-Layer Transition and Heat Transfer on a Highly Polished 8-Inch-Diameter Hemisphere-Cylinder at Mach Numbers up to 3 and Reynolds Numbers Based on a Length of 1 Foot Up to 17.7×10^6." NACA RM L57D18c, May, 1957.

16. Garland, B. J., and Chauvin, L. T. "Measurements on Heat Transfer and Boundary-Layer Transition on an 8-Inch-Diameter Hemisphere-Cylinder in Free Flight for a Mach Number Range of 2.00 to 3.88." NACA RM L57504a, April, 1957.

17. Morkovin, M. V. "On Transition Experiments at Moderate Supersonic Speeds." J. Aero. Sci., 24, (1957).

18. Laufer, J. "Aerodynamic Noise in Supersonic Wind Tunnels." JPL Progress Report 20-378, February 27, 1959.

19. Amick, J. L. "Supersonic Tunnel Design for Transition Studies." Paper presented at 14th STA Meeting, October 17-19, 1960.

20. Ferri, A., and Libby, P. A. "A New Technique for Investigating Heat Transfer and Surface Phenomena Under Hypersonic Flow Conditions." J. Aero. Sci., 24, (1957), 464-465.

21. Kuethe, A. M., and Schetzer, J. D. Foundations of Aerodynamics. New York: John Wiley and Sons, Second Edition, (1959), Chapter 15.

22. Dryden, H. L. "Some Aspects of Transition from Laminar to Turbulent Flow." Lecture Series No. 34, The Institute for Fluid Dynamics and Applied Mechanics, University of Maryland, November, 1955.

23. Gazely, C. "Boundary-Layer Stability and Transition in Subsonic and Supersonic Flow." J. Aero. Sci., 20, (1953), 19-28.

24. Czarnecki, K. R., and Sinclair, A. R. "Factors Affecting Transition at Supersonic Speeds." NACA RML53I18a, November, 1953.

25. Taylor, G. I. "Stability of a Viscous Liquid Contained Between Two Rotating Cylinders." Phil. Trans. Roy. Sco. London: A223, (1923), 289-343.

26. Goertler, H. "Ueber eine dreidimensionale Instabililaet laminarer Grenyschichten an knokaven Waenden." Ges. d. Wiss., Goettingen, Nachr. a. d. Math., Bd. 2, Nr. 1, 1940, (Translated in NACA TM 1375, June, 1954).

27. Liepmann, H. W. "Investigations of Boundary-Layer Transition on Concave Walls." NACA ACR 4J28, 1945.

28. Lees, L. "Note on the Stabilizing Effect of Centrifugal Forces on the Laminar Boundary Layer Over Convex Surfaces." J. Aero. Sci., 25, (1958).

29. Potter, J. L., and Whitfield, J. D. "Effects of Unit Reynolds Number Nose Bluntness, and Roughness on Boundary Layer Transition." AEDC-TR-60-5, March, 1960.

30. Braslow, A. L., Knox, E. C., and Horton, E. A. "Effect of Distributed Three-Dimensional Roughness and Surface Cooling on Boundary-Layer Transition and Lateral Spread of Turbulence at Supersonic Speeds." NASA TN D-53, October, 1959.

31. Cohen, C. B., and Reshotko, E. "Similar Solutions for the Compressible Laminar Boundary Layer with Heat Transfer and Pressure Gradient." NACA Report 1203, 1956.

32. Cohen, C. B., and Reshotko, E. "The Compressible Laminar Boundary Layer with Heat Transfer and Arbitrary Pressure Gradient." NACA Report 1294, 1956.

33. Oliver, R. E. "An Experimental Investigation of Flow Over Simple Blunt Bodies at a Nominal Mach Number of 5.8." J. Aero. Sci., 23, (1956).

34. Beckwith, I. E., and Gallagher, J. J. "Heat Transfer and Recovery Temperatures on a Sphere with Laminar, Transitional, and Turbulent Boundary Layers at Mach Numbers of 2.00 and 4.15." NACA TN 4135, December, 1957.

35. Cooper, M., and Mayo, E. E. "Measurements of Local Heat Transfer and Pressure on Six 2-Inch-Diameter Blunt Bodies at a Mach Number of 4.95 and at Reynolds Numbers Per Foot to 81 x 10^6." NASA Memo 1-3-59L, March, 1959.

36. Kemp, N. H., Rose, P. H., and Detra, R. W. "Laminar Heat Transfer Around Blunt Bodies in Dissociated Air." AVCO Research Report 15, May, 1958.

37. Boison, J. C. "Experimental Investigation of the Hemisphere-Cylinder at Hypervelocities in Air." AEDC-TR-58-20 (ASTIA Document: AD-204392), November, 1958.

38. Kendall, Jr., J. M. "Experiments on Supersonic Blunt-Body Flows." CIT, Progress Report No. 20-372, February, 1959.

39. Lamb, H. Hydrodynamics. New York: Dover Publications, (1945), 42.

40. Morkovin, M. V. "Fluctuations and Hot-Wire Anememetry in Compressible Flows." AGARDograph 24, NATO, November, 1956.

41. Trilling, L., and Hakkinen, R. J. "The Calibration of the Stanton Tube as a Skin-Friction Meter." 50 Jahre Grenzschichtforschung. Edited by H. Goertler and W. Tollmien, Braunschweig: Friedr. Vieweg und Sohn, (1955).

42. Wilkins, M. R., and Darsaw, J. F. "Finishing and Inspection of Model Surfaces for Boundary-Layer-Transition Tests." NASA Memo 1-19-59A, February, 1959.

43. Kuethe, A. M., Willmarth, W. W., and Crocker, G. H. "Stagnation Point Fluctuations and Boundary Layer Stability on Bodies of Revolution with Hemispherical Noses." Presented at AGARD Boundary Layer Symposium, London, England, April 25-29, 1960.

44. Kuethe, A. M., Willmarth, W. W., and Crocker, G. A. "Stagnation Point Fluctuations Near the Nose of Bodies of Revolution." Physics of Fluids, 2, (1959).

45. Potter, J. L., Whitfield, J. D., and Strike, W. T. "Transition Measurements and the Correlation of Transition Sensitive Data." AEDC-TR-59-4, February, 1959.

46. Favre, A. J., Gaviglio, J. J., and Dumas, R. "Space-Time Double Correlations and Spectra in a Turbulent Boundary Layer, Journal of Fluid Mechanics, 2, (1957).

47. Peterson, J. B., and Horton, E. A. "An Investigation of the Effect of a Highly Favorable Pressure Gradient on Boundary-Layer Transition as Caused by Various Types of Roughnesses on a 10-Foot Diameter Hemisphere at Subsonic Speeds." NASA Memo 2-8-59L, April, 1959.

48. Bandetlini, A. and Isler, W. E. "Boundary-Layer-Transition Measurements on Hemispheres of Various Surface Roughnesses in a Wind Tunnel at Mach Numbers from 2.48 to 3.55." NASA Memo 12-25-58A, March, 1959.

49. Cooper, M., Mayo, E. E., and Julius, J. D. "The Influence of Low Wall Temperature on Boundary-Layer Transition and Local Heat Transfer on 2-Inch-Diameter Hemispheres at a Mach Number of 4.95 and a Reynolds Number Per Foot of 73.2×10^6." NASA TN D-391, July, 1960.

50. Hayes, W. D., and Probstein, R. F. Hypersonic Flow Theory. New York: Academic Press Inc., (1959).